

**PHYSICAL TRANSFORMATIONS FOR GREENER CHEMICAL
PROCESSES**

A Thesis
Presented to
The Academic Faculty

by

Ross R. Weikel

In Partial Fulfillment
Of the Requirements for the Degree
Doctor of Philosophy in Chemical Engineering

Georgia Institute of Technology
August, 2005

PHYSICAL TRANSFORMATIONS FOR GREENER CHEMICAL PROCESSES

Approved by:

Dr. Charles A. Eckert, Advisor
College of Engineering
Georgia Institute of Technology

Dr. Dennis Hess
College of Engineering
Georgia Institute of Technology

Dr. Carson Meredith
College of Engineering
Georgia Institute of Technology

Dr. Charles L. Liotta, Co-advisor
College of Sciences
Georgia Institute of Technology

Dr. Rigoberto Hernandez
College of Sciences
Georgia Institute of Technology

Date Approved: July 13, 2005

You ready B...Let's go get 'em

ACKNOWLEDGEMENTS

I would like to thank my advisors, Dr. Charles A. Eckert and Dr. Charles L. Liotta for their tremendous guidance during my tenure at Georgia Tech. Chuck treats every group member as a friend and coworker from the day they walk in the door. He taught me everything I expected to learn about chemical engineering. Moreover, he allowed me to learn how to be a leader in the lab and to learn from my own mistakes. I am amazed at the things other than science that can be learned in a lab.

Dr. Liotta's energetic personality has been an inspiration from the beginning. I enjoyed his comedy more than most, and enjoyed his enthusiasm for research as much as anyone. His ideas got me out of research dead ends several times and made me excited to get back in the lab. The collaboration between these two is impressive not just for the body of research produced, but for all the other things the two manage to do while conducting research.

I also thank the other members of my committee, Dr. Dennis Hess, Dr. Carson Meredith, and Dr. Rigoberto Hernandez. Each of these men provided not only time for the steps along the way, but also research advice whether through research collaboration or personal communication.

I thank Deborah Babykin who keeps the Eckert-Liotta group running and whose work makes all of us more effective than we could come close to without her.

I would like to thank the entire Eckert-Liotta research group of past and present. In my time I have moved a lab, put a lab back together, broken a MS, fixed a MS and much more with a large number of people. I would particularly like to thank the list of post-doctoral scientists who made my research much better and helped it finish much faster than it would have otherwise: Shane Nolen, Tony Belcher, Josh Brown, Jie Lu, Pamela Pollet, Dave Bush, Jason Hallett and Chris Kitchens. I would also like to thank my research collaborators, who obviously had a hand in this body of work and were also friends: Theresa Chamblee, Colin Thomas, Galit Levitin, and Beth Newton. I also had the privilege of working with several undergraduates in the lab who also contributed significantly: Kyle Ross, Kristin Kitigawa, Oxana Selivanova, Chris Shockley, and Craig Simpson. I would also like to thank Beckie Jones who will finish with me and helped push me to get this done. Finally, Malina Janakat, who was an officemate for 4 years, was an ally, a coworker, and a friend who helped make the whole experience.

I would like to thank my family: my parents, Scott and Jean, for raising me to enjoy education and to have the drive to do it; my brother, Colby for setting the bar that was my goal for the first 18 years of my life and being a friend since; the Weikel family for its incredible support, and the Ritchie family for always being so proud of me.

Finally, I thank my wife, Blair, who is my escape valve. Somehow she knows precisely when I need a hug and a bear claw to get back on my feet. She is one of the many blessings I have received that I could never repay. I am truly blessed and give thanks to God.

TABLE OF CONTENTS

ACKNOWLEDGEMENTS		<i>ii</i>
LIST OF TABLES		<i>vii</i>
LIST OF FIGURES		<i>ix</i>
LIST OF SYMBOLS		<i>xiii</i>
SUMMARY		<i>xvi</i>
CHAPTER I.	INTRODUCTION	1
CHAPTER II.	PROPERTIES OF ALKYL CARBONIC ACIDS	7
	Introduction	7
	Experimental Materials	10
	Apparatus and Procedures	10
	Results and Discussion	15
	Conclusion	28
	References	29
CHAPTER III	SELF NEUTRALIZING IN SITU ACID CATALYSIS FOR SINGLE POT SYNTHESIS OF ARYL HALIDES AND AZO DYES IN GAS-EXPANDED LIQUIDS	31
	Introduction	31
	Experimental Materials	37
	Apparatus and Procedures	37
	Results and Discussion	38
	Conclusion	46
	References	47
CHAPTER IV	HYDROLYSIS OF β -PINENE VIA ALKYL CARBONIC ACIDS	49
	Introduction	49
	Experimental Materials	57
	Apparatus and Procedures	58
	Results and Discussion	60
	Conclusion	65

	References	67
CHAPTER V	CONTROLLABLE SURFACTANTS	70
	Introduction	70
	Experimental Materials	76
	Apparatus and Procedures	77
	Results and Discussion	79
	Conclusion	88
	References	90
CHAPTER VI	TUNABLE MELTING POINT DEPRESSION OF IONIC LIQUIDS	93
	Introduction	93
	Experimental Materials	98
	Apparatus and Procedures	98
	Results and Discussion	102
	Conclusion	110
	References	111
CHAPTER VII	SUMMARY AND RECCOMENDATIONS	114
VITA		126

LIST OF TABLES

Table 1-1	12 principles of green chemistry (Anastas)	3
Table 2-1	Parts and manufacturers for dielectric cell construction	13
Table 4-1	Sample of pinene hydration literature	52
Table 4-2	Summary from the literature for product composition for pinene solvolysis reactions (% of product mixture)	53
Table 4-3	pH and dielectric constant values for MeOH/H ₂ O/CO ₂ GXLs	55
Table 4-4	Summary of GXL composition and results	63
Table 6-1	Enthalpy of fusion, enthalpy of transition, melting temperature, and transition temperature values and references	102
Table 6-2	Average water content and standard deviation of ionic liquids tested	107

LIST OF FIGURES

Figure 1-1	Number of environmental laws versus year of passage	2
Figure 2-1	Diagram of dielectric probe and wires	13
Figure 2-2	High pressure pass through for steel wire	14
Figure 2-3	Mechanism for the reaction of DDM with an alkylcarbonic acid forming an ether and a carbonate	16
Figure 2-4	Typical UV-vis spectrum of decreasing DDM absorbance as a function of time	17
Figure 2-5	Pseudo-first order fit for 20 mol % ethylene glycol, 20 mol % CO ₂ , 60 mol % acetone	18
Figure 2-6	Pseudo-first order rate constants for various alcohols at 20 mol % alcohol, 20 mol % CO ₂ , 60 mol % acetone	19
Figure 2-7	Two separate steps required for alkylcarbonic catalysi. Step 1: formation of acid from alcohol and CO ₂ . Step 2: Dissociation of proton from alkylcarbonic acid	20
Figure 2-8	Methanol-CO ₂ at 40°C: DDM reaction rate x 10 ⁴ (diamonds), dielectric constant (squares), and volume expansion (triangles)	21
Figure 2-9	Methanol-CO ₂ at 23°C: DDM reaction rate x 10 ⁴ (squares), dielectric constant (diamonds), and volume expansion (triangles)	22
Figure 2-10	Dielectric constant of methanol-CO ₂ mixture versus mol fraction CO ₂ at 23°C (diamonds) and literature data with linear interpolation (line)	24
Figure 2-11	Dielectric constant of methanol-CO ₂ mixture versus mol fraction CO ₂ at 40°C (diamonds) and literature data with linear interpolation (line)	25
Figure 2-12	Hammett Plot of para substituted benzyl alcohol alkylcarbonic acid reaction with DDM at 40°C.	26

Figure 3-1	Possible synthetic products from the diazonium cation	32
Figure 3-2	Mechanism for the formation of methyl yellow from aniline and nitrous acid	34
Figure 3-3	Mechanism for the formation of benzyl iodide from aniline and nitrous acid	35
Figure 3-4	Alkylcarboxylic acid formation and proton dissociation equilibria	36
Figure 3-5	Synthesis of methyl yellow from aniline	38
Figure 3-6	Formation of carbamic acid from aniline and carbon dioxide	39
Figure 3-7	Effect of nitrite loading on yield	41
Figure 3-8	Effect of CO ₂ loading on yield	41
Figure 3-9	Effect of temperature on yield	42
Figure 3-10	Mass Selective Detector trace for the production of methyl yellow at low CO ₂ addition and low nitrite loading.	44
Figure 3-11	Synthesis of iodobenzene from aniline	45
Figure 4-1	α -terpineol (1) and its isomers	51
Figure 4-2	Classical method for the manufacture of terpineol from pinene	52
Figure 4-3	Pinene based versatile reagents (PVR) from Ramachandran (2002)	53
Figure 4-4	Mechanism for the acid-catalyzed rearrangement and hydrolysis of β -pinene	56
Figure 4-5	β -pinene conversion and product distribution variations with different methanol/water ratios (75°C, 24 hrs)	62
Figure 4-6	β -pinene conversion and product distribution variations with different cosolvents (75°C, 24 hrs)	62
Figure 4-7	Product distribution reproducibility for 6 runs of pinene hydrolysis in the 1:1 MeOH/water GXL	66

Figure 5-1	Structure of n-octyl thiirane-1-oxide	70
Figure 5-2	Critical micelle concentration diagram by surface tension measurement	71
Figure 5-3	Decomposition of n-octyl thiirane-1-oxide to 1-decene, sulfur oxide, and other sulfurous products	76
Figure 5-4	Synthetic scheme for n-octyl thiirane-1-oxide	80
Figure 5-5	¹ H NMR of n-octyl thiirane-1-oxide	81
Figure 5-6	Critical micelle concentration of 1-octyl thiirane-1-oxide in water by capillary rise (diamond), hydrophobic sessile drop contact angle (square), hydrophilic sessile drop contact angle (triangle), and Sudan III dye solubility (x).	83
Figure 5-7	Loss of surface activity by heating the solution for 1 hour at 90°C	86
Figure 5-8	Comparison of the dye solubility of 1-octyl thiirane-1-oxide and sodium dodecyl sulfate before (blue) and after heating (red) at 90°C for one hour and for 10 minutes.	87
Figure 6-1	Most commonly employed ionic liquid cations	94
Figure 6-2	Common ionic liquid cations and anions & their abbreviations	95
Figure 6-3	Schematic of melting point apparatus	99
Figure 6-4	Temperature-composition (T-x) diagram for naphthalene-CO ₂ : (circle- Cheong et al, square-this work, line-ideal solubility, dashed line-MOSCED solubility, triangle-pure component)	103
Figure 6-5	Temperature-composition (T-x) diagram for tetrabutylammonium tetrafluoroborate-CO ₂ : diamonds-this work, line-ideal solubility	105
Figure 6-6	Temperature-composition (T-x) diagram for tetrahexylammonium bromide-CO ₂ : diamond-this work, line-ideal solubility	106
Figure 6-7	Temperature-composition (T-x) diagram for [C16mim][PF ₆]-CO ₂ from the data of Kazarian et al (2002).	108

Figure 7-1	Series of alcohols for further study of alkylcarbonic acids reacting with DDM	116
Figure 7-2	Photolabile analog of thiirane oxide cleavable surfactant	117
Figure 7-3	CO ₂ -philic analogs of thiirane oxide cleavable surfactant	118
Figure 7-4	SO ₂ and CO ₂ emitting cleavable surfactants	119
Figure 7-5	Base catalyzed hydrolysis of benzyl chloride to benzyl alcohol	120
Figure 7-6	Polymerization of acrylamide to polyacrylamide	121
Figure 7-7	Series of cations with decreasing alkylchain length from tetrahexyl to tetramethyl ammonium cation with abbreviations	123

LIST OF SYMBOLS AND ABBREVIATIONS

Abbreviations

GXL	Gas Expanded Liquid
pK _a	-log of the acid dissociation constant
M	moles per liter (concentration)
GC	gas chromatograph
LC	liquid chromatograph
FID	flame ionization detector
MSD	mass selective detector
SCF	supercritical fluid
SFC	supercritical fluid chromatograph
SFE	supercritical fluid extraction
IL	ionic liquid
RTIL	room temperature ionic liquid
VOC	volatile organic compound
MOSCED	Modified Separation of Cohesive Energy Density
PVR	pinene based versatile reagents
DENAB	N,N-diethyl-4-amino-4'-nitroazobenzene
GAS	gas anitsolvent system
DDM	diazodiphenylmethane
NNDMA	N,N-dimethyl aniline

w/o	water in oil emulsion
o/w	oil in water emulsion
w/c	water in CO ₂ emulsion
CMC	critical micelle concentration
SANS	small angle neutron scattering
AOT	bis-(2-ethylhexyl) sulfosuccinate sodium salt
DENAB	N,N-diethyl-4-[(4-nitrophenyl)azo]aniline
HPLC	high performance liquid chromatography
PEEK	polyetheretherketones
LCR	inductance, capacitance, resistance meter

Symbols

α	location of double bond
β	location of double bond
γ	location of double bond
ϵ	dielectric constant
v	molar volume
λ	MOSCED polarizability
τ	MOSCED dipolarity
ψ	MOSCED dipolarity asymmetry term
α	MOSCED hydrogen bonding acidity
β	MOSCED hydrogen bonding basicity
ξ	MOSCED hydrogen bonding asymmetry

q	MOSCED dipolarity
T_m	melting point temperature
T	temperature
R	gas constant
C	capacitance
L	length of dielectric probe
k_e	Coulomb's constant
R_2	outer radius of dielectric probe
R_1	inner radius of dielectric probe
ρ	Hammett reaction sensitivity to electronic effects
σ	Hammett electron donating/ withdrawing constant
k_x	Hammett reaction rate constant
k_0	Hammett base reaction rate
ΔH_{fus}	Enthalpy of fusion
ΔH_{trans}	Enthalpy of solid-solid transition
T_{trans}	Temperature of solid-solid transition

SUMMARY

Homogenous acid catalysts are prevalent throughout the chemical industry but all have the drawback of requiring post reaction neutralization and subsequent downstream removal of the product salt. The use of a base to neutralize the acid and the processing of the salt are ancillary to the process and the disposal of the salt is an environmental concern. The work presented here shows the use of alkylcarbonic acids, which form in situ with CO₂ pressure and neutralize on loss of CO₂ pressure rather than requiring a base. Thus CO₂ can be used to “switch” the acid on and off.

The properties of alkylcarbonic acids are explored to gain understanding of the mechanisms by which they act. The acids are also used to catalyze the synthesis of α -pinene, methyl yellow, and benzyl iodide. These reactions are examples of common acid catalyzed reactions where this technology could be implemented.

The second half of the work explores two other “switches”. The first is using temperature to break an emulsion with a novel thermally cleavable surfactant. This technology has potential applications in a wide range of fields where surfactants are used including polymerization, oil recovery, and biosynthesis. The second is using CO₂ to liquefy a solid ionic compound to allow its use as a solvent. This would greatly increase the number of ionic species available for use in ionic liquid-CO₂ biphasic systems.

CHAPTER I

INTRODUCTION

Since the 1970s, the number of environmental laws in the United States has grown exponentially as shown in Figure 1-1. Most, if not all, of these laws have impacted the chemical industry. Some laws were in direct response to mistakes on the part of the chemical industry while others are goals set to help reach a sustainable future. As a result, a push for more environmentally friendly chemistry grew into what is today called green chemistry or green engineering. The field has been solidified by creation of the Green Chemistry Institute among chemists and the Sustainable Engineering Forum among engineers. Additionally, there is annual recognition by way of the Presidential Green Chemistry Challenge Award and education through the green chemistry summer schools put on in both the U.S. (Bektesevic, Beier et al. 2005), Europe (Holscher 2004), elsewhere (Licence and Asfaw 2005).

Currently the field has matured to point where there are a wide range of efforts by several disciplines all under the umbrella of green chemistry or sustainability. Some of these ideas have even made it to commercialization such as poly-lactic acid, decaffeination of coffee beans by CO₂, and using CO₂ for dry cleaning. Paul Anastas

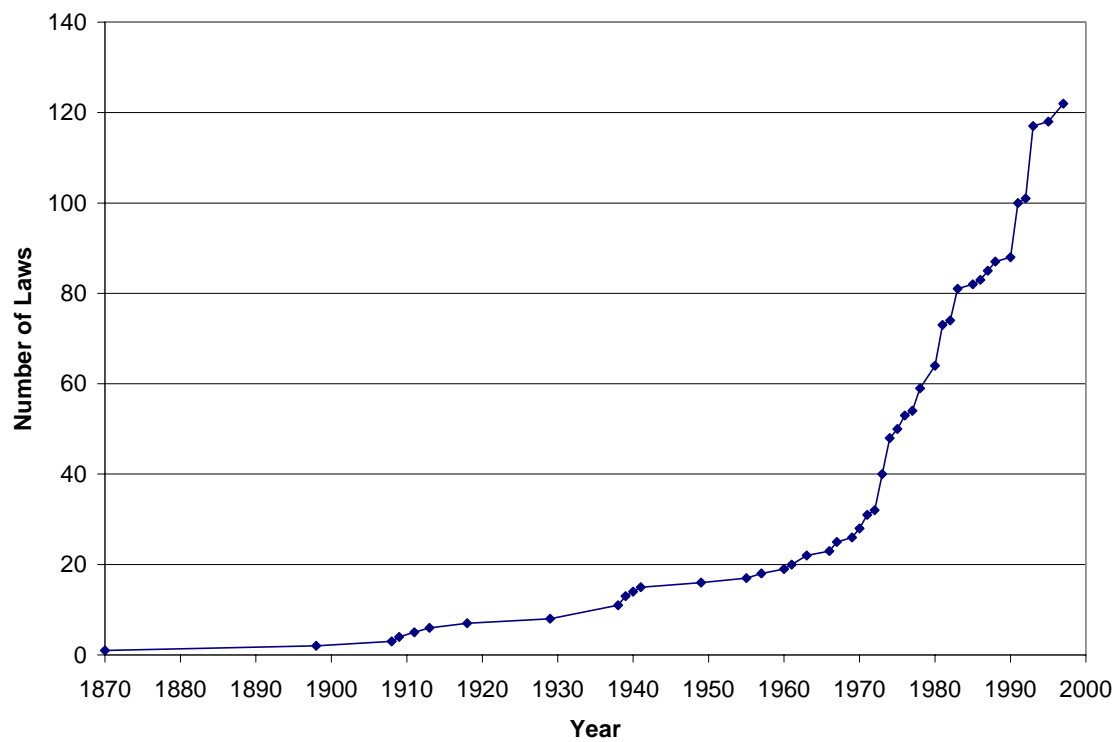


Figure 1-1: Number of U.S. Environmental Laws versus year of passage (Green Chemistry Institute)

Table 1-1: 12 Principles of Green Chemistry (Anastas and Warner 1998)

12 Principles of Green Chemistry		
1	Prevention	It is better to prevent waste than to treat or clean up waste after it has been created.
2	Atom Economy	Synthetic methods should be designed to maximize the incorporation of all materials used in the process into the final product
3	Less Hazardous Chemical Syntheses	Wherever practicable, synthetic methods should be designed to use and generate substances that possess little or no toxicity to human health and the environment
4	Designing Safer Chemicals	Chemical products should be designed to effect their desired function while minimizing their toxicity
5	Safer Solvents and Auxiliaries	The use of auxiliary substances (e.g., solvents, separation agents, etc.) should be made unnecessary wherever possible and innocuous when used
6	Design for Energy Efficiency	Energy requirements of chemical processes should be recognized for their environmental and economic impacts and should be minimized. If possible, synthetic methods should be conducted at ambient temperature and pressure
7	Use of Renewable Feedstocks	A raw material or feedstock should be renewable rather than depleting whenever technically and economically practicable
8	Reduce Derivatives	Unnecessary derivatization (use of blocking groups, protection/ deprotection, temporary modification of physical/chemical processes) should be minimized or avoided if possible, because such steps require additional reagents and can generate waste
9	Catalysis	Catalytic reagents (as selective as possible) are superior to stoichiometric reagents
10	Design for Degradation	Chemical products should be designed so that at the end of their function they break down into innocuous degradation products and do not persist in the environment.
11	Real-time Analysis for Pollution Prevention	Analytical methodologies need to be further developed to allow for real-time, in-process monitoring and control prior to the formation of hazardous substances
12	Inherently Safer Chemistry of Accident Prevention	Substances and the form of a substance used in a chemical process should be chosen to minimize the potential for chemical accidents, including releases, explosions, and fires

summarized the goals of the movement in his 12 principles of green chemistry seen in Table 1-1 (Anastas and Warner 1998).

Using these goals, researchers have been able to find improvements over current chemical technology and search for more sustainable solutions. One of the biggest areas of research and potential impact is safer solvents which led to research of supercritical fluids and more recently, gas-expanded liquids (GXLs). While supercritical fluids are heavily developed, gas-expanded liquids are still being characterized and extensively studied. During the study of GXLs, the presence of alkylcarbonic acids were observed and demonstrated in systems where both alcohol and CO₂ are present. Not only were these acids useful for catalysis, but they were also “switchable,” meaning their acidity could be turned on with CO₂ pressure and turned off by removal of CO₂. The ability to control, or switch, chemistry in order to create greener processes will be exploited in several areas in this thesis.

In Chapter II, a background of GXLs as well as a full explanation of alkylcarbonic acids is presented. The acid catalyzed reaction of diazodiphenyl methane (DDM) is extensively studied as a basis for comparison of various alkylcarbonic acids. Additionally, the dielectric constant of these solvent systems are measured to provide understanding of the mechanisms involved.

Chapter III provides application of alkylcarbonic acids to synthesize dyes in a one pot reaction. Both, N,N-dimethyl aminoazobenzene (also known as methyl yellow) and N,N-diethyl amino-nitroazobenzene (DENAB) were synthesized in a more environmentally friendly process than currently used in industry. Other dyes synthesized through azo coupling could also be made through the same process (such as phenolic

dyes rather than di-alkyl anilines). Similarly, Chapter IV, applies alkylcarbonic acids to acid catalyzed hydrolysis of β -pinene, a model compound for the flavor and fragrance industry. Improved product distribution and yields are reported compared to literature syntheses which are similar to industrial practice.

A different type of switch is introduced in Chapter V. Surfactants are widely used throughout the chemical and petroleum industries for their ability to bring organic and aqueous phases into contact. However, separating the two phases later in the process can prove to be quite difficult and energy intensive. For this reason, having a switch to turn off the emulsion is highly desired. A new surfactant, n-octyl thiirane-1-oxide, is described with the ability to go from a surfactant to a simple organic molecule with external stimulus. The critical micelle concentration of this molecule is reported by several methods and the decomposition of the molecule is also reported.

Chapter VI, provides yet another external switch: phase change from solid to liquid for various ionic compounds. Room temperature ionic liquids have received heavy attention in several areas of research mainly because of their lack of observable vapor pressure which makes them ideal replacements for volatile organic compounds. However, under ambient conditions, the number of ionic species which are liquids is quite limited when compared to the possible combinations of ions. Presented in Chapter VI are measurements of melting points of various ionic solids in the presence of CO₂ pressure. Thus CO₂ provides a 'switch' to control the phase of the ionic species and thereby vastly extending the number of compounds which could be used for ionic liquids in future research and applications.

Finally, Chapter VII, summarizes the work listed above and frames the implications of the work. Also, extensions of the research are put forward where there could be greater impact for the technology developed in this thesis.

References

- Anastas, P. T. and J. C. Warner (1998). Green Chemistry: Theory and Practice. Oxford, England, Oxford University Press.
- Bektesevic, S., J. C. Beier, et al. (2005). "Green Challenges: student perspectives from the 2004 ACS-PRF Summer School on Green Chemistry." Green Chem. **7**(6): 403.
- Holscher, M. (2004). "Sixth Summer School on Green Chemistry." Green Chem. **6**(6): G49.
- Licence, P. and N. Asfaw (2005). "The first Green Chemistry workshop in Ethiopia." Green Chem. **7**(6): 401.

CHAPTER II

SELF-NEUTRALIZING *IN SITU* ACID CATALYSIS FROM CO₂

Introduction

Acids are the most common industrial catalysts but have the disadvantage of requiring post-reaction neutralization and salt disposal. We show the catalytic use of self-neutralizing acids. Carbon dioxide interacts with water and amines to form acidic species. A similar interaction occurs with alcohols to form alkylcarbonic acids. All three solvent systems provide *in situ* acid formation which can be easily neutralized. Therefore, all three solvent systems provide *in situ* acid formation for catalysis. However, water has poor organic solubility and amines form salts, so only alkylcarbonic acids combine good organic solubility with simple neutralization via depressurization. The use of *in situ* acid also completely eliminates the solid salt wastes associated with many acid processes. To elucidate how to implement these systems in place of a standard acid system we compare the reaction rates of several alkylcarbonic acids. We report also the effect of CO₂ pressure on rate.

Acids are widely used industrial catalysts but often have environmental limitations. Common acids include Brønsted acids such as HCl, H₂SO₄ and H₃PO₄ and Lewis acids such as AlCl₃ and BF₃. Problems such as large amounts of waste, toxicity, corrosion, and difficulty of separation plague acids used in industry. For instance, in the Friedel-Crafts acylation of methyl benzoate with acetic anhydride, around twenty

kilograms of AlCl_3 are used per kilogram of product (Eissen and Metzger 2002).

Generally when HCl is used it is neutralized with NaOH resulting in one mole of NaCl for every mole of acid. This solid must be removed to avoid accumulation and is contaminated with whatever else is in the process stream and so must be disposed of as toxic waste. One approach to solving these problems has been solid acids. However, they often bind irreversibly with anything in the system which is basic which destroys activity. Therefore, there is significant demand for an easily recycled, environmentally benign acid.

The use of carbon dioxide as a solvent has been the subject of a wide range of research (Eckert, Knutson et al. 1996; Eckert and Chandler 1998; Eckert, Bush et al. 2000). However, solubility limitations lead to the use of cosolvents which in turn lead to the development of gas-expanded liquids (GXLs). GXLs are organic solvents which are expanded by a soluble gas, usually CO_2 , thereby increasing mass transfer and serving as an environmentally benign solvent replacement. GXLs also offer solubility which is more in the range of traditional organic solvents and tunable with pressure. These GXLs have been used for a range of reactions (Blanchard and Brennecke 2001; Musie, Wei et al. 2001; Wei, Musie et al. 2001) and separations (Chang and Randolph 1990; Eckert, Bush et al. 2000; Zhao and Olesik 2001; Xie, Brown et al. 2002; Lin, Muhrer et al. 2003).

During the development of these GXLs, an interaction between alcohols and CO_2 was shown to change the color of Reichardt's dye. West et al. explained this phenomenon by demonstrating the presence of alkylcarbonic acids (Figure 2-5) in such systems (West, Wheeler et al. 2001). These acids are reversible with CO_2 pressure and the CO_2 is easily separated by depressurization and recycled. Thus alkylcarbonic acids

offer simple neutralization and do not require any waste disposal. West et al. used diazodiphenylmethane (DDM) as a probe to measure relative rates of these acids (scheme 2) as well as carbonic acid from water (West, Wheeler et al. 2001). Since then, some work has been done to find applications for alkylcarbonic acids. Xie et al. used CO₂-expanded methanol and ethylene glycol for acetal formation on cyclohexanone (Xie, Liotta et al. 2004). In work shown in Chapter IV, Chamblee et al. used a mixture of methanol and water with CO₂ to catalyze the hydrolysis of β -pinene (Chamblee, Weikel et al. 2004). Chapter III also shows the use of this acid to catalyze diazotization reactions. Finally, Hulme et al. used methylcarbonic acid to catalyze some Ugi reactions (Keating and Armstrong 1998; Hulme, Ma et al. 2000).

In this work, DDM is again used as a reactive probe to find more information about alkylcarbonic acids and to further understand how to employ them in the future. DDM has been used as a probe for benzoic and naphthoic acids (Buckley, Chapman et al. 1968) and many carboxylic acids (Roberts and Watanabe 1950; Roberts and Regan 1952) in addition to its previous use with alkylcarbonic acids. DDM has also previously been used in Hammett plots (Hine and Bailey Jr. 1959), as it is here.

The dielectric constant of gas expanded liquids has never been fully investigated. Several research groups have obtained data for mixtures of CO₂ and organic solvents above the mixture critical point (Dombro, McHugh et al. 1991; Roskar, Dombro et al. 1992; Golfarb, Fernandez et al. 1999; Lee, Smith et al. 2000). In this paper, we investigate the gas expanded region where there is vapor-liquid equilibrium rather than a single supercritical phase. It is important in the case of acid catalysis to know the

dielectric constant because it gives some indication of the solvent's ability to support ions such as a proton.

Experimental Materials

All Chemicals were obtained and used without further purification except CO₂ which was filtered before use. These chemicals include: methanol (Aldrich, anhydrous, 99.5+%), acetone (Aldrich, HPLC grade, 99.9+%), ethanol (Aldrich, anhydrous), ethylene glycol (Aldrich, anhydrous, 99.8%), propylene glycol (Aldrich, 99.5+%), benzyl alcohol (Aldrich, 99+%), water (Aldrich, HPLC grade), isopropanol (Aldrich, HPLC grade, 99.5 %), tertiary butyl alcohol (Aldrich, HPLC grade, 99%), 4-methoxybenzyl alcohol (Aldrich, 98%), 4-nitrobenzyl alcohol (Pfaltz and Bauer Inc.), 4-chlorobenzyl alcohol (Acros, 99%), benzophenone hydrazone (Aldrich, 96%), Mercury (II) Oxide, yellow (Aldrich, 99+%), hexanes (Fischer, HPLC grade, 99.9+%) and carbon dioxide (Matheson, SFC grade).

Apparatus and Procedures

Diazodiphenylmethane (DDM) Synthesis

Diazodiphenylmethane was synthesized following a slightly modified procedure from the literature (Smith and Howard 1944). A molar ratio of 6:1 of mercury oxide to benzophenone hydrazone was dissolved in hexane and stirred in an Erlenmeyer flask which was placed in a water bath for around four hours. The resulting red colored solution was filtered and concentrated. Because the analysis of the DDM reaction does

not require knowledge of purity, no further purification from the starting materials was required.

DDM Reaction Apparatus

All reactions of diazodiphenylmethane were carried out in a machined pressure cell (316 stainless steel) with three sapphire windows. Temperature was controlled with a heating/cooling tunnel bored through the cell with water flowing from a heated water bath (Thermo NESLAB RTE-740). Agitation was from a magnetic stir bar controlled to 500 rpm \pm 5 by controller (H+P Labortechnik AG Telemodul 20C). The temperature of the cell was measured to within \pm 0.1°C using type K thermocouples (Omega) calibrated in a water bath (ThermoNESLAB RTE-740) with digital temperature indicators (Omega). The pressure of the reactor was measured \pm 0.07bar with a pressure transducer (Druck Limited, DPI 260 readout, PDCR-4010 transducer) calibrated against a hydraulic deadweight tester (Ruska).

DDM Reaction Procedure

For rate comparison between alcohols, 0.024 mol of alcohol was added to 0.073 mol of acetone and ~25mg of diazodiphenyl methane previously synthesized. The mixture was then heated to 40.0°C and then 0.024 mol of CO₂ was added by a syringe pump (ISCO 500D). The reactor was then placed in an ultraviolet-visible spectrometer (UV-Vis, Hewlett-Packard 8453) and absorbance of DDM was taken periodically. The resulting liquid phase was analyzed using a gas chromatograph (GC, Hewlett-Packard

6890) with a mass selective detector (MS, Hewlett-Packard 5973). The MS was used for compound identification and product ratio quantification.

DDM Hammett Plot Procedure

For Hammett plot runs, 5.4 mmol of alcohol was added to 0.092 mol of acetone and 25mg of DDM in the same reactor and again heated to 40.0°C. Then 9.8 mmol of CO₂ were added and the same analysis as previous was carried out. For rate versus pressure runs, 5.0mL methanol was added to 25mg of DDM in the same reactor vessel and heated to 40.0°C. Various amounts of CO₂ were added via syringe pump and analysis was done the same.

Dielectric Constant Measurement Procedure

A custom concentric cylinder dielectric probe was constructed out of stainless steel and shown in Figure 2-1. The inner cylinder has a diameter of 1.750” and the outer cylinder has a diameter of 2.000”. Both cylinders are 0.900” tall and are connected via Teflon screws through tapped holes. Thus the geometry of the probe is set. Standard stainless steel screws attach a solid stainless steel wire to the circuit and provide the support for the probe. The wires are insulated with Teflon tubing inside of the reactor. The steel wire passes through a PEEK pipe fitting and a PEEK ferrule and nut out of the vessel and then is connected to a Hewlett Packard LCR model 4284A via alligator clips. All parts are listed in Table 2-1 with part numbers and manufacturer. The probe is suspended in a 300mL Parr model 4560 pressure vessel with windows and overhead

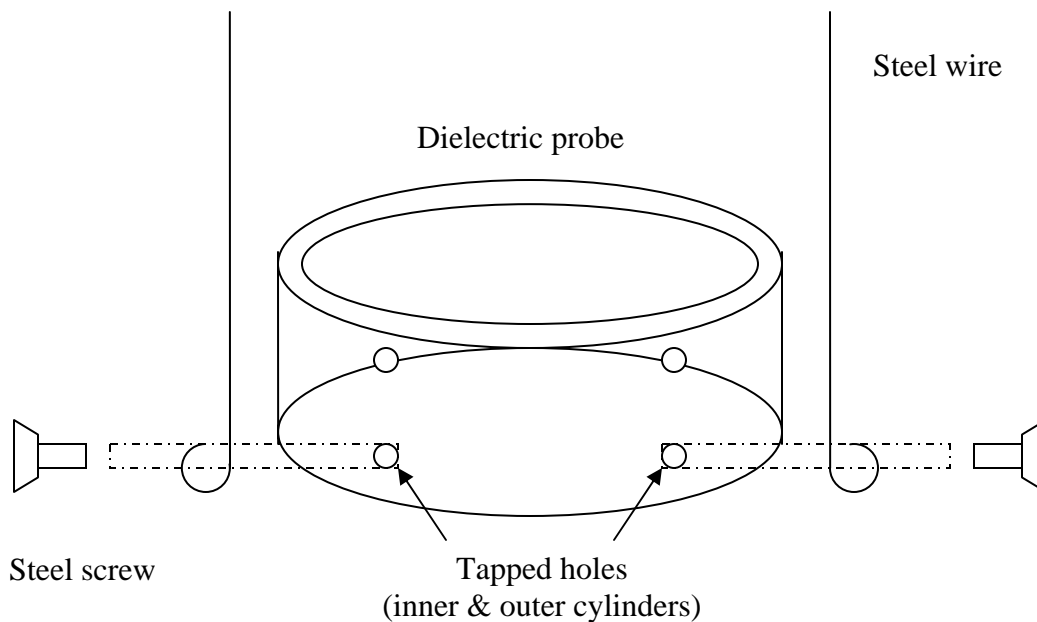


Figure 2-1: Diagram of Dielectric probe and wires

Table 2-1: Parts and manufacturer for dielectric cell construction

Part	Manufacturer	Part Number
PEEK pipe adapter fitting (bored from .062" to .060")	Valco Instruments Co Inc	CPA2PK
PEEK nut & ferrule kit	Valco Instruments Co Inc	CFL1PK (CFL-CB1PK for ferrules only)
Teflon tubing (bored from 0.062" to 0.060")	Valco Instruments Co Inc	TTF260-10
Stainless steel wire (1/16" x 36", 10 lbs)	Linde gas	620084
Teflon screws (8-32 x 1/2")	McMaster Carr	94701A194
Steel screws (8-32 x 3/16")	McMaster Carr	91773A189

stirring. The temperature was regulated to within 1°C of the set point using the accompanying Parr 4842 controller.

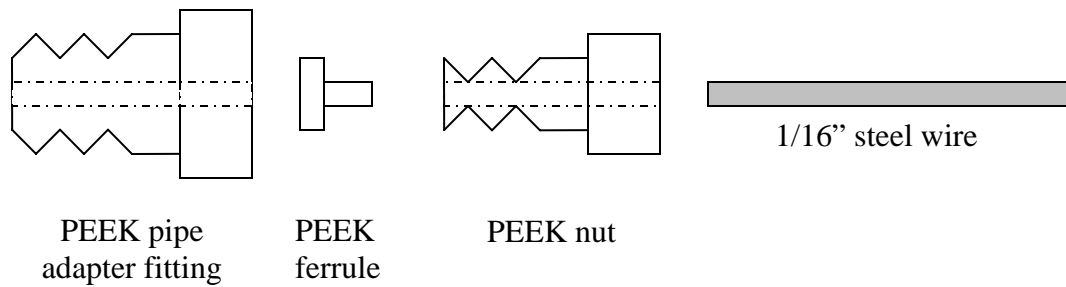


Figure 2-2: High pressure pass through for steel wire

The capacitance is then recorded at 10 kHz and 1 MHz and used to calculate the dielectric constant using equation 2-1. In Equation 1, C is capacitance, ϵ is the dielectric constant being calculated, L is the length of the cylinder, k_e is Coulomb's constant and is equal to $8.99 \times 10^9 \text{ N m}^2 \text{ C}^{-2}$, R_2 is the radius of the outer cylinder and R_1 is the radius of the inner cylinder.

$$C = \frac{\epsilon L}{2k_e \ln \frac{R_2}{R_1}}$$

Equation 2-1: Dielectric constant calculation based on capacitance and geometry.

Several fluids were tested at atmospheric conditions prior to use under pressure. Water, methanol, acetone, and tetrahydrofuran were all tested at ambient temperature and pressure and gave values within 2% of their literature values. All measurements were done with sufficient volume to ensure that the entire probe was covered with liquid. A windowed vessel was employed at high pressures to confirm this visually. The mole fraction of CO₂ in the liquid phase was calculated from the measured pressure and interpolating the VLE data of Chang(Chang, Kou-Lung et al. 1998).

Results and Discussion

Since alkylcarbonic acids are not isolable at standard conditions, DDM was used as a reactive probe molecule which not only gives a relative reaction rate based on acid strength, but also traps the acid species as shown in Figure 2-3. By dissolving DDM in 60 mol% acetone, 20 mol% alcohol, and 20 mol% CO₂ in a pressure vessel one can compare the relative rates of various alkylcarbonic acids. Since the DDM is very dilute and the amount of actual acid formed is large but not measurable, a pseudo-first order rate constant was calculated. Figure 2-4 shows a typical UV-vis spectrum for this reaction at various times. Figure 2-4 shows a typical fit for these reactions for the $\ln(1/(1-X))$, with X being conversion, versus the time which should yield a straight line with the slope being the pseudo-first order rate constant. These results found that the fastest rate was for ethylene glycol while methanol and propylene glycol had very similar rates (see Figure 2-6). The trend from ethylene glycol to propylene glycol agrees with the trend from methanol to tertiary butanol of increasing alkyl chain length and

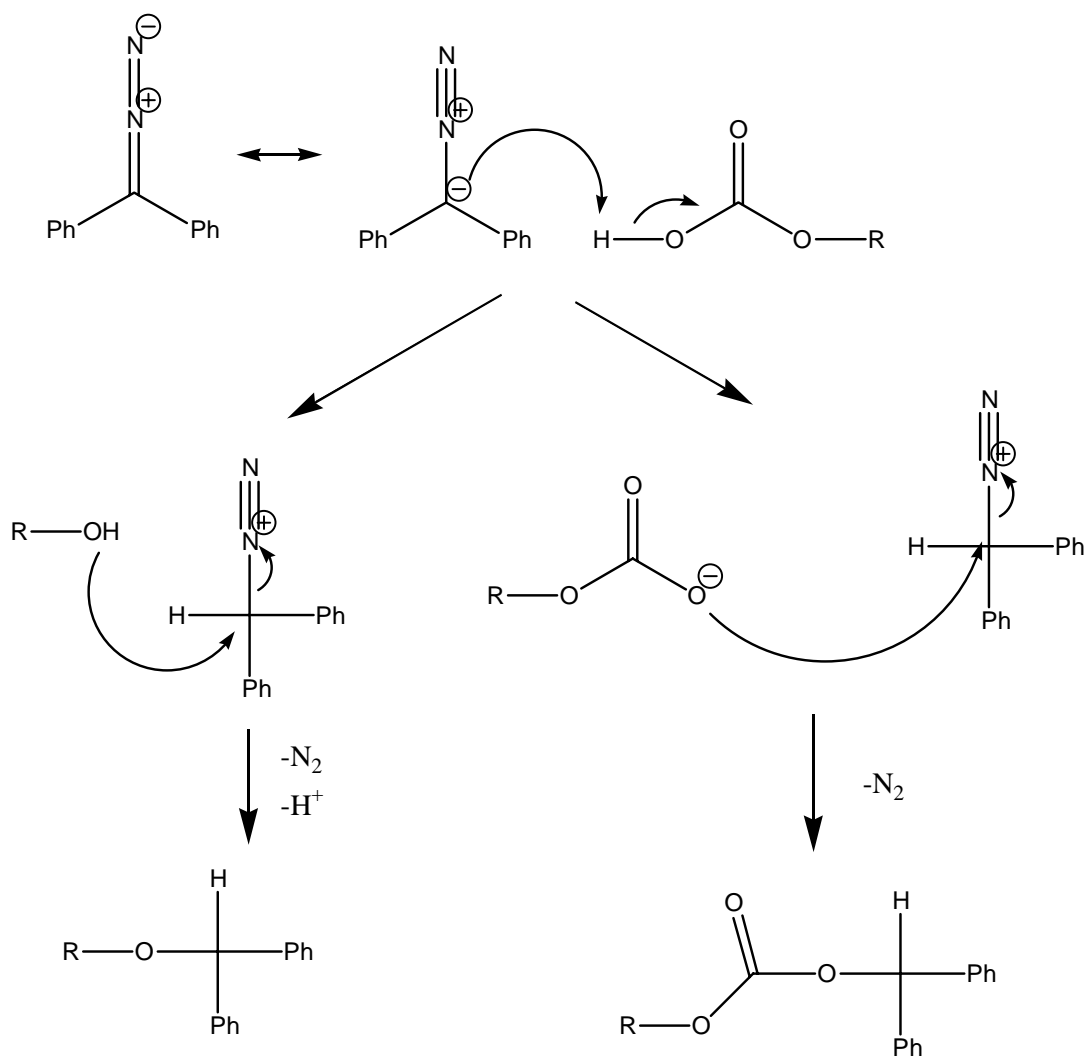


Figure 2-3: Mechanism for the reaction of DDM with an alkylcarboxylic acid forming an ether and a carbonate.

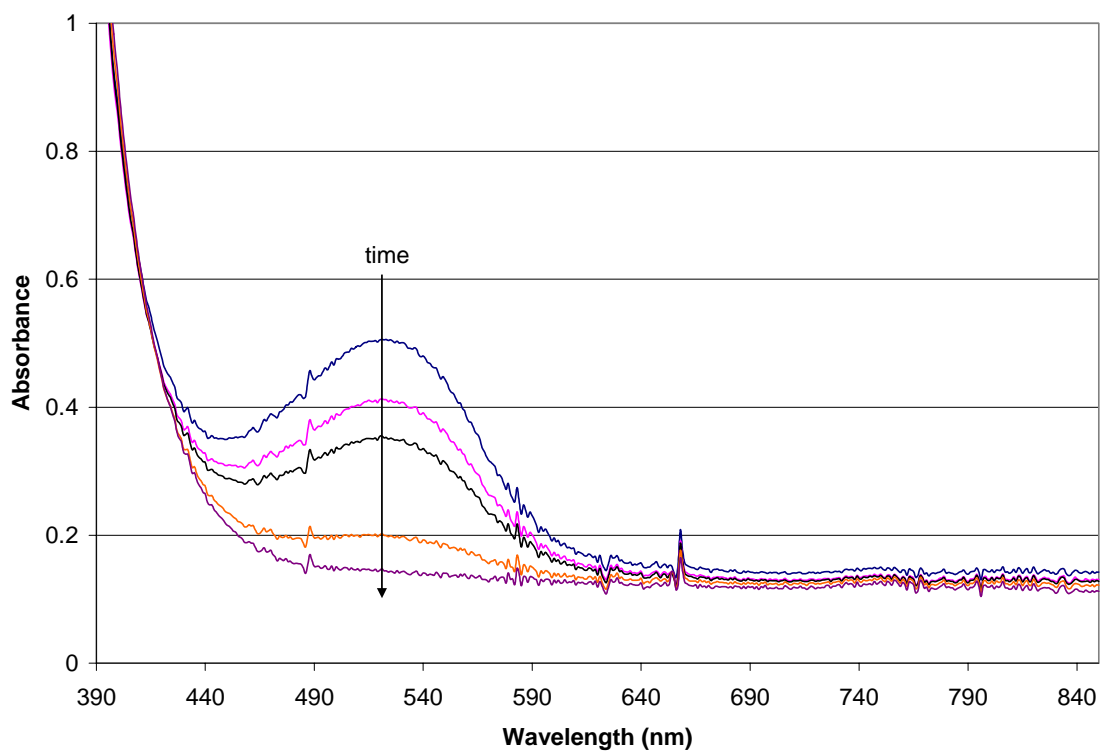


Figure 2-4: Typical UV-vis spectrum of decreasing DDM absorbance as a function of time.

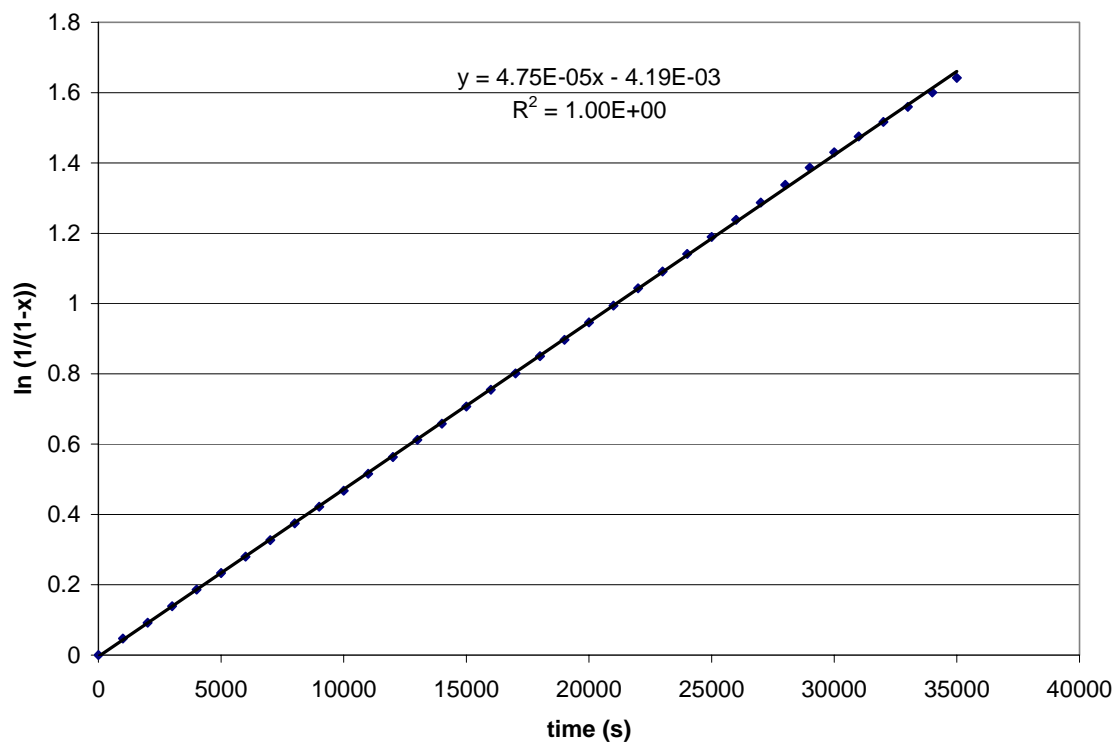


Figure 2-5: Pseudo-first order fit for 20 mol % ethylene glycol, 20 mol % CO₂, 60 mol % acetone.

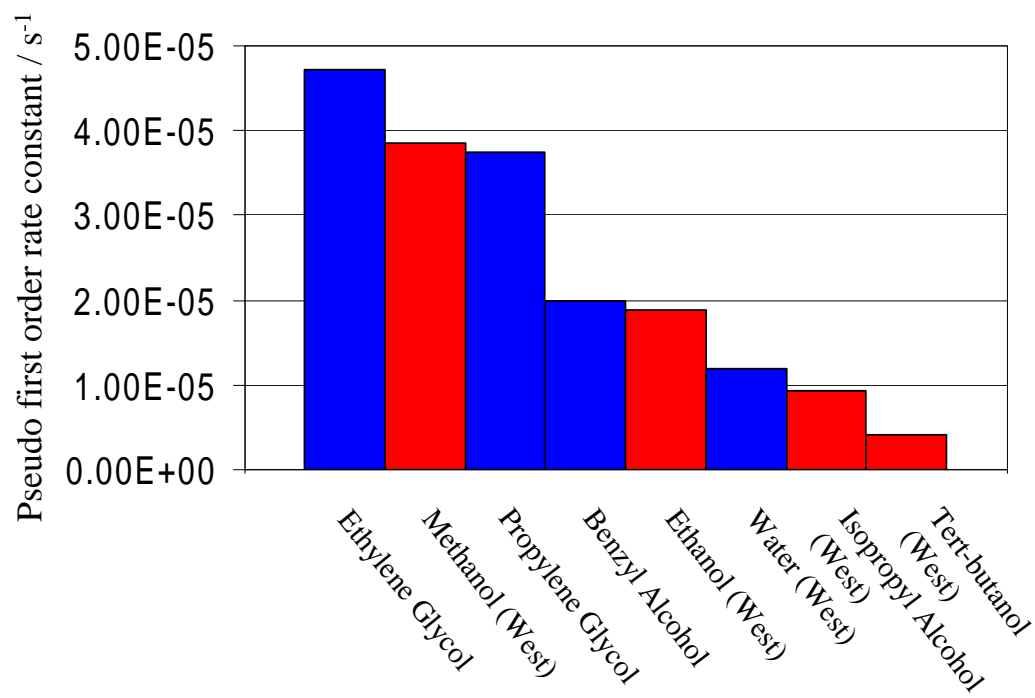


Figure 2-6: Pseudo-first order rate constants for various alcohols at 20 mol % alcohol, 20 mol % CO₂, and 60 mol % acetone at 40°C.

decreasing rate. This decreasing rate agrees with the trend of decreasing basicity and nucleophilicity of the oxygen in the alcohol. However, the ethylene glycol is significantly faster than ethanol. One possible explanation is that the second alcohol group helps stabilize the alkylcarbonic acid through hydrogen bonding.

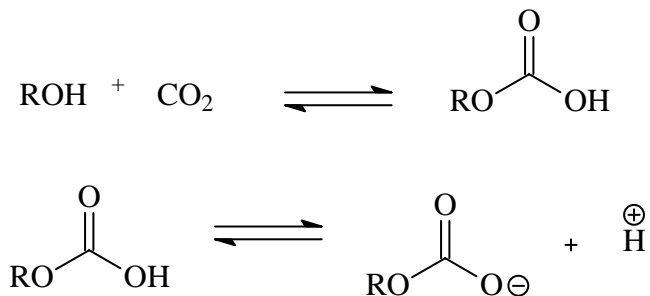


Figure 2-7: Two separate steps required for alkylcarbonic acid catalysis. Step 1: formation of acid from alcohol and CO₂. Step 2: Dissociation of proton from alkylcarbonic acid.

To investigate further the rates of alkylcarbonic acids, a series of experiments were run without the acetone diluent. Pure methanol was run at a range of pressures as shown in Figure 2-8. A maximum rate is observed at 60 bar of CO₂ pressure. The presence of a maximum means there are at least two counteracting effects. Figure 2-7 demonstrates these two effects. The first is the addition of CO₂ pressure drives the first equilibrium to form the acid. The second effect is the drop in polarity of the solvent with increasing concentration of CO₂ in the solvent thus hindering the dissociation of a proton from the acid. This second effect is seen in the dielectric constant also in Figure 2-8. The maximum rate is also 3 orders of magnitude faster than the rate without any CO₂ pressure. Figure 2-8 also includes the volume expansion of the solvent which could have

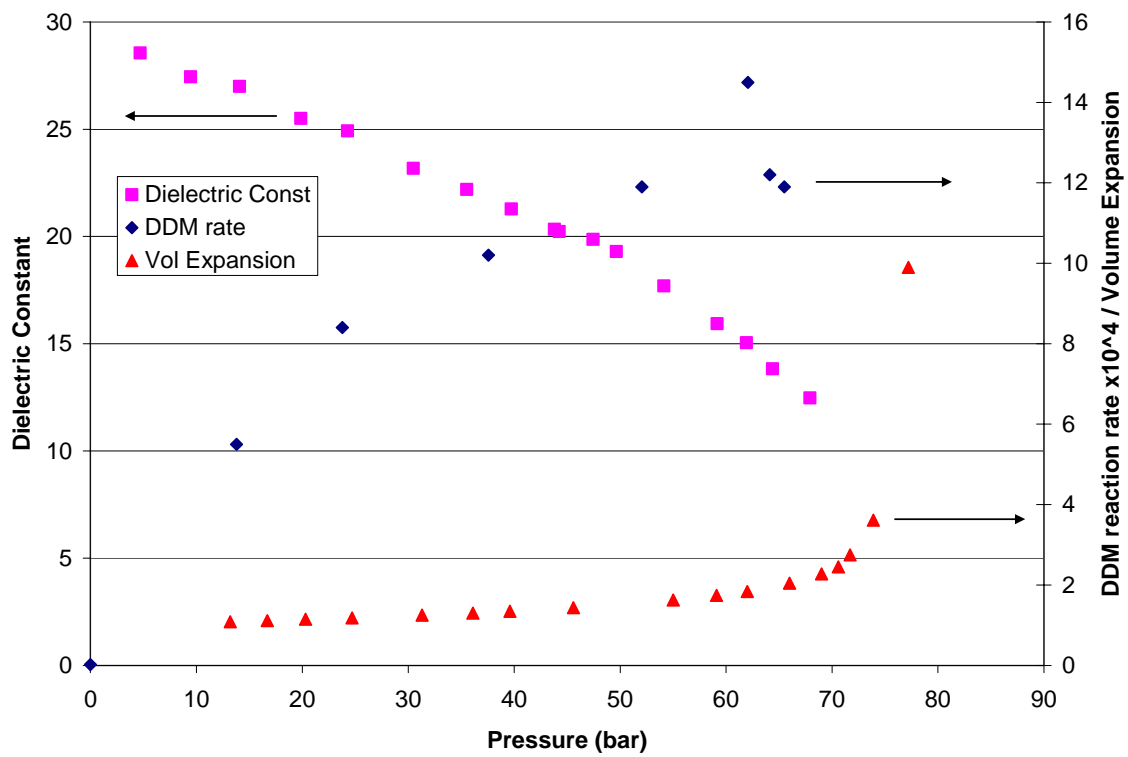


Figure 2-8: Methanol-CO₂ at 40°C: DDM reaction rate x 10⁴ (diamonds), dielectric constant at 1 MHz (squares), and volume expansion (triangles).

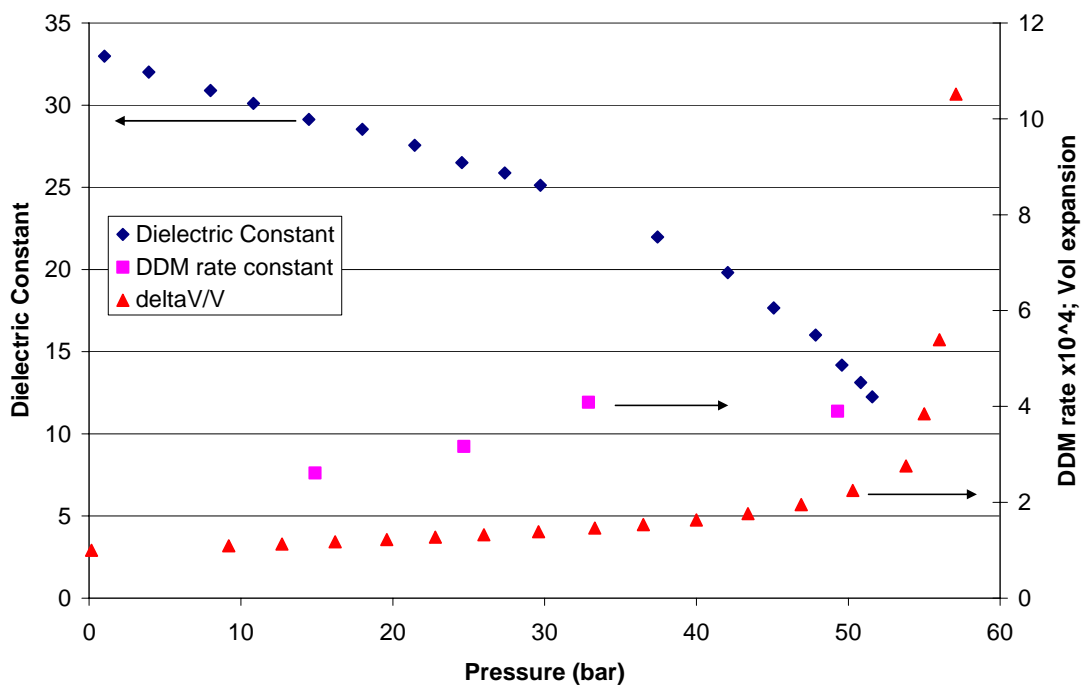


Figure 2-9: Methanol-CO₂ at 23°C: DDM reaction rate x 10⁴ (squares), dielectric constant at 1 MHz (diamonds), and volume expansion (triangles).

been a possible explanation of the decreased reaction rate but the expansion changes little until at least 70 bar of CO₂ pressure.

Figure 2-9 shows a similar plot for the same system at 23°C rather than 40°C. Qualitatively the same behavior is observed. There seems to be a maximum or plateau in the DDM reaction rate, in this case at a pressure near 45 bar. This is a pressure below the point where the volume expands quickly and where the dielectric constant is dropping quickly.

The dielectric constant was also measured as a function of mole fraction for both 23 and 40°C. These results are presented in Figures 2-10 and 2-11. Similar behavior is seen in both cases where the dielectric constant drops below the straight line between the pure components. This indicates that the CO₂ is breaking up the hydrogen bonding network and making the solvent less supportive of ions more than other nonpolar solvents such as hexane. The values above 0.5 mol % CO₂ are difficult to measure because of the volume expansion of the solvent. These values were also not important to this body of research.

Benzyl alcohol also has a moderate rate. The presence of the phenyl ring allowed for the possibility of studying electronic effects with a Hammett plot. The alcohols 4-nitro-, 4-chloro-, and 4-methoxy- benzyl alcohols (see Figure 2-12) were chosen in addition to benzyl alcohol and all were run in duplicate. These alcohols corresponding Hammett σ values are 0.78, 0.23, -0.27, and 0. Due to the substituted alcohols being solids at room temperature and the overlapping of UV absorbance with DDM at high concentrations, all runs were done with an overall loading of 85 mol% acetone, 5 mol% alcohol, and 10 mol% CO₂.

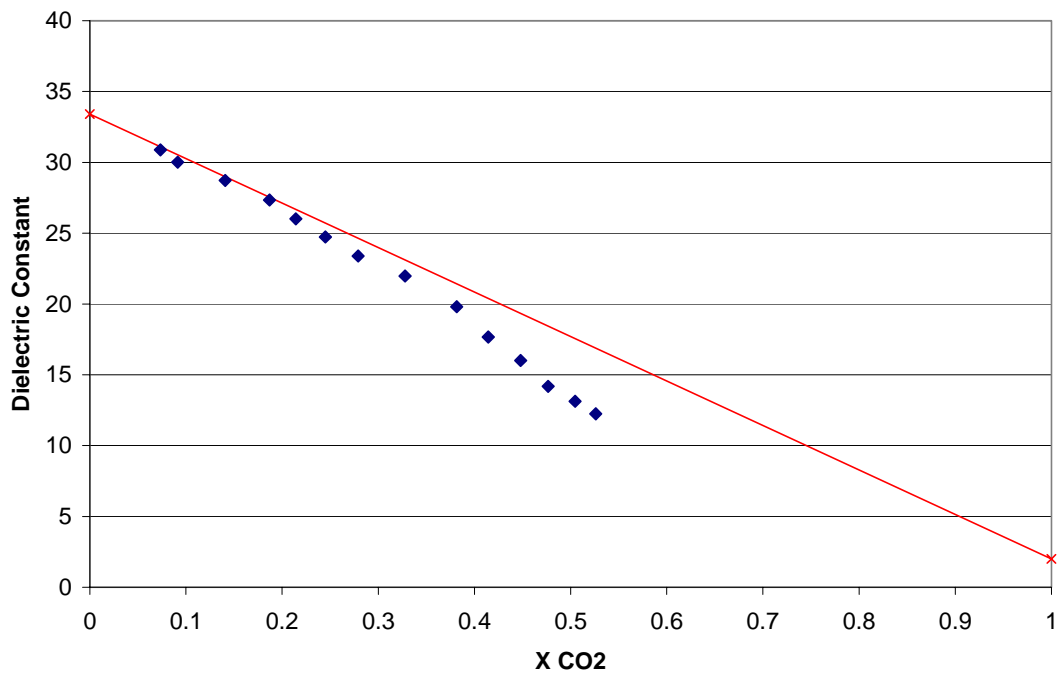


Figure 2-10: Dielectric constant of methanol-CO₂ mixture versus mol fraction CO₂ at 23°C (diamonds) and literature data (squares) with linear interpolation of literature data (line).

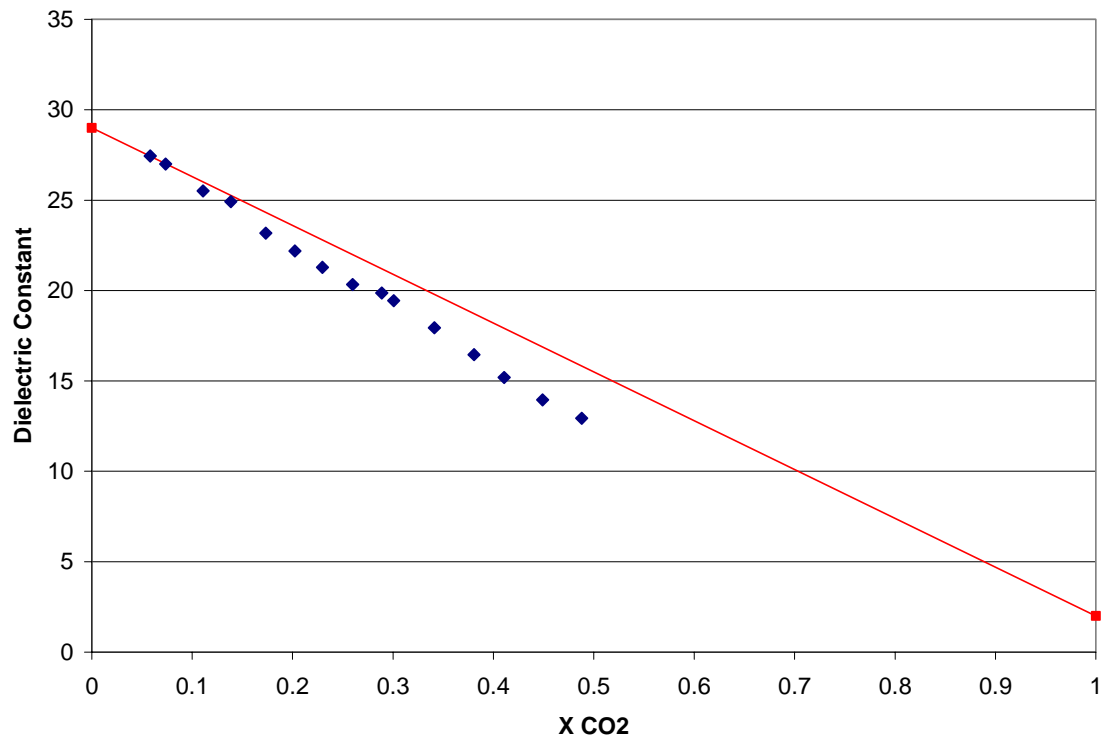


Figure 2-11: Dielectric constant of methanol-CO₂ mixture versus mol fraction CO₂ at 40°C (diamonds) and literature data (squares) with linear interpolation of literature data (line).

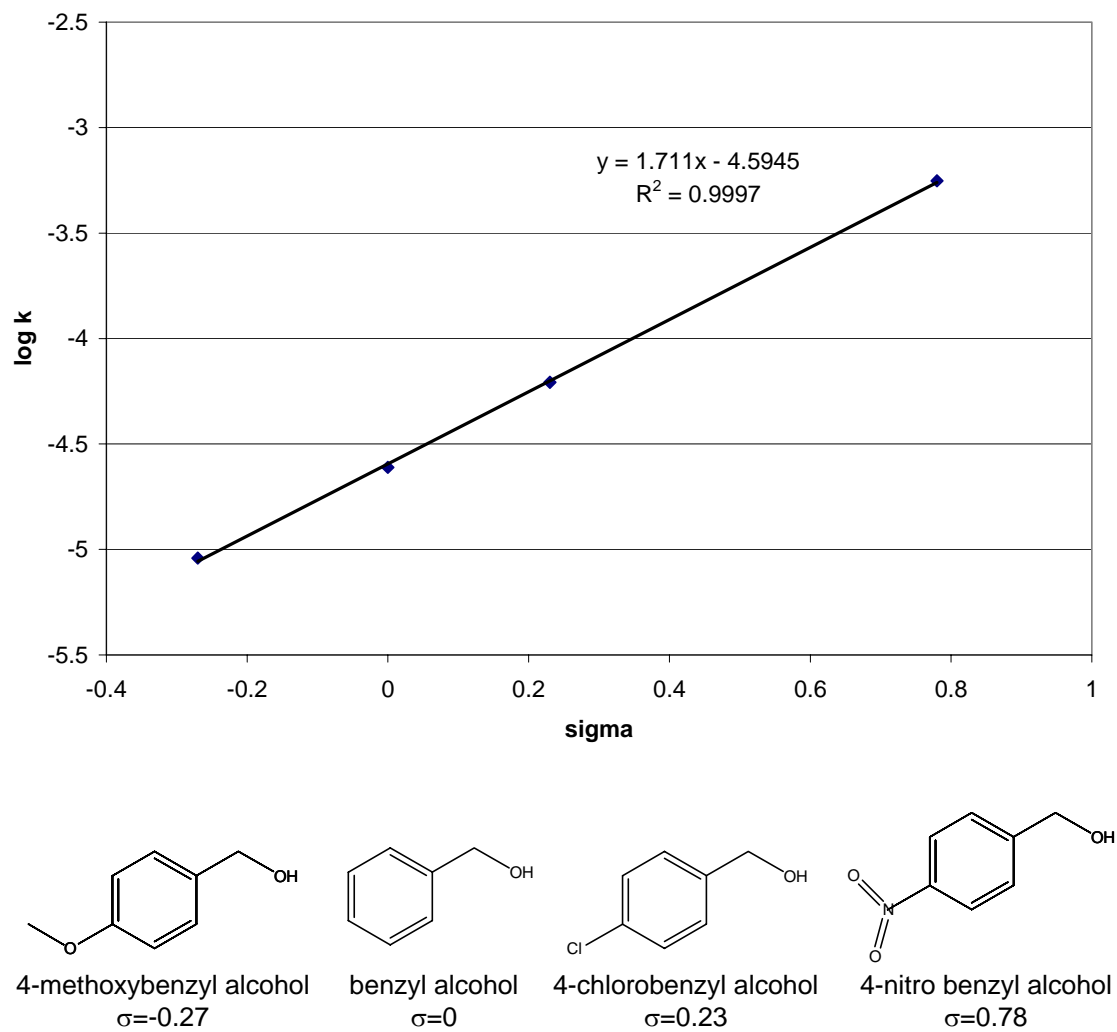


Figure 2-12: Hammett Plot of para substituted benzyl alcohol alkylcarboxylic acid reaction with DDM at 40°C.

$$\log \frac{k_x}{k_0} = \rho\sigma$$

Equation 2-1: Hammett equation for a reaction

The results of the Hammett plot are seen in Figure 2-12. An excellent linear fit was found with a ρ of 1.71 according to the Hammett equation (Equation 2-1) where k_x is the rate of disappearance of DDM, σ is a constant based on electron withdrawing/donating ability, and ρ is the reaction sensitivity. Since all rates are divided by the same k_0 , it is not necessary to find this value. The value ρ value of 1.71 is very similar to the ρ value of 1.93 for DDM and benzoic acid in acetone at 30°C (Buckley, Chapman et al. 1968). A high ρ means that the reaction is very sensitive to electronic effects. Since the fastest rate occurred with the highly electron withdrawing nitro substitution, this means that the second step in scheme 1 is most affected by electronic effects. This is because the first step is nucleophilic attack of the carbon in CO_2 which should be increased by an electron donating group and conversely decreased by an electron withdrawing group. The second step of proton dissociation should be increased by electron withdrawing group and decreased with electron donating group. The fact that benzoic acid, which must only undergo the second step (proton dissociation) has a similar ρ value, is consistent with the hypothesis that the acid formation step for alkylcarbonic acids is not limiting. The Hammett plot also shows a two order of magnitude difference between the most electron withdrawing and the most electron donating groups so clearly, the dissociation of the proton is greatly affected by electronics.

Conclusions

Alkylcarbonic acids are further demonstrated as useful environmentally benign acids. Several new alcohols are used to further demonstrate the wide ranging applicability of the concept. A comparison of the rate of reaction of DDM with the acid versus pressure gives indication of where the maximum in rate may occur. The dielectric constant of CO₂ expanded methanol was also measured to explain the presence of the maximum. The dielectric constant in conjunction with volume expansion data proves the solvent eventually loses the ability to support ions as CO₂ concentration increases. A Hammett plot of the reaction of DDM with a series of benzyl alcohol alkylcarbonic acids gives a ρ of 1.7 which proves that the acidity of the alkylcarbonic acid formed is more important than the nucleophilicity of the alcohol.

References

- Blanchard, L. A. and J. F. Brennecke (2001). "Esterification of Acetic Acid with Ethanol in Carbon Dioxide." Green Chem. **3**(1): 17.
- Buckley, A., N. B. Chapman, et al. (1968). "The Separation of Polar and Steric Effects. Part VIII. The Influence of the Solvent on the Kinetics of the Reactions of Benzoic Acid and meta- or para-Substituted Benzoic Acids with Diazodiphenylmethane." J. Chem. Soc. B **2**: 631.
- Chamblee, T. S., R. R. Weikel, et al. (2004). "Reversible *in situ* acid formation from β -pinene hydrolysis using CO₂ expanded liquid and hot water." Green Chem. **6**.
- Chang, C. J., C. Kou-Lung, et al. (1998). "A new apparatus for the determination of P-x-y diagrams and Henry's constants in high pressure alcohols with critical carbon dioxide." J. Supercrit. Fluids **12**(3): 223.
- Chang, C. J. and A. D. Randolph (1990). "Solvent Expansion and Solute Solubility Prediction in Gas Expanded Liquids." AIChE J. **36**(6): 939.
- Dombro, R. A., M. A. McHugh, et al. (1991). "Dielectric Constant Behavior of Carbon Dioxide-Methanol Mixtures in the Mixture-Critical and Liquid-Phase Regions." Fluid Phase Equilibria **61**: 227.
- Eckert, C. A., D. Bush, et al. (2000). "Tuning Solvents for Sustainable Technology." Ind. Eng. Chem. Res. **39**: 4615.
- Eckert, C. A. and K. Chandler (1998). "Tuning Fluid Solvents for Chemical Reactions." J. Supercrit. Fluids **13**(1-3): 187.
- Eckert, C. A., B. L. Knutson, et al. (1996). "Supercritical Fluids as Solvents for Chemical and Materials Processing." Nature **383**: 313.
- Eissen, M. and J. O. Metzger (2002). "Environmental Performance Metrics for Daily Use in Synthetic Chemistry." Chem. Eur. J. **8**(16): 3580.
- Golfarb, D. L., D. P. Fernandez, et al. (1999). "Dielectric and volumetric properties of supercritical carbon dioxide(1) + methanol(2) mixtures at 323.15 K." Fluid Phase Equilibria **158-160**: 1011.
- Hine, J. and W. C. Bailey Jr. (1959). "A Hammett Equation Correlation for trans-3-Substituted Acrylic Acids." J. Am. Chem. Soc. **81**: 2075.
- Hulme, C., L. Ma, et al. (2000). "Novel applications of carbon dioxide/MeOH for the synthesis of hydantions and cyclic ureas via the Ugi reaction." Tetrahedron Lett. **41**: 1889.

- Keating, T. A. and R. W. Armstrong (1998). "The Ugi Five-Component Condensation Using CO₂, CS₂, and COS as Oxidized Carbon Sources." J. Org. Chem. **63**: 867.
- Lee, S. B., R. L. Smith, et al. (2000). "Coaxial probe and apparatus for measuring the dielectric spectra of high pressure liquids and supercritical fluid mixtures." Review of Scientific Instruments **71**(11): 4226.
- Lin, C., G. Muhrer, et al. (2003). "Vapor-liquid mass transfer during gas antisolvent recrystallization: Modeling and experiments." Ind. Eng. Chem. Res. **42**(10): 2171.
- Musie, G. T., M. Wei, et al. (2001). "Catalytic Oxidations in Carbon Dioxide-based Reaction Media, Including Novel CO₂-expanded Phases." Coor. Chem. Rev. **219-221**: 789.
- Roberts, J. D. and C. Regan, McG. (1952). "Analysis of Mixtures of Carboxylic Acids." Anal. Chem. **24**(2): 360.
- Roberts, J. D. and W. Watanabe (1950). "The Kinetics and Mechanism of the Acid-Catalyzed Reaction of Diphenyldiazomethane with Ethyl Alcohol." J. Am. Chem. Soc. **72**(11): 4869.
- Roskar, V., R. A. Dombro, et al. (1992). "Comparison of the dielectric behavior of mixtures of methanol with carbon dioxide and ethane in the mixture-critical and liquid regions." Fluid Phase Equilibria **77**: 241.
- Smith, L. I. and K. L. Howard (1944). "Diazodiphenylmethane." Organic Synthesis **3**: 351.
- Wei, M., G. T. Musie, et al. (2001). "CO₂-expanded Solvents: Unique and Versatile Media for Performing Homogeneous Catalytic Oxidations." J. Am. Chem. Soc. **124**: 2513.
- West, K. N., C. Wheeler, et al. (2001). "In Situ Formation of Alkylcarbonic Acid with CO₂." J. Phys. Chem. A **105**: 3947.
- Xie, X., J. S. Brown, et al. (2002). "Phase-transfer catalyst separation by CO₂ enhanced aqueous extraction." Chem. Commun.: 1156.
- Xie, X., C. L. Liotta, et al. (2004). "CO₂-Catalyzed Acetal Formation in CO₂-Expanded Methanol and Ethylene Glycol." Industrial and Engineering Chemistry Research **43**: 2605.
- Zhao, J. and S. V. Olesik (2001). "Separation of dimer acids using enhanced-fluidity liquid chromatography." Anal. Chim. Acta **449**: 221.

CHAPTER III

SELF NEUTRALIZING IN SITU ACID CATALYSIS FOR SINGLE POT SYNTHESIS OF ARYL HALIDES AND AZO DYES IN GAS-EXPANDED LIQUIDS

Introduction

Despite widespread use, homogeneous acid catalysis has the drawback requiring downstream neutralization resulting in salt waste. Methylcarbonic acid is a self-neutralizing acid which forms *in situ* in methanol-CO₂ systems and decomposes by depressurization. In the work presented here, methylcarbonic acid catalyzes the diazotization of aniline which is either coupled with N,N-dimethyl aniline to form methyl yellow or reacted with iodide to form iodobenzene. The synthesis of methyl yellow and iodobenzene represent a class of industrially important reactions.

The diazotization of aniline and aniline derivatives is a useful reaction for a wide range of products as shown in Figure 3-1. The vast majority of all processes use a strong acid such as HCl or H₂SO₄ to promote the diazotization reaction (Leverenz 1981; Hartmann and Zug 2000; Heemestra and Moore 2004). At the end of the reaction, base must be added to neutralize the acid. This results in salts which must be removed from the process stream and treated as toxic waste.

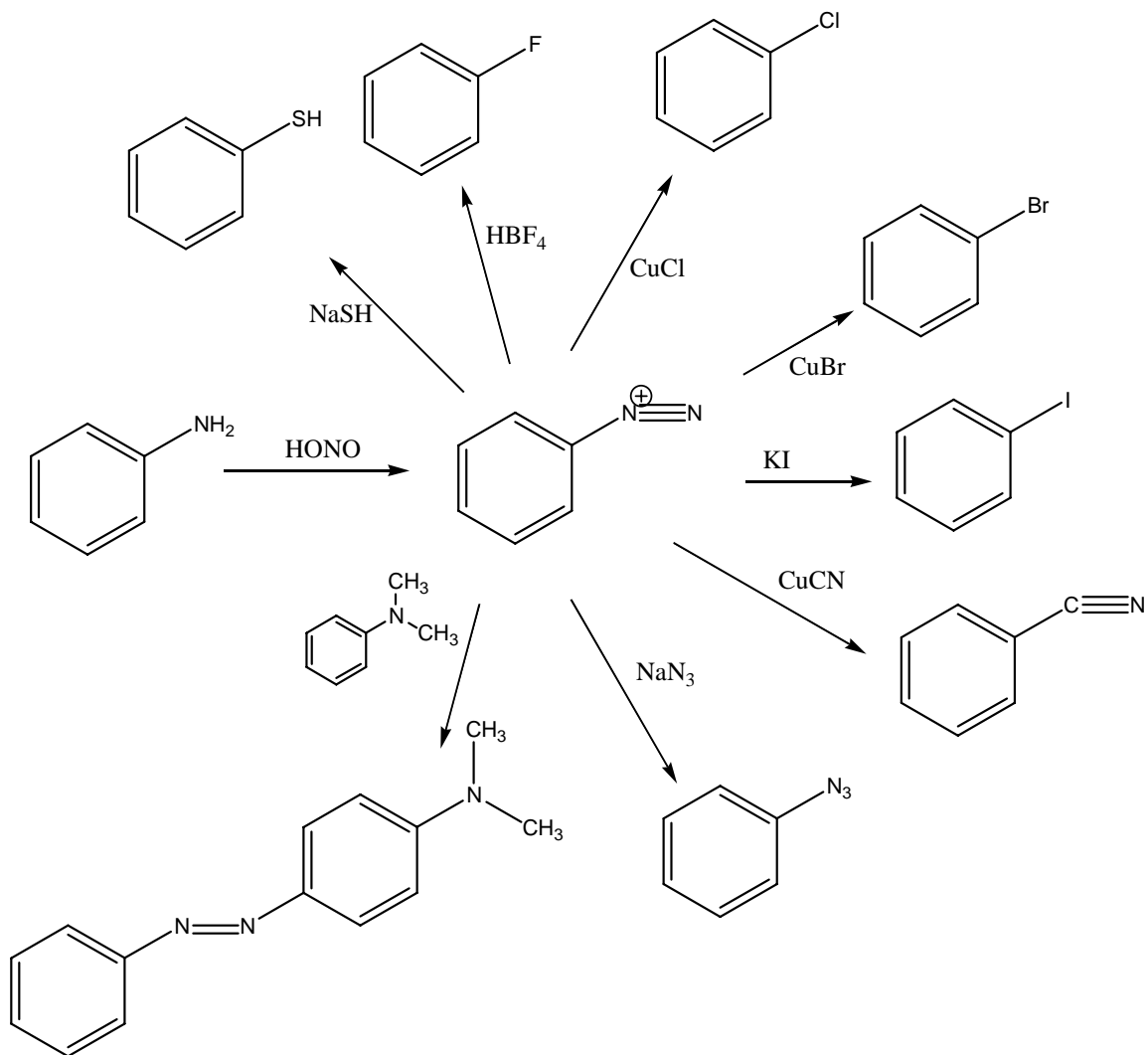


Figure 3-1: Possible synthetic products from the diazonium cation.

The strong acid used in the diazotization reacts with a nitrite to form nitrous acid *in situ*. Then, nitrous acid releases the active species, nitrosyl cation, which reacts with the amine to form the diazonium cation through several steps. Recent research has looked into using NO directly as a gas (Itoh, Nagata et al. 1997) or as NOCl (Kaupp, Herrmann et al. 2002) but these methods have not gained industrial acceptance. Generally, after the diazonium ion is formed there are two possible outcomes. Either there is substitution or a coupling with an activated arene. The first group is represented in this paper by the synthesis of iodobenzene and the latter by synthesis of methyl yellow (N,N-dimethyl-4-aminoazobenzene).

The coupling of diazonium salts with activated arenes is of significant industrial importance. The activated arenes include dialkylaniline and phenol derivatives to produce a wide variety of azo products. The resulting azo products are commonly used for dyeing in textiles (Hooker, Hinks et al. 2002; Bahulayan, John et al. 2003) and inks for jet printing (Heinz 2002). The textile industry has recently faced pressure to reduce the amount of electrolytes and colored wastewater released into the environment thus there has been research into ways to alleviate these concerns. These ideas include using ion exchange resins (Wolff, Wolf et al. 1988), running solid-solid reactions (Kaupp, Herrmann et al. 2002), running the reaction in polyethylene glycol solvent (Suzuki, Azuma et al. 1987), supporting the diazonium ion on clays (Bahulayan, John et al. 2003), polymers (Calderelli, Baxendale et al. 2000), or resins (Merrington, James et al. 2000), or using carbonic acid from water and CO₂ for catalysis (Raue, Brack et al. 1996; Raue, Lange et al. 1996; Hooker, Hinks et al. 2002).

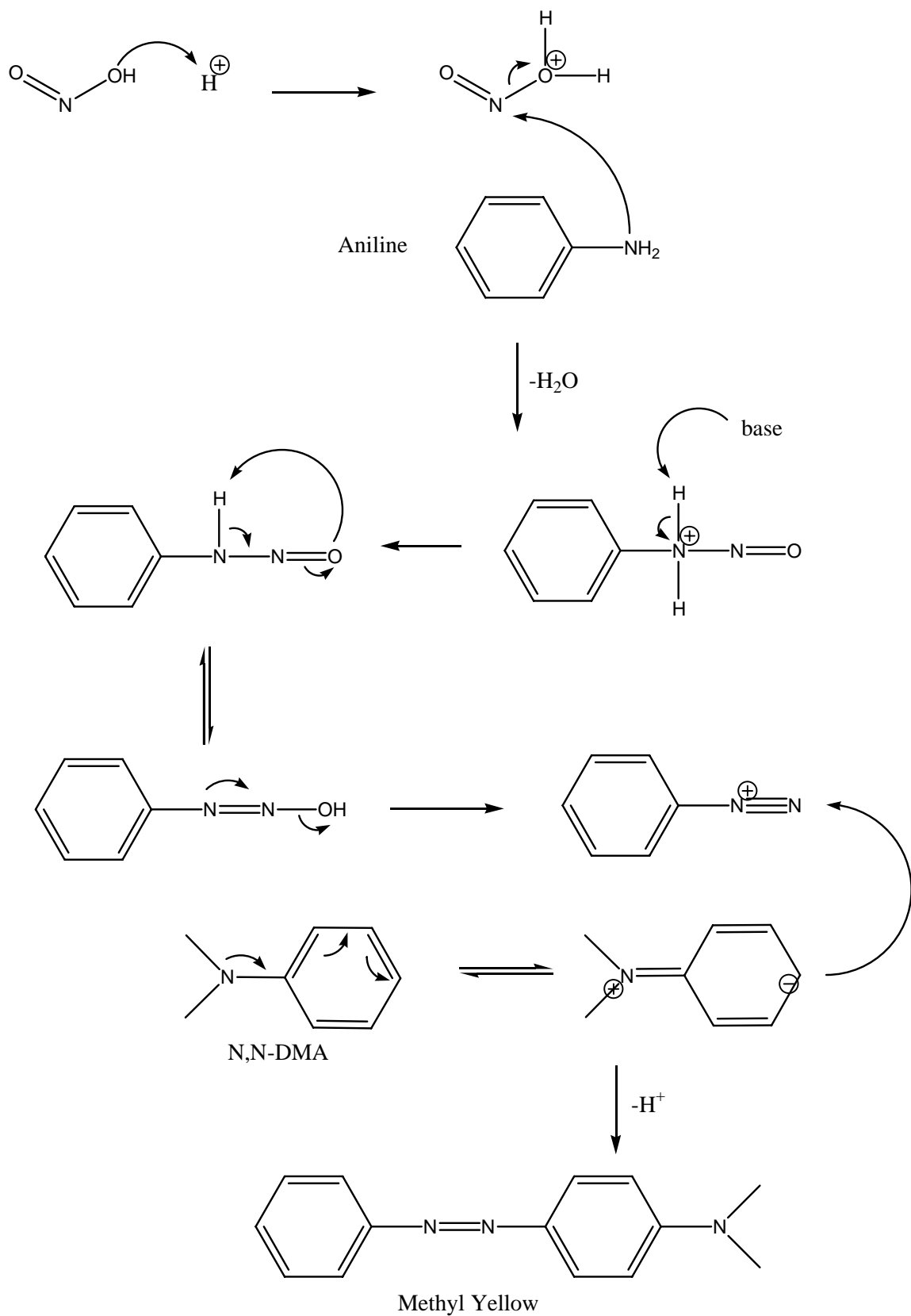


Figure 3-2: Mechanism for the formation of methyl yellow from aniline and nitrous acid

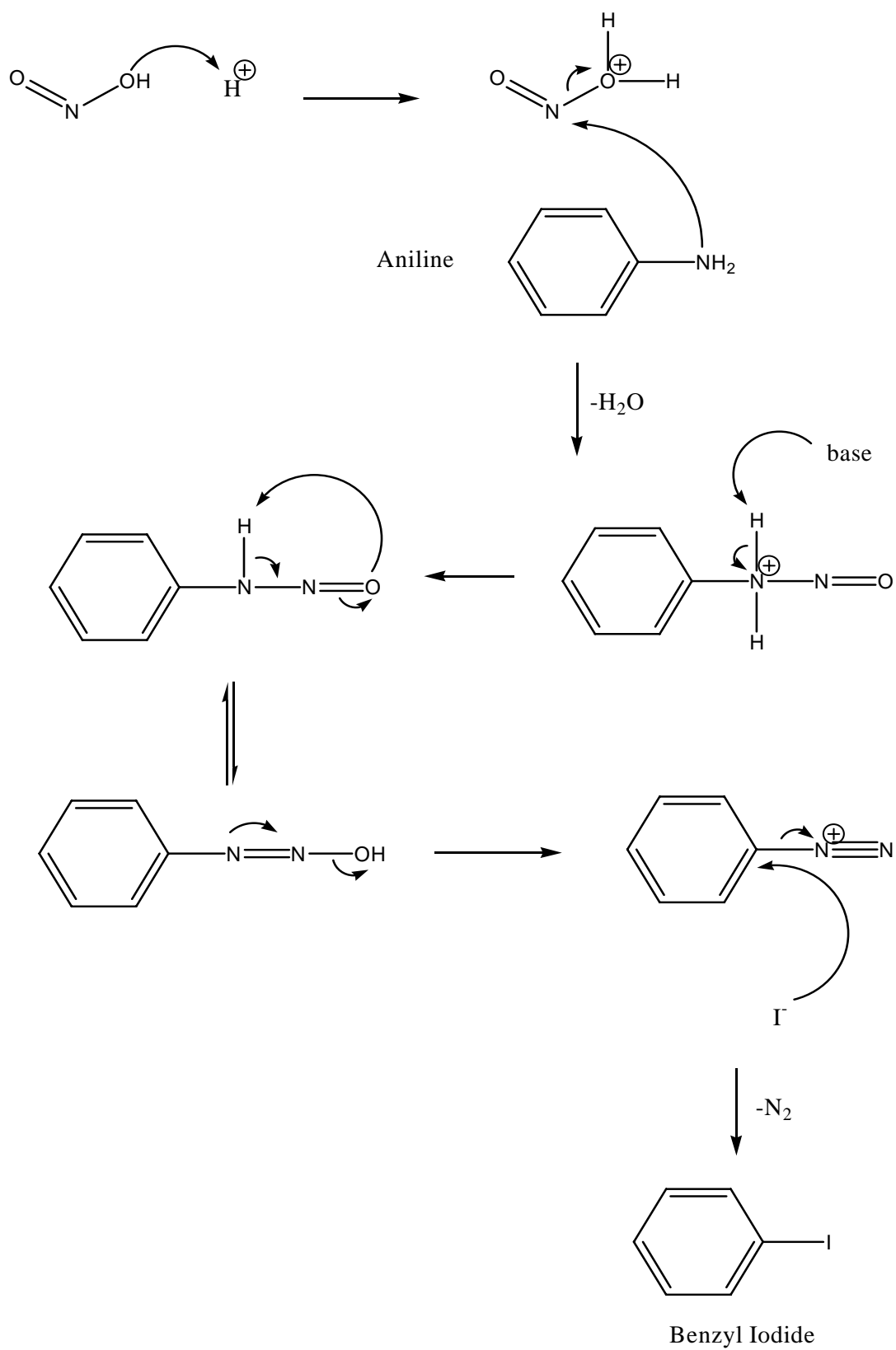


Figure 3-3: Mechanism for the formation of benzyl iodide from aniline and nitrous acid

The reaction of diazonium salts to form chlorobenzene, bromobenzene, benzonitrile is catalyzed by copper salts whereas the other substitution reactions (Figure 3-1) take place simply with alkali metal salts of the nucleophilic anion. In particular, in the case of iodobenzene, only an iodide salt (generally sodium or potassium iodide) is needed to form the product from the diazonium salt.

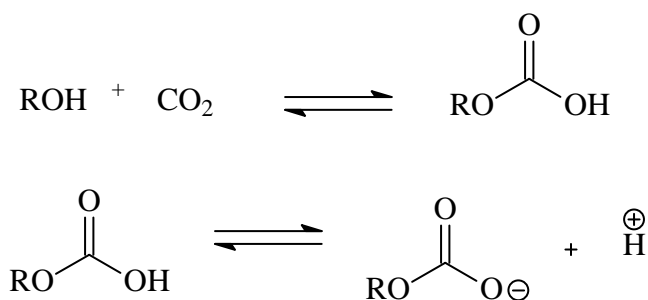


Figure 3-4: Alkylcarbonic acid formation and proton dissociation equilibriums

The work reported here proposes the use of methylcarbonic acid from methanol and CO₂ (Figure 3-4) to catalyze the synthesis of the diazonium cation. The use of CO₂ as a benign component of a reaction medium is well known (Eckert, Knutson et al. 1996; Eckert, Bush et al. 2000). The development of gas expanded liquids (GXLs) of CO₂ and organic solvents has also seen significant research for both reactions (Musie, Wei et al. 2001; Subramaniam, Lyon et al. 2002) and separations (Xie, Brown et al. 2002; Eckert, Liotta et al. 2004). Alkylcarbonic acids were first observed in alcohol-CO₂ GXL systems by West et al (West, Wheeler et al. 2001) and further characterized in Chapter II. Alkylcarbonic acids have been used to catalyze acetal formation (Xie, Liotta et al. 2004), hydrolysis of β-pinene (Chamblee, Weikel et al. 2004), and Ugi reactions (Hulme, Ma et al. 2000). Alkylcarbonic acids form when alcohols are in the presence of CO₂ and

naturally decompose when CO₂ is depressurized. Therefore there is no need for addition of base to neutralize the acid which eliminates the salt waste produced from acid neutralization.

Experimental Materials

All chemicals were obtained from Acros and used as purchased unless otherwise stated including: aniline (99.5%), methanol (HPLC grade, 99.93%), sodium nitrite (Sigma 99.5%), N,N-dimethyl aniline (99%), potassium iodide (Sigma 99.0%), toluene internal standard (HPLC), tetrahydrofuran (anhydrous 99.9%), 4-nitroaniline (Aldrich 99+%), N,N-diethyl aniline (Aldrich 99+%), CuBr (Aldrich 99%), CuCN (Aldrich 99%). The carbon dioxide (SFC/SFE grade) was from Airgas and was filtered prior to use.

Apparatus and Procedures

All reactions were run in a 300mL Parr model 4560 pressure vessel with windows and overhead stirring. The temperature was regulated to within 1°C of the set point using the accompanying Parr 4842 controller. The windows allowed for simple visual observation of dye formation from colorless reactants. All reactions were run for 24 hours with the following loading unless specifically noted otherwise: 140 mL methanol (3.9 mol), 0.6 mL aniline (6.5 mmol), and 1.0 g sodium nitrite (14.5 mmol). The coupling reactions had 2.5 mL of N,N-dimethyl aniline (19.6 mmol) while the halogenation reactions had 3.3 g potassium iodide (19.9 mmol). All reactants were loaded into the autoclave and then heated or cooled to temperature at a stirring rate of 725 rpm for one hour. Then the CO₂ was added (either 0.54 mol for low loading or 1.25 mol

for high loading) by an ISCO 500D syringe pump with series D controller and the reaction started. The reaction was run under temperature, pressure, and stirring for 24 hours and then depressurized which generally takes +/- 1 hour. Then 0.69 mL of toluene internal standard (6.5 mmol) are added and samples collected. These samples are run on a Hewlett Packard 6890 Gas Chromatograph with flame ionization detector (GC-FID) for quantification of yield. Samples were also run on a Hewlett Packard GC with Mass Selective Detector 5972 (GC-MS) for peak identification. All yields reported are averages of 3 runs.

Results and Discussion

Synthesis of Methyl Yellow

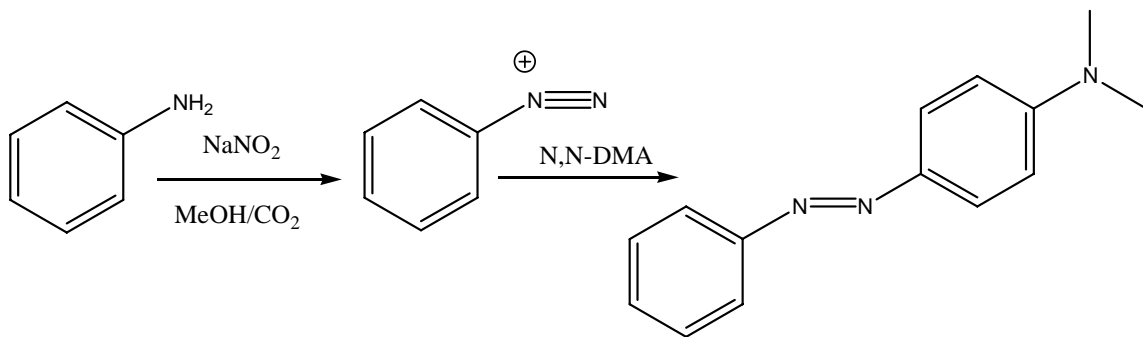


Figure 3-5: Synthesis of methyl yellow from aniline

Methyl yellow was synthesized in a single pot reaction from aniline, sodium nitrite, N,N-dimethyl aniline and CO₂ in methanol as shown in Figure 3-x. Aniline was the limiting reagent with both the nitrite and N,N-dimethyl aniline in excess. All reactants except CO₂ were loaded and stirred for an hour to allow the temperature to equilibrate. Then the CO₂ was added and the reaction began. The CO₂ and methanol

form methylcarbonic acid which reacts with the nitrite to form nitrous acid. The nitrous acid reacts with the aniline to form a diazonium salt which couples with N,N-dimethyl aniline to form methyl yellow.

The most successful coupling reaction conditions were at 5°C with excess nitrite salt and a high CO₂ loading. The reaction was run for 24 hours and produced an average yield of 72% methyl yellow and 97% conversion of aniline. The product was confirmed by GC-MS and ¹H NMR. Two different nitrite loadings, two different CO₂ loadings, and three temperatures were run for the coupling reaction all in triplicate. Also several experiments were run to ensure that the catalysis was due to methylcarbonic acid. The first experiment was to run the normal loading without any added CO₂. This resulted in no visual color change and no measurable yield. Next, the reaction was run with tetrahydrofuran as the solvent rather than methanol because it should not form an *in situ* acid with CO₂. This reaction resulted in a yield of 0.3% which is likely due to the formation of carbamic acid from aniline and CO₂ (Salvatore, Flanders et al. 2000) as shown in Figure 3-6. To verify this result, the reaction was run without any solvent and resulted in a methyl yellow yield of 14%. So while the aniline can catalyze the reaction to trace yield, the methylcarbonic acid clearly provides the major catalysis.

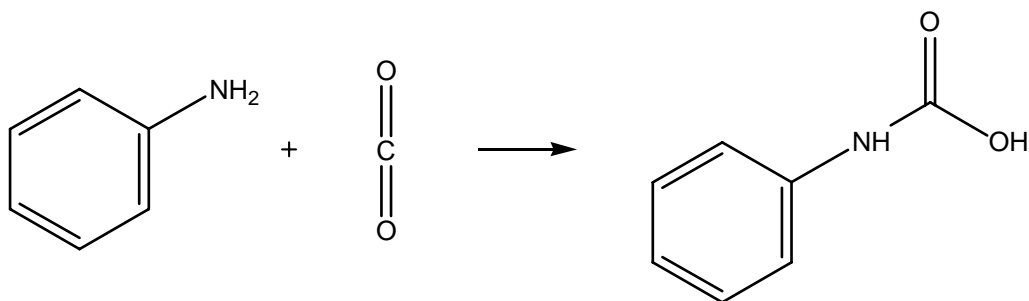


Figure 3-6: Formation of carbamic acid from aniline and carbon dioxide

The effect of nitrite type and loading was also investigated. Initially both isoamyl nitrite and sodium nitrite were used in slight excess. The isoamyl nitrite gave yields roughly half of that of sodium nitrite. All further reactions were run with sodium nitrite. Next the amount of excess sodium nitrite was investigated by comparing the yield and rate for a slight excess (1.04 times) and for 2.2 times excess. The results in Figure 3-7 show a significant increase with the large excess of nitrite.

The amount of CO₂ loaded was also varied. A small loading of 0.54 moles was compared to a higher loading of 1.25 moles. The low CO₂ loading at low temperatures gave a pressure close to 10 bar while a high CO₂ loading and high temperature gave pressures as high as 47 bar. Figure 3-8 shows that the higher CO₂ loading gave improved yields. This was expected because increased CO₂ concentration will increase the alkylcarbonic acid concentration. However, there was the possibility that the increased CO₂ concentration could sufficiently lower the dielectric constant of the solvent to hinder proton dissociation as discussed in Chapter II.

A range of temperatures was run for the coupling reaction. Typically diazotizations are run at low temperature because of the instability of the diazonium salt. Then after the coupling agent or substitution reactant is added, the temperature is allowed to rise to increase the reaction rate. So in a one pot synthesis, it is assumed that a low temperature will do best. However this was not the case in the coupling to form N,N-diethyl-4-[(4-nitrophenyl)azo]aniline (DENAB) in Hooker et al where the highest yields were found at 80°C (Hooker, Hinks et al. 2002). Figure 3-9 shows the results for temperatures of 5, 25, and 50°C with the highest yields at 5°C and decreasing yield with increased temperature.

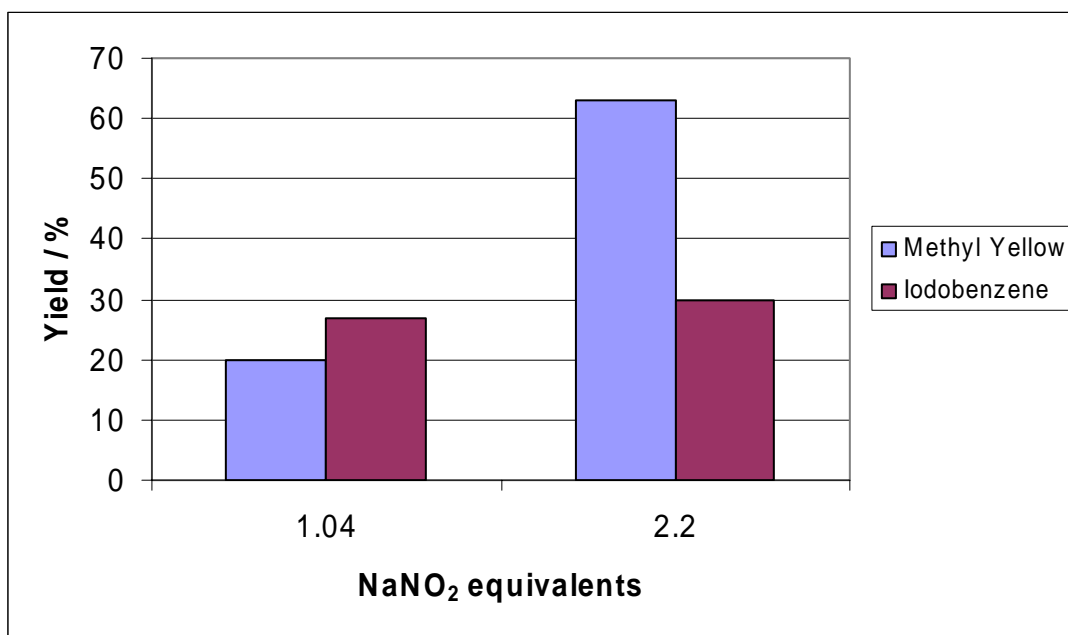


Figure 3-7: Effect of nitrite loading on yield

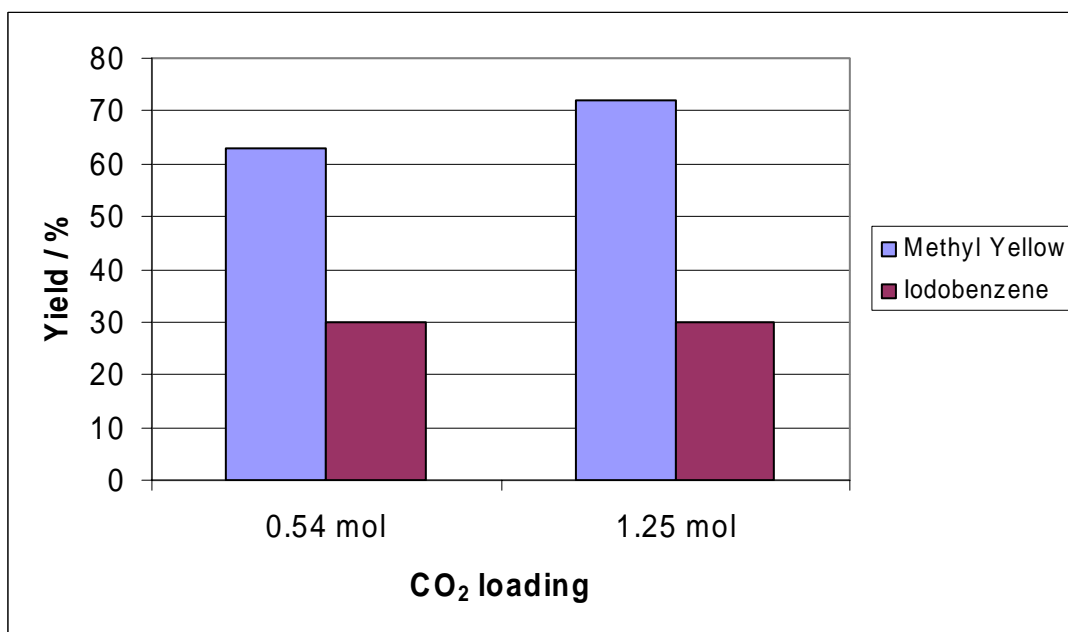


Figure 3-8: Effect of CO₂ loading on yield

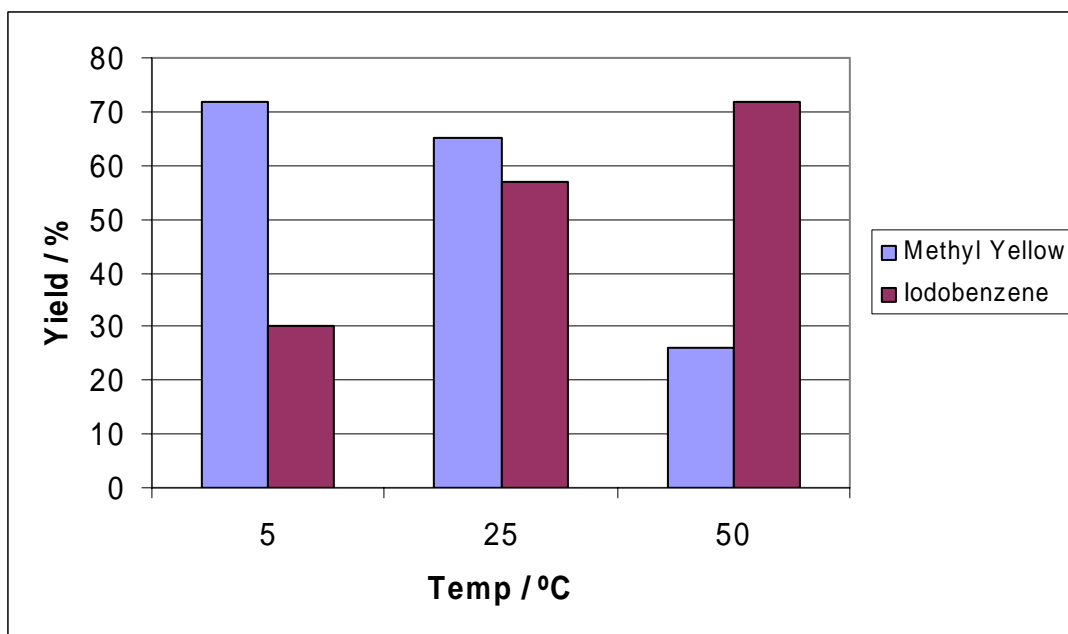


Figure 3-9: Effect of temperature on yield

This shows that the stability of the diazonium cation is more important than the reaction kinetics in this case.

Additionally, the reaction was run under the corresponding conditions from Hooker et al (Hooker, Hinks et al. 2002) who synthesized DENAB in a water-CO₂ system with carbonic acid in yields up to 91%. When the reaction was replicated for methyl yellow resulted in a yield of only 11%. This is due to the probable lower water solubility of the aniline versus 4-nitroaniline and the lack of stabilizing effect from the nitro group on the diazonium ion as well. The reaction could not be duplicated with DENAB because it's high melting point prevented it from running through a GC. The reaction was also attempted with ethanol and CO₂ to form ethylcarbonic acid but while there was some conversion of aniline, no yield was observed.

All reactions had similar byproducts and product ratios with an example shown in figure 3-8. The major byproduct from all reactions by GC-MS was benzene through deamination of the diazonium cation which was expected but not shown in figure 3-8 due to a solvent delay. Other common byproducts were azobenzene, diphenyl amine, aminobiphenyl, and biphenyl although all were generally in small amounts. The conversion on aniline was reproducible for each reaction condition, however, the value only varied from 93-99% for all coupling reactions.

Synthesis of Iodobenzene

The synthesis of iodobenzene proceeded just as the coupling reaction in a single pot with potassium iodide in place of N,N-dimethyl aniline (Figure 3-x). All reactants but CO₂ were loaded into the pressure vessel and stirred for an hour while waiting for

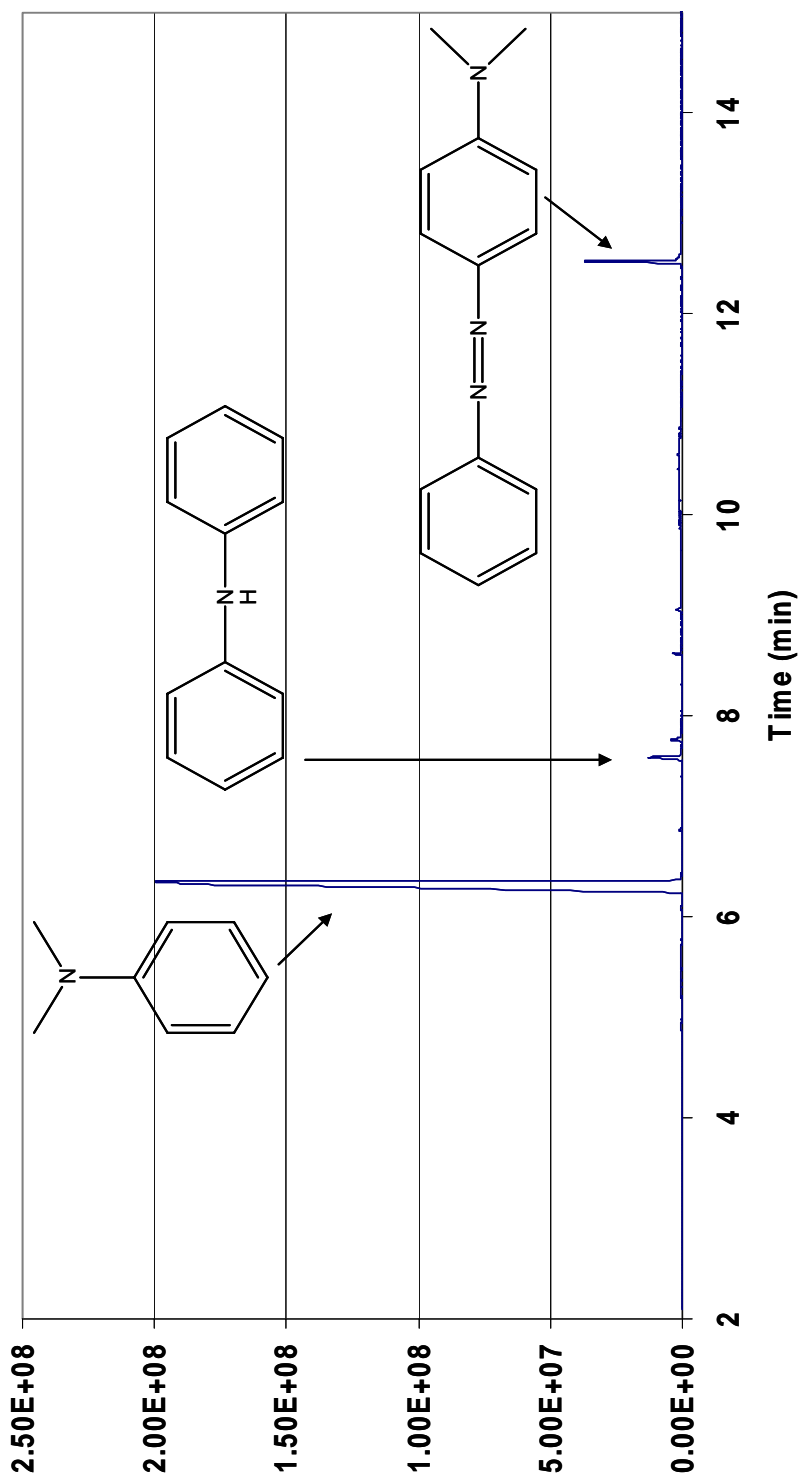


Figure 3-10: Mass selective detector trace for the production of methyl yellow at low CO₂ addition and low nitrite loading

thermal equilibrium. When the CO₂ was added, the reaction began and the same process occurs to form the diazonium ion. Then the diazonium ion reacts with the nucleophilic iodide which form iodobenzene.

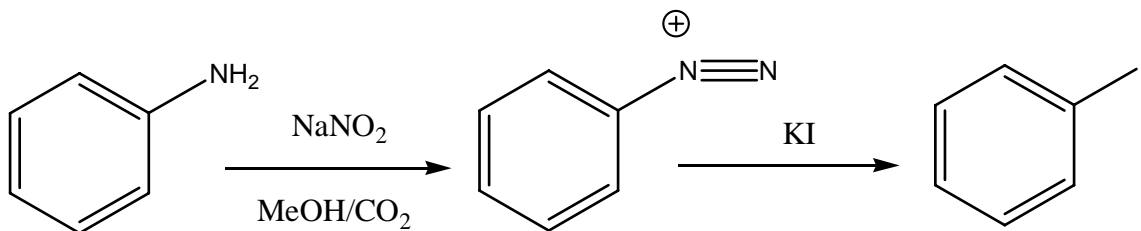


Figure 3-11: Synthesis of iodobenzene from aniline

The most effective conditions for the synthesis of iodobenzene were similar to that of the coupling reaction except in the case of temperature. The best yield was an average of 72% for 3 runs at a high nitrite loading (2.2 times excess) and CO₂ loading (1.25 mol) and at high temperature (50°C). The product was confirmed by GC-MS. The effect of nitrite, temperature, and CO₂ loading was tested in triplicate as well. Additionally, several runs were carried out to show that alkylcarboxylic acids were catalyzing the reaction. The normal loading at 5°C without CO₂ resulted in a yield of 5%, which though higher than expected, is still quite small. The reaction was run in tetrahydrofuran with CO₂ pressure and no product was observed. This suggests that the methanol was acidic enough to catalyze the reaction slightly but that alkylcarboxylic acids significantly increased the rate.

The effect of nitrite loading was not as pronounced for benzyl iodide as it was for methyl yellow. The increase in yield shown in Figure 3-5 was very slight (3%). One possible explanation is that the nitrite was near the solubility limit in methanol at 5°C and thus an increase in loading did not have a significant impact on the actual concentration

in solution. The results from increased CO₂ loading agree with this hypothesis since more CO₂ (and thus more acid) did not have an effect on the yield (Figure 3-6).

However, for the benzyl iodide, an increase in temperature had a significant impact on yield as shown in Figure 3-7. The yield increased with temperature which could be an effect of both increased reaction rate and improved salt solubility. The only observed byproduct for the substitution reactions was benzene. The conversion of aniline was reproducible but again only varied from 94-99% for all reactions.

The Sandmeyer reaction was also run under the same conditions with CuBr to form benzyl bromide. The theoretical yield of benzyl bromide was found to be 58%. However, when the reaction was run without any CO₂, a yield of 43% was still observed. Also, when the reaction was run in tetrahydrofuran and CO₂, there was a yield of 13%. Because the yield increase because of alkylcarbonic acid was not significant, no further experiments were conducted.

Conclusion

Methylcarbonic acid is demonstrated as a green substitute for strong acids for the diazotization of aniline and subsequent coupling to form methyl yellow or substitution to form benzyl iodide. The use of methylcarbonic acid eliminated the salt waste associated with use of strong acids generally used in the synthesis of these chemicals. Several variables were varied to improve yields and optimal conditions for both reactions were at reasonable temperatures and pressures (below the critical pressure of CO₂).

References

- Bahulayan, D., L. John, et al. (2003). "Modified Clays as Efficient Acid-Base Catalyst Systems for Diazotization and Diazocoupling Reactions." Synthetic Communications **33**(6): 863.
- Calderelli, M., I. R. Baxendale, et al. (2000). "Clean and Efficient Synthesis of Azo Dyes Using Polymer-Supported Reagents." Green Chem. **2**(2): 43.
- Chamblee, T. S., R. R. Weikel, et al. (2004). "Reversible *in situ* acid formation from β -pinene hydrolysis using CO₂ expanded liquid and hot water." Green Chem. **6**.
- Eckert, C. A., D. Bush, et al. (2000). "Tuning Solvents for Sustainable Technology." Ind. Eng. Chem. Res. **39**: 4615.
- Eckert, C. A., B. L. Knutson, et al. (1996). "Supercritical Fluids as Solvents for Chemical and Materials Processing." Nature **383**: 313.
- Eckert, C. A., C. L. Liotta, et al. (2004). "Sustainable Reactions in Tunable Solvents." J. Phys. Chem. B **108**(47): 18108.
- Hartmann, H. and I. Zug (2000). "On the coupling of aryldiazonium salts with N,N-disubstituted 2-aminothiophenes and some of their carboxylic and heterocyclic analogues." J. Chem. Soc., Perkin Trans. 1: 4316.
- Heemestra, J. M. and J. S. Moore (2004). "A novel indicator series for measuring pK_a values in acetonitrile." Tetrahedron **60**: 7287.
- Heinz, P. (2002). Black dyes for use in jet-printing inks. Switzerland.
- Hooker, J., D. Hinks, et al. (2002). "Synthesis of *N,N*-diethyl-*N*-{4-[(*E*)-(4-nitrophenyl)diazonyl]phenyl}amine via *in situ* Diazotisation of coupling in supercritical carbon dioxide." Color. Technol. **118**: 273.
- Hulme, C., L. Ma, et al. (2000). "Novel applications of carbon dioxide/MeOH for the synthesis of hydantions and cyclic ureas via the Ugi reaction." Tetrahedron Lett. **41**: 1889.
- Itoh, T., K. Nagata, et al. (1997). "Reaction of Nitric Oxide with Amines." J. Org. Chem. **62**(3582-3585).
- Kaupp, G., A. Herrmann, et al. (2002). "Waste-Free Chemistry of Diazonium Salts and Benign Separation of Coupling Products in Solid Salt Reactions." Chem., Eur J. **8**(6): 1395.
- Leverenz, K. (1981). Process for Diazotizing Aromatic Amines. US.

- Merrington, J., M. James, et al. (2000). "Supported diazonium salts-convenient reagents for the combinatorial synthesis of azo dye." Chem. Commun.: 140.
- Musie, G. T., M. Wei, et al. (2001). "Catalytic Oxidations in Carbon Dioxide-based Reaction Media, Including Novel CO₂-expanded Phases." Coor. Chem. Rev. **219-221**: 789.
- Raue, R., A. Brack, et al. (1996). Process for the Preparation of Dyestuffs. US.
- Raue, R., K.-H. Lange, et al. (1996). Process for the Preparation of Dyestuffs. US.
- Salvatore, R. N., V. L. Flanders, et al. (2000). "Cs₂CO₃-Promoted Efficient Carbonate and Carbamate Synthesis on Solid Phase." Organic Letters **2**(18): 2797.
- Subramaniam, B., C. J. Lyon, et al. (2002). "Environmentally Benign multiphase catalysis with dense phase carbon dioxide." Appl. Catal. B **37**: 279.
- Suzuki, N., T. Azuma, et al. (1987). "Diazotization and Sandmeyer Reactions of Arylamines in Poly(ethylene glycol)-Methylene Dichloride: Usefulness of PEG in Synthetic Reactions." J. Chem. Soc., Perkin Trans. 1: 645.
- West, K. N., C. Wheeler, et al. (2001). "In Situ Formation of Alkylcarbonic Acid with CO₂." J. Phys. Chem. A **105**: 3947.
- Wolff, J., K. Wolf, et al. (1988). Process For Preparing Aromatic Diazonium Salts by Diazotization of Amines. US.
- Xie, X., J. S. Brown, et al. (2002). "Phase-transfer catalyst separation by CO₂ enhanced aqueous extraction." Chem. Commun.: 1156.
- Xie, X., C. L. Liotta, et al. (2004). "CO₂-Catalyzed Acetal Formation in CO₂-Expanded Methanol and Ethylene Glycol." Industrial and Engineering Chemistry Research **43**: 2605.

CHAPTER IV

HYDROLYSIS OF β -PINENE USING ALKYL CARBONIC ACIDS

Introduction

Large amounts of waste may result from the neutralization of homogeneous acid catalysts following reaction. Here we present examples of *in situ* acid formation and self-neutralization, thus eliminating waste and offering advantages for product recovery. The formation of α -terpineol (**2**) from β -pinene (**1**) is a reaction of commercial significance that is typically run with strong acid. We demonstrate that the reaction can be performed under more environmentally benign conditions using the *in situ* acid formation of CO₂ expanded liquids. The relative rates and product distributions achieved are presented and discussed.

β -pinene is a member of the terpene class of compounds which are very important to the flavor and fragrance industry. Terpenes occur naturally in fruits, spices, flowers, leaves and other natural sources. Terpenes are also commercially produced from both natural and synthetic sources with production in the millions of pounds a year (Bedoukian 1967). Naturally derived compounds generally demand a premium cost on the market due to limited supply and perceived higher quality. α -terpineol was chosen as the target product from hydrolysis of β -pinene because of its importance in the flavor and fragrance industry and because strong acids are used in the industrial synthesis, resulting in significant salt waste.

The term terpineol is commonly used for a mixture of terpene alcohol isomers with the isomer α -terpineol(1) being the dominant compound. (Figure 4-1: β -terpineol (2), γ -terpineol (3), terpinen-1-ol (4), and terpinen-4-ol (5)). The aroma associated with the mixture varies based on the relative composition of the isomers and what other compounds are isolated in the mixture. This composition is heavily dependant on the natural source of β -pinene. The aroma ranges from a delicate lilac commonly employed by perfumists to a harsher pine aroma which is associated with cleaning materials. Terpineol can also have a citrus character and is used in distilled lime oil at around ten percent by mass (Clark Jr. and Chamblee 1992). α -terpineol exist as the optical isomers (4R)(+), which is floral, and (4S)(-), which is coniferous and tarry (Ravid, Putievsky et al. 1995). α -terpineol has been isolated from over 150 essential oils but is generally found in small amounts (with the exception of yellow pine oil at around 70%) and/or the oil itself is not widely available (Wagner 1951; Bedoukian 1967). Therefore most terpineol is synthesized from pinene.

Synthesis of terpineol began in the late nineteenth century (Bedoukian 1967). In this process, a mixture of α - and β -pinene are taken from turpentine and then transformed to terpineol in a two step reaction (see Figure 4-2). The first step is reaction in strong aqueous acid with low heating which yields 1,8 terpin diol (8). After isolation of the diol, the second step involves dehydration to terpineol in dilute acid. The pure product α -terpineol is a white crystalline powder which melts at 35°C and boils at 218-219°C. Commercially, terpineol is a mixture of isomers which is a colorless, viscous liquid. The mixture is slightly soluble in water and soluble at a ratio of 1:8 in a 50% alcohol mixture (1995).

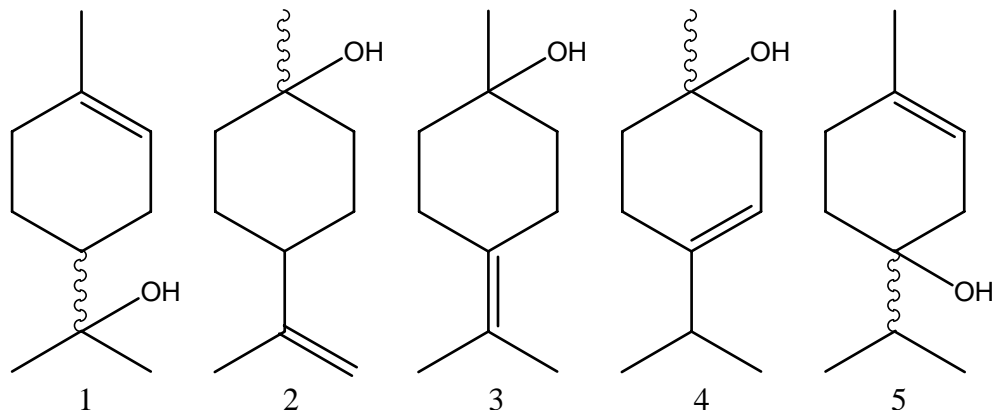


Figure 4-1: α -terpineol (1) and its isomers

Pinene is a bicyclic unsaturated terpene with two isomers: α - (6) which has an endocyclic double bond and β - (7) which has an exocyclic double bond. The isomers have different reactivities because of the difference in structure. In the case of acid catalyzed hydrolysis, β -pinene reacts approximately ten times faster than α -pinene because of steric and electronic effects. The exocyclic double bond is much more accessible to protons and is less substituted and therefore less stable (Egloff, Hulla et al. 1942; Banthorpe and Whittaker 1966). Both isomers are colorless liquids that are insoluble in water and soluble in alcohol or ether. The boiling points are 155-156°C for α -pinene and 165-166°C for β -pinene (1989).

Pinene is generally found as a mixture of the two isomers and over 400 different essential oil sources have been documented. One significant source is pine trees and the turpentine taken from them. Turpentine is composed of as much as 90% pinene with around twice as much α - as β - depending on the specific type of pine tree (Bedoukian 1967). Other common sources of pinene include sage, rosemary, thyme, lavender, neroli,

lemon, and ylang ylang (1995). Optical activity also varies according to source. In American and Russian pines (+)- β -pinene is the predominant isomer while in French pines the (-)- β -pinene is more prevalent (Bedoukian 1967). Interestingly, the distribution of optical isomers of pinene is specific enough that adulteration of citrus essential oils can be checked from using the known optical activities (Mondello, Dugo et al. 2002).

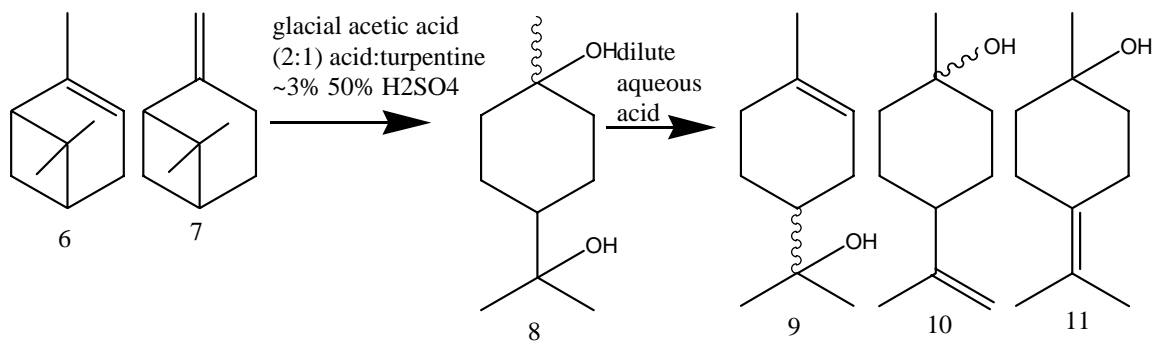


Figure 4-2: Classical method for the manufacture of terpineol from pinene

Pinene is a common reagent in organic chemistry for synthesis of flavor and fragrance compounds, resins, medicines, among others. A recent review covers a wide range of asymmetric applications of pinene based reagents (Ramachandran 2002). (see Figure 4-3) Other uses of pinene as a starting material include the synthesis of menthol (Nicolaou and Sorenson 1996), pinane (Chouchi 2000; Tan, Lin et al. 2000), a taxol C-ring precursor (Wender, Loreancig et al. 1995), camphene (Severino, Vital et al. 1993), and α -terpineol (Teunissen and DeBont 1995).

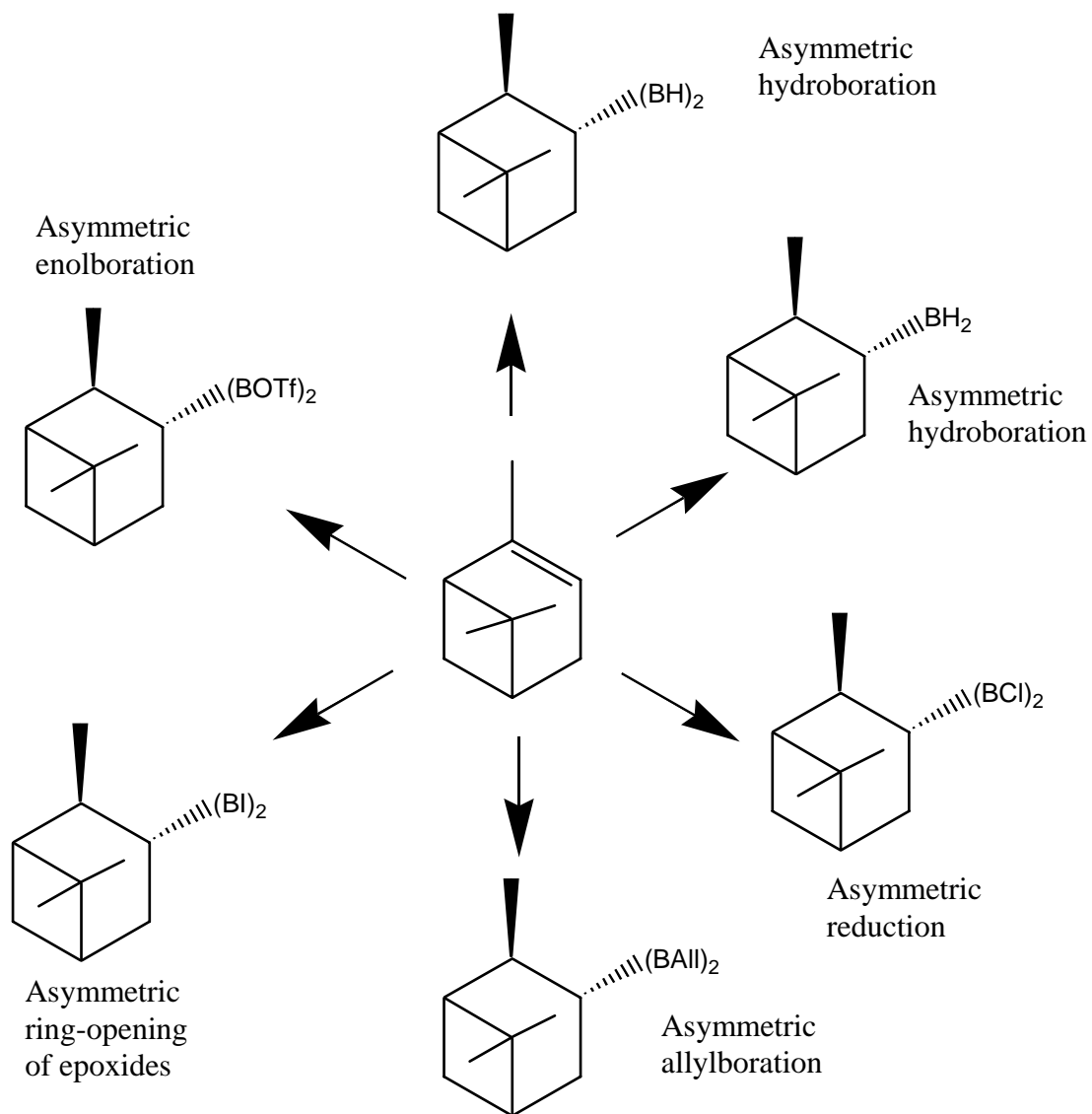


Figure 4-3: Pinene based versatile reagents (PVR) from Ramachandran (2002)

The reaction carried out in this work is the acid-catalyzed hydrolysis of β -pinene. Table 4-1 lays out the history of this reaction from the original two step process already detailed to several more modern references. The early two step processes took days to months to carry out and were performed at high temperatures (Betram and Walbaum 1892). In the mid-twentieth century cosolvents and surfactants were employed to overcome the poor water solubility of pinene which resulted in much shorter reaction times (Weissenborn 1942; Williams and Whittaker 1971). More recently cation exchange resins and several acids have been utilized but yields above 50 % are rare (Chaves Das Neves and Marques Vital 1984; Tanaka, Yamamoto et al. 1996). In all these processes, neutralization and/or separation of the resulting salts are not addressed.

Table 4-1. Sample of pinene hydration literature

Reagents	Temp/ time	Yield	Ref/ Year
1 kg turpentine, 2 kg glacial acetic acid, 100g 50% H ₂ SO ₄			18, 1892
500 parts turpentine, 2000 parts 25% H ₂ SO ₄ , 5-10 parts polyglycol emulsifier followed by: 7.5 parts phthalic anhydride, 3000 parts water	~3 days 30-40°C	95% terpineol	19, 1942
β -pinene, 95% acetone/water, 0.73N H ₂ SO ₄	1hr, 75°C	42% terpineol	20, 1971
α -pinene, Dowex 50W-X8 cation exchange resin, aqueous acetone (4% water)	10-17hrs, 75°C	30-40% terpineol	21, 1984
α - or β -pinene, chloroacetic acid, Sc triflate	2 hrs, 60°C	57% terpineol	22, 1996

Hydration of pinene involves unique ring opening and rearrangement reactions which attracted significant research both academically and industrially until the mid-twentieth century (Winstein and Appel 1964). The research allowed full understanding of the carbocation chemistry involved in the reaction and the full mechanism elucidated. Clark and Chamblee outline this mechanism as well as kinetics in a review (Clark Jr. and

Chamblee 1992). Figure 4-4 visually demonstrates the mechanism for hydrolysis of β -pinene and shows the dominant products: α -terpineol(1), broneol(16), camphene(17), fenchol(22), fenchene(21), terpinolene(18), and limonene(19). Table 4-2 shows a summary of the literature for this reaction (Valkanias and Iconomou 1963). The products are grouped into terpineols, hydrocarbons, and bicyclic alcohols. The table shows that increasing temperature brings increasing hydrocarbon yield from dehydration and that there is little difference in product distribution between α - and β -pinene.

Table 4-2. Summary from the literature for product composition for pinene solvolysis reactions (% of product mixture)

Conditions (Ref)	pinene remaining	hydrocarbons	terpineol	bicyclic alcohols
α -pinene, pH=2.2, buffered aqueous plant gum emulsion, 25°C, 73 hrs (1)	6.8	12.4	71.7	10.4
α -pinene, 0.073N H ₂ SO ₄ , 95% acetone/water, 75°C, 4 hr (20)	9	39	41	20
β -pinene, 0.073N H ₂ SO ₄ , 95% acetone/water, 75°C, 1 hr (20)	12	38	42	19
α -pinene, 0.06N H ₂ SO ₄ , 95% acetone/water, 75°C, 7 hr (37)	10	37.4	52	7
α -pinene, 0.05M HClO ₄ , dioxane/water, 75°C, 24 hr (24)	17	33	55	12
β -pinene, 0.05M HClO ₄ , dioxane/water, 75°C, 3 hr (24)	19	30	56	9

The hydrolysis reactions in this work were carried out in gas-expanded liquids (GXLs) as described in previous chapters. As before, the presence of alkylcarbonic acids will allow for simple neutralization via depressurization, completely eliminating salt waste. The major difference in this work is the presence of water in the GXL. Water will also contribute to *in situ* acid creation through the formation of carbonic acid. Previous

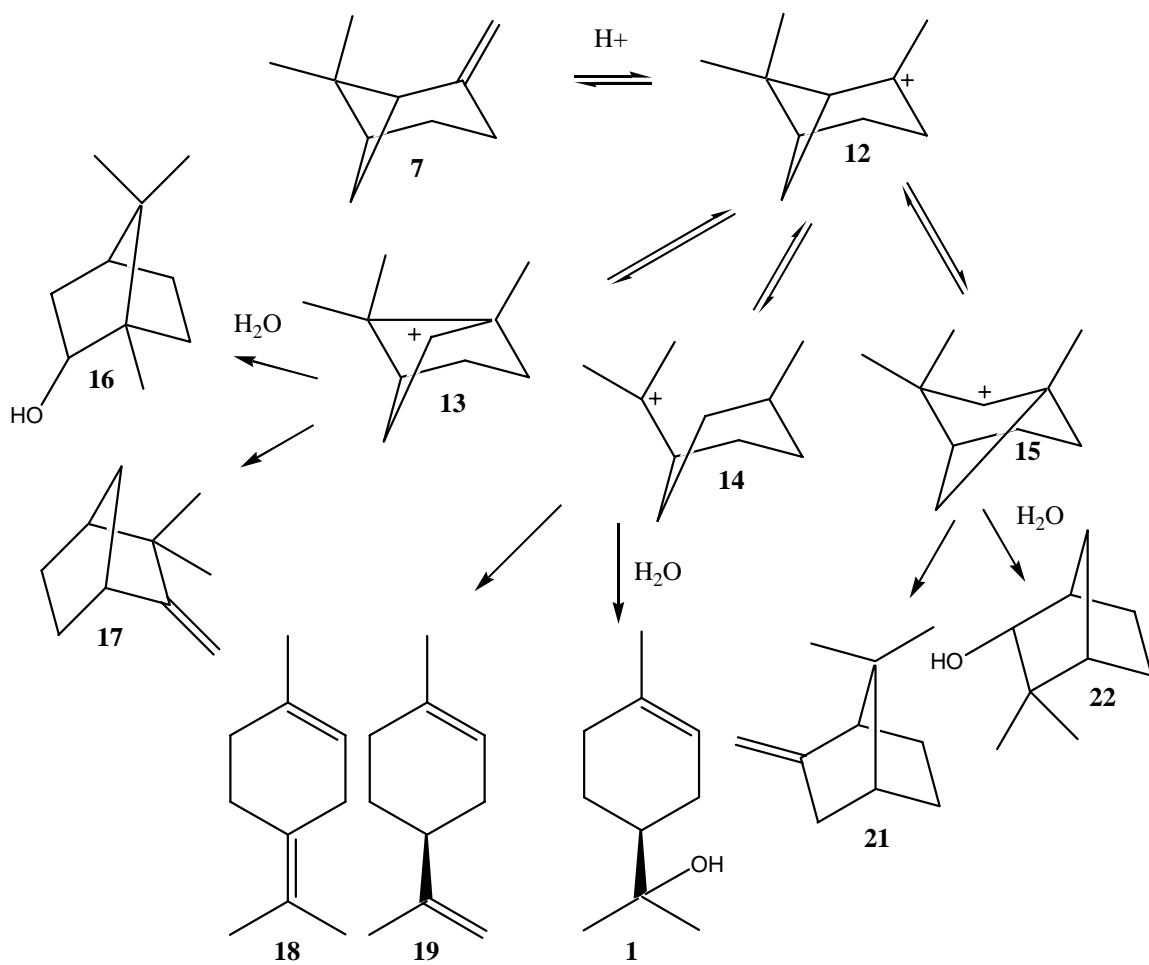


Figure 4-4: Mechanism for the acid-catalyzed rearrangement and hydrolysis of β -pinene

work done on CO₂/water systems has shown that a pH as low as 2.8 can be attained (Towes, Shroll et al. 1995). Wen and Olesik measured pH of CO₂/water/methanol systems using pH indicators and UV/visible spectrum measurements. They found a minimum pH of 4.22 at 5.6 mole percent CO₂ (see table 4-3) (Wen and Olesik 2000). They attribute this phenomenon to competition between increased acid concentration and decreased dielectric constant as CO₂ composition is increased. They do not assume any alkylcarbonic acid is formed but the argument would be the same for carbonic acid. They compare the addition of CO₂ to that of a nonpolar alkane and assume the dielectric constant is proportional to the amount of nonpolar component added. Using this idea with known dielectric values for methanol/water mixtures (Jaz and Tomkins 1972) and known CO₂ concentrations, a dielectric for the CO₂/methanol/water mixture can be calculated (see Table 4-3). Wen and Olesik also reported that pressure has little effect on pH in CO₂/methanol/water systems from 100-200 atmospheres.

Table 4-3. pH and dielectric constant values for MeOH/H₂O/CO₂ GXLs

MeOH/H ₂ O/CO ₂ mol ratio	pH	Dielectric constant	MeOH/water system w/ equiv. dielec. const. mol ratio
68.2/30.6/1.2	4.54	42	70/30
65.1/29.3/5.6	4.22	40	75/25
61.7/27.7/10.6	4.38	38	81.4/18.6
55.7/25.1/19.2	4.73	34	95.6/4.4

Experimental Materials

(1S)-(-)- β -Pinene (99% by GC) from Aldrich Chemical Company was used. HPLC grade solvents were obtained from Aldrich: water; methanol (anhydrous 99.8%); ethanol (reagent grade, anhydrous); acetone (Aldrich, 99.9+%); tetrahydrofuran;

isopropanol. Methylene chloride was obtained from Fisher. Tetradecane internal standard (99% by GC) was obtained from Fluka. Carbon dioxide (SFC/SFE grade) was obtained from AirGas. All materials were used as purchased.

Apparatus and Procedures

The reactions were performed in a Model 4560, inconel, 100 mL Parr reactor fitted with an overhead magnetic stirrer controlled by a Model 4842 stirrer and heater controller. The temperature of the reactor was maintained within 1 °C of the setpoint and stirring was maintained at 725 rpm. The CO₂ was added to the reactor using an Isco 500D syringe pump with a Series D controller. The pressure of the Parr reactor was monitored using an Ashcroft pressure gauge. The pressure of the reactor was typically 200–300 psi (14–21 bar). At the end of the reaction period the reactor was allowed to cool to room temperature (~ 1–1.5 hr) and the pressure was released into a 250 mL degassing flask fitted with a glass frit filter and ~ 200 mL of acetone. The degassing process continued for ~ 5 min.

At the end of the degassing period, the entire contents of the reactor were poured into a 200mL separatory funnel. Tetradecane (0.05 mL) was added as an internal standard using an Eppendorf pipet. The reactor, and as much of the stirring mechanism as possible, were thoroughly rinsed with methylene chloride. The rinse solvent was added to the separatory funnel (~50 mL solvent) and the mixture was extracted and allowed to separate. The extraction was repeated two more times. The final organic layer (~150 mL) was concentrated to ~15 mL using a Kuderna Danish (KD) evaporator and hot water bath (~75°C). Previous work in the Coca-Cola laboratory confirms that the

KD evaporator is suitable for quantitative concentration of methylene chloride samples. The efficiency of the work-up procedure was checked by taking a 50 mL solution of methanol/water containing 1 mL of β -pinene through the extraction and concentration steps. The percent recovery of β -pinene was 96 % as determined by GC-FID. Internal standard (0.05 mL tetradecane) was also added to the acetone degassing solvent which was then concentrated to ~15 mL using a rotavap set to relatively mild conditions (40°C, 20 in Hg). The degas solvent generally contained less than 5 % of the recovered mass. However, the levels rose to ~20 % in a few cases, probably due to degas flows that were set too fast. All concentrated samples were analyzed by GC-FID and GC-MSD.

An HP 5890 GC equipped with a 6890 series autosampler was used for GC-FID analysis with a DB-5 capillary column. The oven temperature program was as follows: initial temperature 70°C; initial hold 10 min; 2 °/min to 200°C; final hold 50 min. Other settings of the GC were: injector temperature 200°C; detector temperature 240°C; carrier gas helium; column flow at initial temperature 1.91 mL/min; carrier gas pressure (constant pressure) 10 psi; split ratio 20:1; 1 μ L injection. An Agilent GC Chemstation was used for peak integration and data analysis. Response factors were calculated for all of the major compounds based on the internal standard tetradecane and the results were reported as absolute concentration values (mg/mL). These were then converted to percent of reaction products. GC-MS analysis was conducted on an HP 5972 MSD coupled with an HP 5890 GC. A DB-5 capillary column (30 m x 0.32 mm x 1 μ m film thickness) was used with temperature program (10 min initial hold at 60°C, 2 °/min to 200°C, 50 min final hold at 200°C). The GC injector temperature was 190°C and MSD transfer line temperature was 280°C. The GC was operated in constant flow mode at 1.2 mL/min with

vacuum compensation. Peak identifications were made using an in house citrus.l library, the Wiley 6th edition MS library and retention time data found in the literature (Adams 1995).

Phase equilibria studies were conducted in a 300 mL Parr vessel equipped with two observation windows. The same temperature and stirring controller as previously described were used. The total volume of reaction mixture was doubled to 100 mL to put the meniscus in the visible part of the reactor. CO₂ was added to the Parr as previously described. The phase behavior of the system was observed at the window as the reactor temperature was increased.

Results and Discussion

Initially, a series of control reactions were run to provide proof of the in situ acid formation of gas expanded liquids (GXLs). Reactions were run in 1:1 volume ratio of methanol water for 24 hours with no heat and/or no CO₂. The first reaction was run at room temperature (25°C) and 0.013 M β-pinene. As expected, with no heat or CO₂ pressure, there was no reaction and 98 % recovery of starting material. Next the reaction was run at 25°C at 0.128 M β-pinene and CO₂ pressure. There was virtually no reaction and 97 % recovery of starting material so the temperature was increased to help the kinetics. A loading of 0.128 M β-pinene at 75°C showed no hydrolysis reaction but only 82 % of the starting material and 84 % of the starting mass was recovered. This suggests that oligomerization could occur at elevated temperatures over long periods of time. Also, the solubility and volatility of pinene could play a role. Further phase behavior work was done to investigate this possibility.

Pinene is not very soluble in water, likely similar to limonene(19) at 1.01×10^{-4} M (Massaldi and King 1973). Experiments were done below the solubility limit in water to be sure of a single phase mixture, but wide variances in recovery did not allow for accurate product analysis. Thus all reaction were run at 0.128 M, well above the solubility limit of 1:1 volume methanol/water mixtures to ensure repeatability of experiments. Additional phase behavior experiments were done to look into the phase behavior of methanol/water mixtures at high temperature and pressure. Experiments in a windowed vessel very similar to the reaction vessel showed that methanol and water are miscible at every condition attempted in this work. However, the β -pinene is still not fully soluble so there was always a second liquid phase. The upper phase will be predominantly β -pinene. At 75°C , there will be a significant concentration of β -pinene in the gas phase. Additionally, the stirring mechanism is not sealed from the reactor and also not heated, so pinene could condense in the stirrer which would account for the low recovery for pinene at elevated temperatures. After several runs the stirring mechanism was opened and the odor of β -pinene was very evident which seems to support this hypothesis.

Polymerization and oligomerization are both concerns for this type of reaction system. In order to investigate this, 1 mL of β -pinene was sealed in a small titanium tube and heated at 75°C for 24 hours without agitation. Analysis of the reaction showed an 8 % loss of starting material but no observed reaction product which is consistent with polymerization. Bicyclic unsaturated terpene polymerization has been shown to be a concern in the literature. Oxidation reactions of 3-carene and α -pinene were conducted at room temperature to avoid polymerization (Rothenberg, Yatziv et al. 1998).

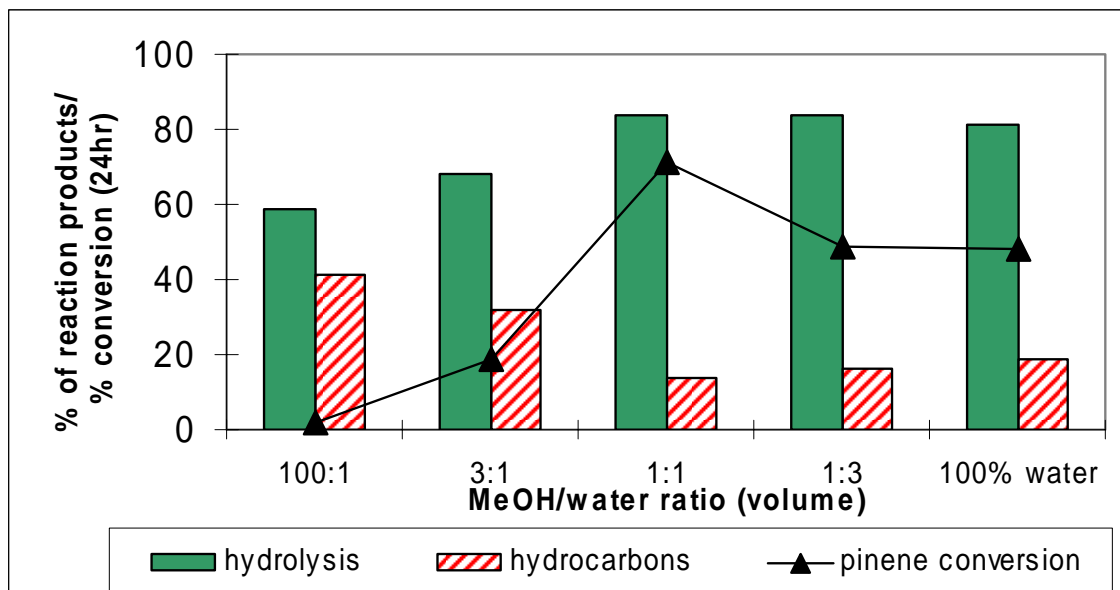


Figure 4-5: β -pinene conversion and product distribution variations with different methanol/water ratios (75°C, 24 hrs)

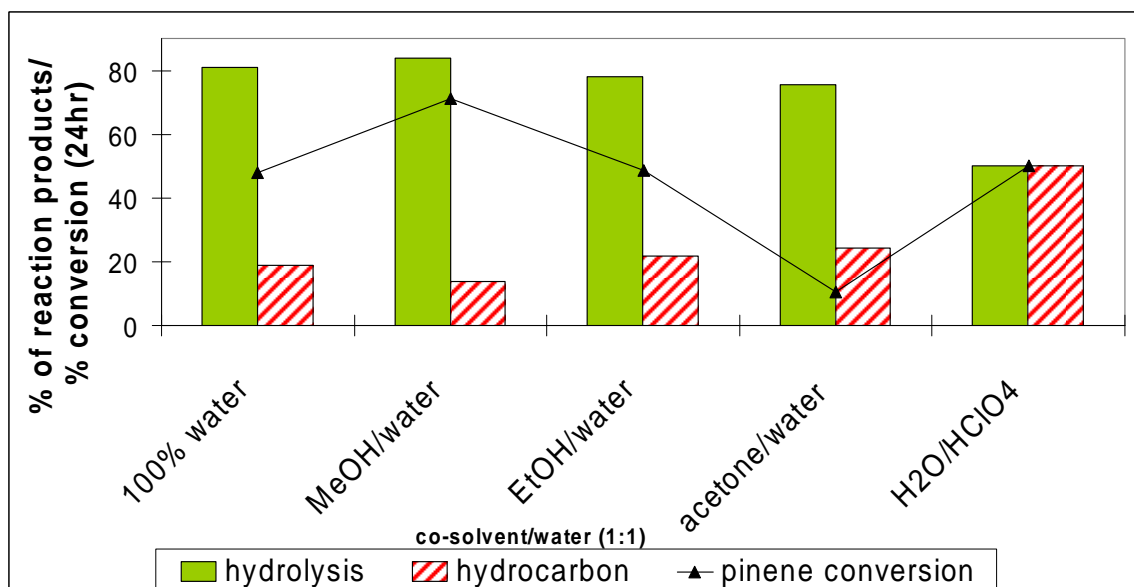


Figure 4-6: β -pinene conversion and product distribution variations with different cosolvents (75°C, 24 hrs)

Additionally, α -pinene polymerization products have been reported after extended reaction times (Valkanas and Iconomou 1963). In acid catalyzed reactions of the similar molecules farnesol and nerolidol, nonvolatile triols or triterpenes were used to explain a low mass recovery (Gutschie, Maycock et al. 1968). There were some late eluting unidentified peaks which could be triols, bis-ether compounds, hydroxy ethers or other polar, nonvolatile compounds. These unidentified peaks only accounted for around two percent of the total area of the chromatogram. There are clearly difficulties in using β -pinene at elevated temperatures; however, the temperature is required for reasonable reaction rates.

When both CO₂ and elevated temperatures (75°C) were employed, significant hydrolysis products were detected after 24 hours. Generally greater than fifty percent of the starting material was converted in this time frame. Because of the difficulties in recovery and possibility of polymerization, it was necessary to do several runs to ensure repeatability. Figure 4-7 shows six runs of 1:1 volume methanol/water GXL hydrolysis of β -pinene experiments. Additionally, when extreme care was taken, duplicate runs gave conversions of 71 +/- 1 % and mass recovery of 92 +/- 4 % with similar certainties for the product distribution.

Since the reaction requires the presence of water but methylcarbonic acid (pK_a of 5.61) (Gattow and Behrendt 1972) is a stronger acid than carbonic acid (pK_a of 6.37) (Teisseire 1994) there should be a tradeoff in amount of water versus methanol. A range of methanol to water ratios, from a stoichiometric amount of water (100:1 vol methanol/water) to all water, was run to investigate this tradeoff. Figure 4-5 summarizes the reaction rate and product distribution for these experiments. Hydrolysis products are

oxygenated species and generally have a more favorable fragrance while the hydrocarbon products are dehydrated which are generally malodorous and undesired. The figure shows that the maximum conversion of 71 % occurred at 1:1 volume ratio of methanol/water. The conversion drops off quickly at higher methanol ratios. This could be attributed to the lowering of dielectric constant which could increase the pK_a of a weak acid (Xue and Traina 1996; Muinasmaa, Rafols et al. 1997; Sarmini and Kenndler 1999). The lower the dielectric constant, the more difficult it is for the proton to dissociate and catalyze the reaction. So since methanol ($\epsilon=32$) has a much lower dielectric constant than water ($\epsilon=80$), this would be expected. The conversion also drops off with increasing water content which agrees with the previously stated pK_a values. Interestingly, the product distribution followed the same trend as conversion with a maximum of 6:1 hydrolysis to hydrocarbon products. Thus the most favorable product distribution and the highest conversion occurred at the same point, 1:1 volume methanol/water.

Further experiments were run with a 1:1 by volume ethanol/water mixture and a 1:1 by volume acetone/water mixture. The ethanol should provide catalysis via both carbonic acid and ethylcarbonic acid while the acetone will only have carbonic acid. Thus it was expected that the reaction in ethanol would be faster than the acetone. Also, previous work by West et al showed that methylcarbonic acid generally gives faster rates than ethylcarbonic acid (West, Wheeler et al. 2001). So the 1:1 volume methanol/water mixture would be expected to have the highest conversion of all of these mixtures. Figure 4-6 compares the results of all of the different types of solvents to the literature source of Keranen (Keranen 1979) which uses perchloric acid in water for 24 hours. The

1:1 methanol/water mixture again had the highest conversion while the 100% water, 1:1 ethanol water, and literature source all had similar conversions. The acetone/water mixture was the slowest since the acetone could not contribute any *in situ* acid. The 1:1 methanol/water also had the most favorable product distribution but all of the GXL reactions had a better product distribution than the perchloric acid reaction. In fact, the literature for strong acid catalyzed hydrolysis gives 30-50 % for hydrocarbons which is also higher than all of the GXL systems (Valkanas and Iconomou 1963; Williams and Whittaker 1971; Indyk and Whittaker 1974; Charwath 1981; Chaves Das Neves and Marques Vital 1984).

Table 4-4: Summary of GXL composition and results

Volume (mL) [MeOH/H ₂ O volume ratio]	mol frac %	% conversion of β -pinene after 24 hr	product distribution		mass recovery
			hydrolysis	hydrocarbons	
MeOH/water	MeOH/water/CO₂				
50/0.5 [100:1]	94/2/4	2.1	59.2	40.8	101.2
37/13 [3:1]	53/42/4	18.9	68.1	31.9	84.6
25/25 [1:1]	30/67/3	70.9	84	14	94.2
13/37 [1:3]	13/84/3	49.3	84	16	68.9
0/50 [100% water]	0/97/3	47.6	80.9	19.1	65.8
EtOH/water	EtOH/water/CO₂				
25/25	23/74/3	48.6	78.2	21.8	62.3
Acetone/water	Acetone/water/CO₂				
25/25	19/77/4	10.4	75.6	24.4	94.9

Conclusion

Gas expanded liquids were shown to be green substitutes for acid-catalyzed hydrolysis of β -pinene. Commonly strong acid is used which requires post reaction

neutralization and resulting salt waste disposal. Using mild CO₂ pressures and simple aqueous mixtures, similar conversion and improved product distributions were attained. A series of experiments showed an optimum in amount of cosolvent used with water as well as choice of cosolvent to be used with water. 1:1 volume methanol/water showed the highest conversion and most favorable product distribution. Ethanol also proved to give slightly lower conversions and slightly less favorable products. However, it would provide a food safe and “natural” route to flavors since ethanol and CO₂ are both considered to be natural chemicals.

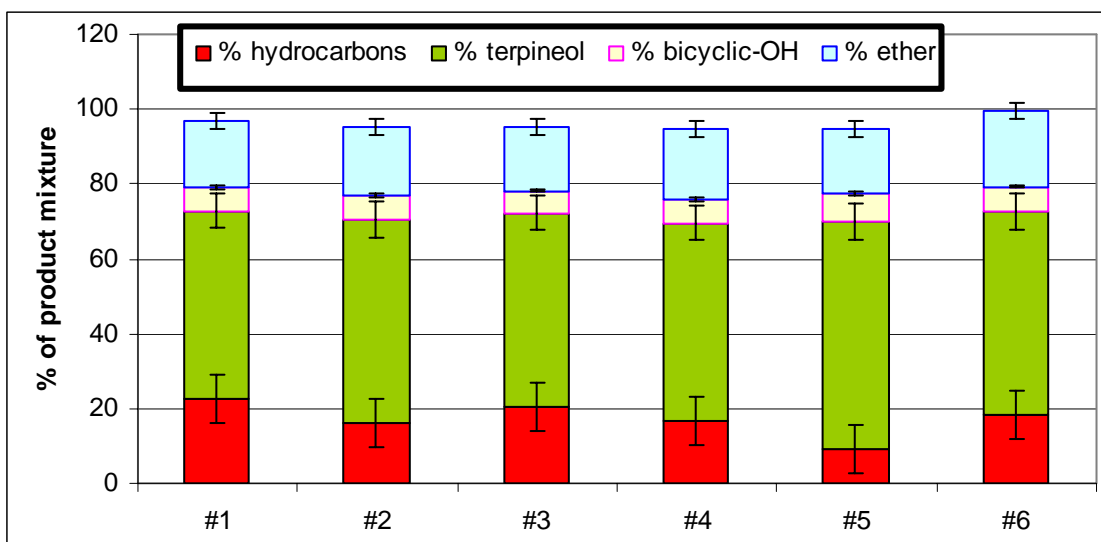


Figure 4-7: Product distribution reproducibility for 6 runs of pinene hydrolysis in the 1:1 MeOH/water GXL

Referenes

- (1989). Merck Index. Rahway, NJ, Merck and Co.
- (1995). Fenaroli's Handbook of Flavor Ingredients, CRC Press.
- Adams, R. P. (1995). Identification of Essential Oil Components by Gas Chromatography/ Mass Spectroscopy. Carol Stream, Ill., Allured Publishing.
- Banthorpe, D. V. and D. Whittaker (1966). "The preparation and stereochemistry of pinane derivatives." Chem. Rev. **66**: 643.
- Bedoukian, P. Z. (1967). Terpiniol. Amsterdam, Elsevier Publishing Co.
- Betram and Walbaum (1892). DE 67255. Germany.
- Charwath, M. K.-C. G. (1981). EP35703 (Cl. C07C33/14).
- Chaves Das Neves, H. J. and J. S. Marques Vital (1984). "Isomerizacao hidratacao do α -pineno catalisada por resinas cationcas de permute ionica." Rev. Port. Quim. **26**: 183.
- Chouchi, D. (2000). Hydrogenation of pinene in a supercritical medium. Portugal. **PT 99-102321 199990611**.
- Clark Jr., B. C. and T. Chamblee (1992). Acid-Catalyzed Reactions of Citrus Oils and Other Terpene-Containing Flavors. Off-Flavors In Foods and Beverages. G. Charalambous, Elsevier: 229-285.
- Egloff, G., G. Hulla, et al. (1942). Isomerization of Pure Hydrocarbons. New York, Reinhold Publishing Corp.
- Gattow, G. and W. Behrendt (1972). "Methyl Hydrogen Carbonate." Angew. Chem. Internat. Edit. **11**(6): 534.
- Gutschie, C. D., J. R. Maycock, et al. (1968). Tetrahedron **24**(2): 859.
- Indyk, H. and D. Whittaker (1974). "Rearrangements of pinane derivatives. Part V. The influence on rearrangements of a neutral nucleophile associated with the carbonium ion." J. Chem. Soc. Perkin Trans. 2: 313.
- Jaaz, G. J. and R. P. T. Tomkins (1972). Nonaqueous Electrolytes Handbook. New York, Academic Press.
- Keranen (1979). Paperi ja Puu-Papperoch Tra **61**: 165.

- Massaldi, H. A. and C. J. King (1973). "Simple technique to determine solubilities of sparingly soluble organics: solubility and activity coefficients of d-limonene, n-butylbenzene, and n-hexyl acetate in water and sucrose solutions." J. Chem. Eng. Data **18**(4): 393.
- Mondello, L., P. Dugo, et al. (2002). The chiral compounds of citrus essential oils. Citrus, The genus Citrus. G. Dugo and A. DiGiacomo, Taylor and Francis: 461-495.
- Muinasmaa, U., C. Rafols, et al. (1997). "Ionic equilibria in aqueous organic solvent mixtures. The dissociation constants of acids and salts in tetrahydrofuran/water mixtures." Analytica Chimica Acta **340**: 133.
- Nicolaou, K. C. and E. J. Sorenson (1996). Menthol. Classics in Total Synthesis, VCH Publishers: 343-379.
- Ramachandran, P. V. (2002). "Pinane-based versatile "allyl boranes"." Alrichimica Acta **35**(1): 23.
- Ravid, U., E. Putievsky, et al. (1995). "Determination of the enantiomeric composition of α -terpeniol in essential oils." Flavour and Fragrance Journal **10**: 281.
- Rothenberg, G., Y. Yatziv, et al. (1998). "Comparitive autoxidation of 3-carene and α -pinene: factors governing regioselective hydrogen abstraction reactions." Tetrahedron **54**: 593.
- Sarmini, K. and E. Kenndler (1999). "Ionization constants of weak acids and bases in organic solvents." J. Biochem. Biophys. Methods **38**: 123.
- Severino, A., J. Vital, et al. (1993). "Isomerization of α -pinene over titania: kinetics and catalyst optimization." Stud. Surf. Sci. Catal. **78**: 685.
- Tan, X., F. Lin, et al. (2000). Improved process for preparation of cis-pinane by catalytic hydrogenation of pinene. China. **CN 99-117276 19991207**.
- Tanaka, S., J. Yamamoto, et al. (1996). Japan.
- Teisseire, P. J. (1994). Chemistry of Fragrant Substances. New York, NY, VCH Publishers, Inc.
- Teunissen, M. J. and J. A. M. DeBont (1995). Will terpenes be of any significance in future biotechnology. Colloques-Institut National de la Recherche Agronomique. **75**: 329-37.
- Towes, K. L., R. Shroll, et al. (1995). "pH-defining equilibrium between water and supercritical CO₂. Influence on SFE of organics and metal chelates." Anal. Chem. **67**: 4040.

- Valkanas, G. and N. Iconomou (1963). "121. Reaktionen in der terpen-reihe, I. Mitteilung, Hydratisierung von α -pinen." Helv. Chim. Acta **46**: 1089.
- Wagner, A. (1951). "Manufacture of Terpinol." Manufacturing Chemist **XXII**.
- Weissenborn (1942). United States.
- Wen, D. and S. V. Olesik (2000). "Characterization of pH in Liquid Mixtures of Methanol/H₂O/CO₂." Anal. Chem. **72**: 475.
- Wender, P. A., P. E. Lorencig, et al. (1995). "Toward the synthesis of taxol and its analogs: incorporation of non-aromatic C-rings in the pinene pathway." Tetrahedron Lett. **36**(28): 4939.
- West, K. N., C. Wheeler, et al. (2001). "In Situ Formation of Alkylcarbonic Acid with CO₂." J. Phys. Chem. A **105**: 3947.
- Williams, C. M. and D. Whittaker (1971). "Rearrangements of pinane derivatives. Part 1. Products of acid-catalyzed hydration of α -pinene and β -pinene." J. Chem. Soc. B: 688.
- Winstein, S. and B. R. Appel (1964). "Estimation of nonassisted solvolysis rates. The structures of the nopinyl p-bromobenzenesulfonates." J. Am. Chem. Soc. **86**: 2722.
- Xue, Y. and S. J. Traina (1996). "Stability of metal-organic complexes in acetone and methanol water mixtures." Environ. Sci. Technol. **30**: 3177.

CHAPTER V

THIIRANE OXIDE BASED THERMALLY CLEAVABLE SURFACTANTS

Introduction

Surfactants are widely used industrially and in laboratories to allow contact between immiscible phases. However, the resulting emulsion is often difficult or costly to separate. We demonstrate a surfactant that can be cleaved into a gas and a hydrophobic alkene which will easily destroy the emulsion and create separate phases. N-octyl thiirane-1-oxide was synthesized from commercially available starting materials, characterized, and purified. We measured the critical micelle concentration (CMC) of the novel surfactant in water to verify its amphiphilicity. Then we thermally decomposed the surfactant to 1-decene and sulfurous gases. Finally, we verified the loss of surface activity for the decomposed surfactant.

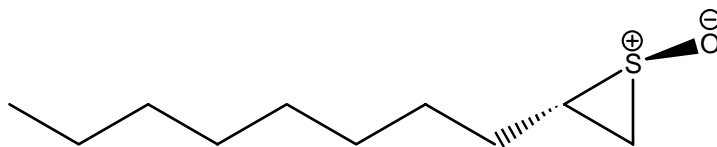


Figure 5-1: Structure of n-octyl thiirane-1-oxide

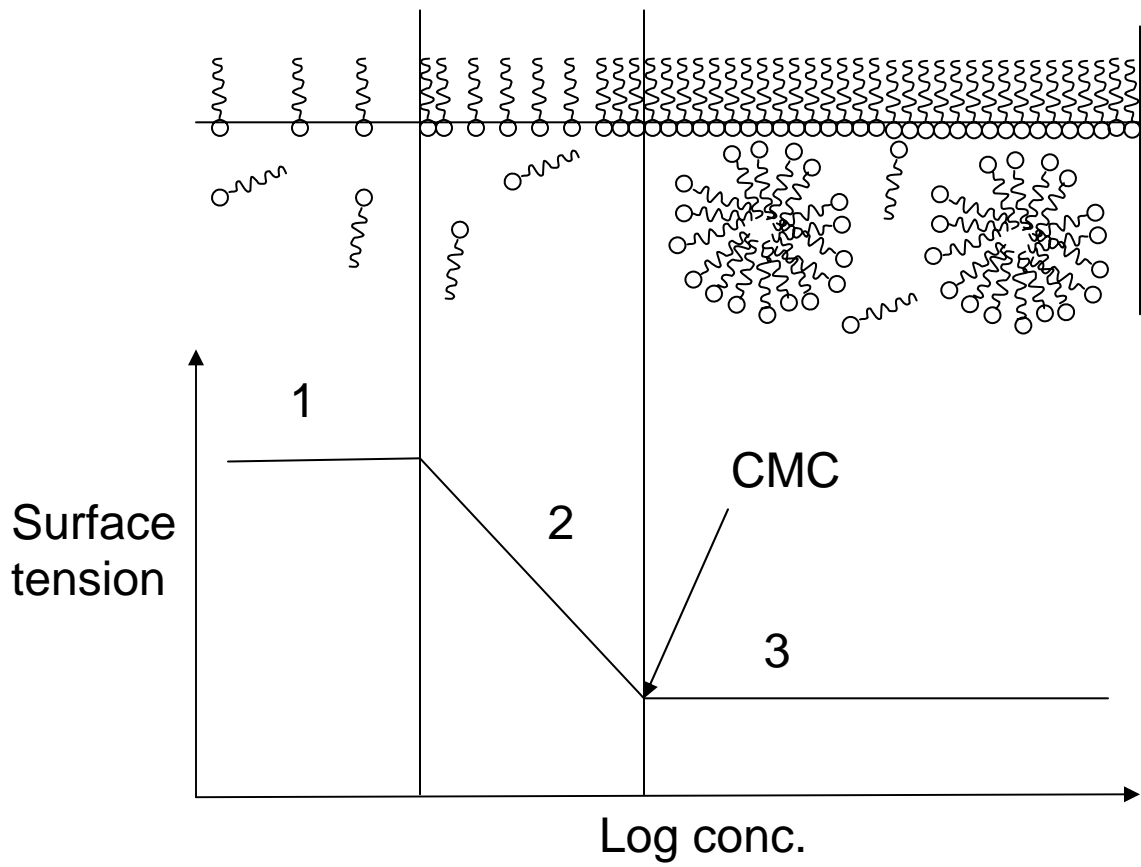


Figure 5-2: Critical Micelle Concentration diagram by surface tension measurement.

Surfactants have been studied and characterized since the 1830's for applications in the dyeing of textiles and synthetic surfactants began appearing by the 1920's (Kastens and Ayo Jr. 1950). Surfactants contain a polar head group and a nonpolar tail and thus are soluble in both aqueous and organic environments. Additionally, surfactants will aggregate into micelles above a specific minimum concentration. This property, called a critical micelle concentration or CMC, allows intimate contact between otherwise immiscible phases and provides the greatest number of applications for surfactants. The creation of micelles significantly changes many physical properties as well as the solubility of organics in aqueous micelles or vice versa. These changes in properties make measuring CMC's fairly simple with a wide variety of possible techniques. These include sessile drop (Fromyr, Hansen et al. 2001), dye solubilization (Schott 1966; Schott 1967), capillary rise (Fuerstenau 2002), keto-enol isomerization, conductance, and fluorescence (Dominguez, Fernandez et al. 1997), among many others.

Above the CMC, many different phenomena can occur. At lower concentrations above the CMC, microemulsions are formed. Microemulsions are thermodynamically stable and are of the order of 2-50nm in diameter (Jonsson, Lindman et al. 1998). These small microphases can have surface areas of 10^5 m²/L of solution. At higher surfactant concentrations, emulsions, which are only kinetically stable, form with sizes of 0.5-10 μ m. Emulsions can be stable without agitation for anywhere from seconds to days depending on the temperature, concentrations, and species involved (Adamson and Gast 1997). Additionally, the shape of emulsions does not have to be spherical. Other common shapes are rods (cylindrical), lamellar, and spherical bilayer which is common of cellular vesicles (Shah 1992). Light scattering is commonly employed to determine

shape information of the emulsion (Iyer, Hayes et al. 2001). It is also important to note that the continuous phase is not necessarily water. While oil in water (o/w) emulsions are the most familiar (i.e. detergents), water in oil (w/o) or reverse micelles and water in carbon dioxide (Johnston, Harrison et al. 1996; Ryoo, Webb et al. 2003) (w/c) are both important industrially and are heavily researched.

Surfactants have developed significantly since the first commercial soaps to the point where they are widely used in industry today. Emulsion polymerization constitutes a significant quantity of industrial output of polymers. Some polymers made in this way are polytetrafluoroethylene (PTFE or Teflon®), poly(vinyl acetate), polychloroprene, polyvinylchloride (PVC), polymethylmethacrylate (PMMA), polyacrylamide (Mathias), and many others. Recently, Dupont started making Teflon in w/c emulsions using a new CO₂-phillic surfactant in an effort to reduce the environmental impact of the process (DeSimone, Guan et al. 1992). Other examples of current and potential industrial surfactant use include enzymatic catalysis, precipitation reactions (Texter 2001), enhanced oil recovery, and extraction from aqueous of proteins and other biological species (Bartscherer, Minier et al. 1995).

In addition to industry, synthetic organic chemistry employs many applications of emulsions to increase contact between immiscible phases, thereby decreasing reaction times (Texter 2001). In either case, when the reaction is complete, the product must be recovered from the emulsion for further reaction or isolation. If there is a microemulsion, the system is thermodynamically stable and thus recovery is difficult or expensive. The most common solution is heating the mixture until it separates into two phases. This procedure is energy intensive since the entire volume must be heated to reach the two

phase region. Additionally, this cannot be employed if the product is thermally sensitive. In the case of emulsions, the mixture is only kinetically stable. However, as previously stated, emulsions can be stable almost indefinitely and rarely is the separation quick enough to ignore in processing. On laboratory quantities, the centrifuge is a common solution to the meta-stable emulsion separation issue. This is a process that does not scale well for both energy and throughput reasons so a better solution to the problem is still required. In drug delivery applications (Holmberg 2003), a water insoluble drug must be injected in a water continuous phase so surfactants are present. However, if the emulsion does not break, the drug will never be delivered.

The separation issues involved with emulsions forced researchers to rethink the way that surfactants are designed. Historically surfactants were created for durability and longevity. However, longevity can also be termed persistence. Not surprisingly there is current research looking into the impact of pharmaceuticals and personal care products (like soaps) on the environment (Smital, Luckenbach et al. 2004) and their biodegradability (Masuyama, Endo et al. 2000). The solution that is proposed is cleavable surfactants. Cleavable surfactants generally break into a hydrophobic molecule and a hydrophilic molecule thus breaking the emulsion. This class of novel surfactants has the potential to lower industrial separation costs, facilitate drug delivery, and reduce environmental surfactant concerns (Holmberg 2003).

A range of possible “triggers” could be used to facilitate the cleaving of the surfactant. These include pH (Jaegar, Mohebalian et al. 1990; Jaegar, Wettstein et al. 1998; Iyer, Hayes et al. 2001) (acid or base addition), ozone (Masuyama, Endo et al. 2000), ultraviolet light (Epstein, Jones et al. 1982; Metzner, Meindl et al. 1994; Nuyken,

Meindl et al. 1994; Nuyken, Meindl et al. 1995; Itoh, Nagata et al. 1997), and heat (Hayashi, Shirai et al. 1985; McElhanon, Zifer et al. 2005). The most common stimulus is a change in pH. Iyer et al decompose a cyclic ketal with a polyethylene glycol polar group attached by adding a buffer of pH 5. They observed complete hydrolysis in three hours at that pH and as fast as fifteen minutes by adding 3% hydrochloric acid. Jaeger et al created a quaternary hydrazinium based acid labile surfactant which was able to be decomposed in acidic conditions in approximately 16 hours. Jaeger et al. also demonstrated base labile surfactants with sulfone moieties as the polar head group. Ozone is employed as a cleaving agent in hopes of mimicking natural biodegradation. These bis(sulfonate) and bis(carboxylate) double chain surfactants showed very similar biodegradability to sodium dodecyl sulfate (SDS) thus limiting their potential (Masuyama, Endo et al. 2000). Epstein et al developed a photolabile surfactant that decomposes into an alkyl chain and an acetyl benzenesulfonate molecule that will still likely have a CMC due to its organic and ionic character. Nuyken produced diazosulfonate based surfactants that degrade into a sulfate ion and a highly reactive diazonium ion. Thus the hydrophobic molecule could easily react with product and the ion will be present in the wastewater. The groups of Hiyahsi and Simmons have developed thermally cleavable surfactants that break into a hydrophobic molecule and a hydrophilic molecule which still leaves the possibility of amphiphilicity and requirement of waste water treatment.

What we set out to create was a surfactant that when given input will go from having a CMC to none at all. So in essence, the molecule must lose its amphiphilicity with stimulus. While this idea does not necessarily require the surfactant molecule to

decompose into a hydrophilic part and a hydrophobic part, that model is the simplest way to lose amphiphilicity. Several examples of this idea have been shown above but all face drawbacks, mainly with the resulting hydrophilic molecule. This hydrophilic molecule is generally organic and thus can be a surfactant. Also, in every case it will be in the water phase requiring downstream removal. The novel surfactant, n-decyl thiirane-1-oxide, produces sulfur oxide (Hartzel and Paige 1966), a gas, from the polar head group, eliminating these concerns. The downside to decomposition as a means of changing physical properties is its irreversibility. Therefore, any surfactant based on this concept would not be able to be easily recycled. However, surfactants are used in small quantities, so recycling is not imperative.

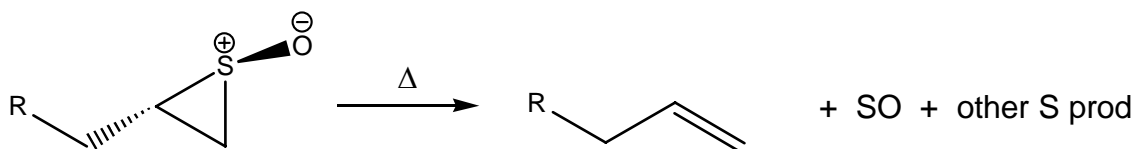


Figure 5-3: Decomposition of n-octyl thiirane-1-oxide to 1-decene, sulfur oxide, and other sulfurous products.

Experimental Materials

All chemicals were purchased from Aldrich and used as received unless otherwise noted. Water (HPLC grade), Sudan III, 1-decene (96%), methyltrioxorhenium, 2,2'-bipyridine-N,N'-dioxide (reagent grade), hydrogen peroxide (35%), sodium thiocyanate (98%), ethanol (reagent grade), m-chloroperbenzoic acid (77%), sodium dodecyl sulfate (Fluka, >99%).

Apparatus and Procedures

Synthesis of surfactant

The entire synthesis of n-octyl thiirane-1-oxide was done on Schlenk tubing under nitrogen atmosphere to avoid problems with atmospheric air and water. The first step in the synthesis is the oxidation of 1-decene with methyltrioxorhenium, 4,4'-bipyridine N,N'-dioxide, 35% hydrogen peroxide in dichloromethane for 16 hrs. The product, 1-decene epoxide is formed with a 96% yield (by NMR) and does not require further purification before further reaction. The epoxide is then reacted with 1.5 molar equivalents of sodium thiocyanate in a 50/50 v/v water/ethanol mixture. The product, n-octyl thiirane, is formed in 76% yield (by NMR) and does not require purification either. Finally, the episulfide is oxidized with 77% m-chloroperbenzoic acid in dichloromethane forming the final product, n-octyl thiirane-1-oxide. Purification is carried out on a silica gel column with 50/50 v/v hexane/ethyl acetate resulting in 35% recovered yield. All NMR were carried out on a Varian Mercury Vx 400 MHz using CDCl₃ as both the solvent and the reference. A Hewlett Packard 1100 LC-MS with positive electrospray ionization (ESI) was used for molecular mass identification. A Bruker Vector 22 Infrared Spectrometer was used for functional group identification. Elemental Analysis was sent to Atlantic Microlabs in Norcross, Georgia.

Determination of Critical Micelle Concentrations

Several techniques were used to confirm the critical micelle concentration of n-octyl thiirane-1-oxide in water. In all cases, a range of surfactant concentrations was made gravimetrically. Capillary rise was carried out by dipping capillary tubes into the

mixture to the bottom, marking the height of the liquid in the tube and measuring the distance. This was repeated three times. Sudan III dye solubility was conducted as has been done in the literature (McElhanon, Zifer et al. 2005). Excess Sudan III was added to each surfactant solution. The samples were then sonicated for thirty minutes and allowed to settle for at least two hours before filtering. A Hewlett Packard model 8453 UV-visible spectrophotometer analyzes the filtered solution and gives an absorbance proportional to dye concentration. These dye experiments were carried out in duplicate. Hydrophilic and hydrophobic sessile drop measurements were done on a VCA 2500 XE system (AST Products, Inc.) to measure the contact angle of the solutions on both hydrophilic and hydrophobic surfaces. The hydrophilic surface used was a glass slide and the hydrophobic surface used was a Teflon sheet. The accompanying software package calculated angles from a digital image of each drop. Both sessile drop methods were carried out in duplicate as well. Since the spreading of the drop on the surface is time dependent, 30 seconds was used the time to wait for the drop to spread. Thus a consistent static measurement could be made from a dynamic property.

Surfactant Decomposition

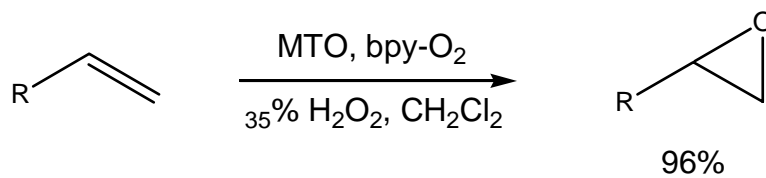
The first test of decomposition was running a solution of the surfactant in acetone on an HP 6890 gas chromatograph with an HP 5973 mass selective detector. This indicated that the inlet heater broke down all of the injected surfactant since only 1-decene was observed. The next tests of surfactant decomposition were done with neat surfactant in a heated oil bath at 120°C and then 100°C. Samples were taken at five and fifteen minutes and analyzed on a Hewlett Packard Series 1100 LC-MS (ESI). A

calibration of n-octyl thiirane-1-oxide and 1-decene was run to quantify the decomposition of the surfactant. For a test of loss of solubility when the surfactant is decomposed, the most concentrated surfactant solutions from the CMC dye experiment were heated at 90°C for 10 minutes and an hour. The solutions were then sonicated for 30 minutes and allowed to settle for at least two hours prior to filtering; the same procedure as was used for the initial solution work up. Then the UV-vis absorbance was taken again to determine the dye concentration after decomposition. The same experiment was carried out with sodium dodecyl sulfate as a comparison to traditional surfactants.

Results and Discussion

Synthesis of Surfactant

The final product, n-octyl thiirane oxide, was synthesized and purified as previously described and shown in figure 5-4 with an overall isolated yield of 25%. Chemical identification was done by ^1H NMR, ^{13}C NMR, ESI-MS, elemental analysis and IR. The proton NMR is shown in figure 5-5 and shows the appropriate peaks for 3 ring protons at 3.0, 2.8, and 2.0 and the alkyl chain protons at 0.9, 1.2, and 1.5. The assignments for ^1H NMR are δ = 0.9, 1.2, 1.5, 2.0, 2.8, and 3.0. The carbon NMR also shows two different carbon species on the ring and the assignments are ^{13}C NMR δ = 14.0, 22.5, 27.5, 28.9, 29.0, 29.2, 29.4, 31.7, 41.5, 50.3.



MTO = Methyltrioxorhenium; bpy-O₂ = 2,2'-bipyridine-N,N'-dioxide

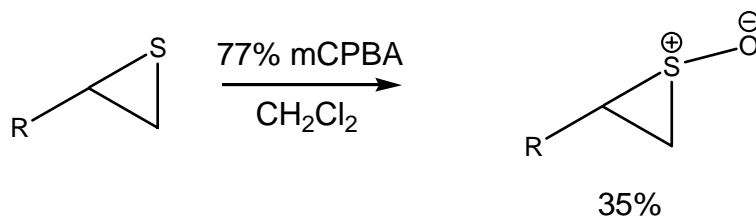
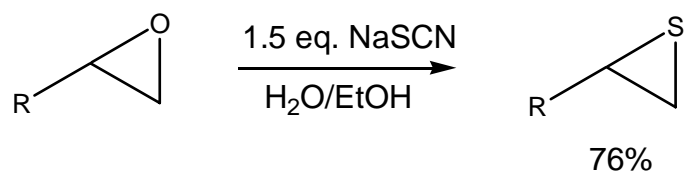


Figure 5-4: Synthetic Scheme for n-octyl thiirane-1-oxide from 1-decene.

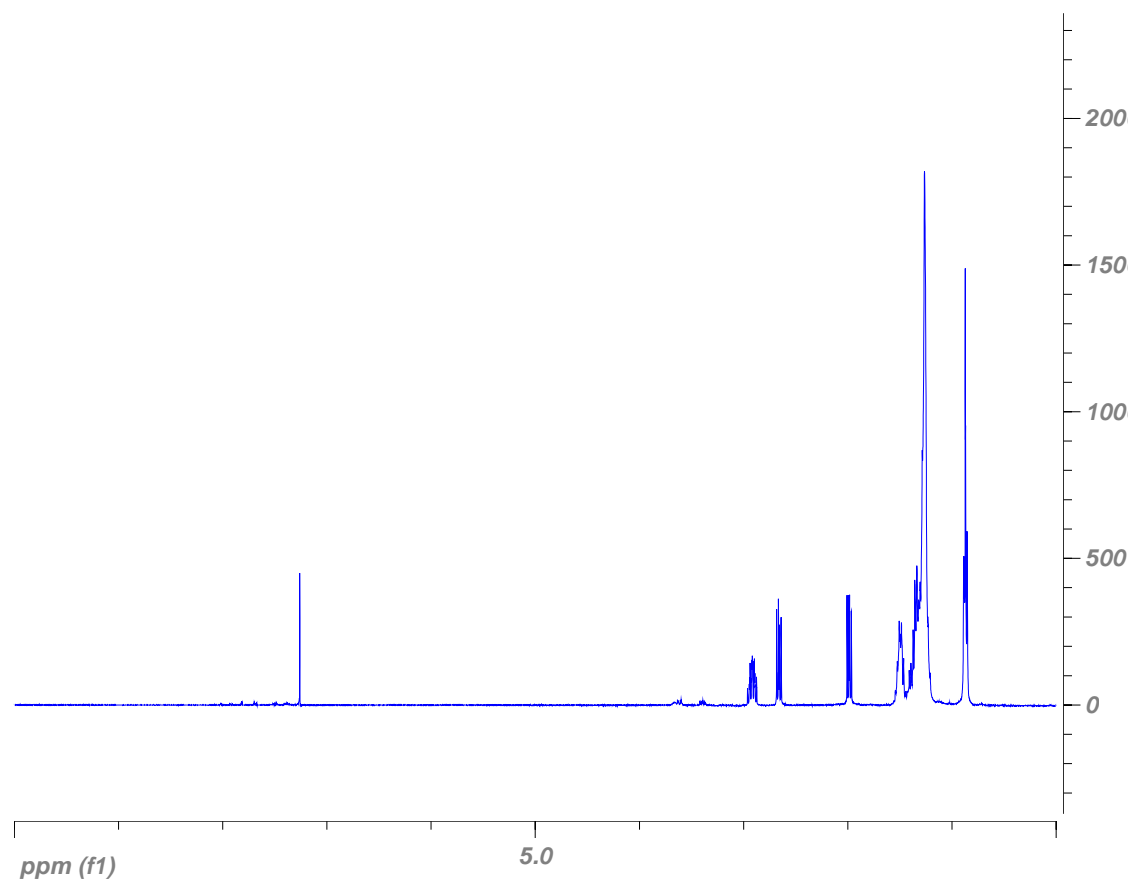


Figure 5-5: ^1H NMR of n-octyl thirane-1-oxide in CDCl_3 .

A LC-MS with positive electrospray ionization gave a mass to charge ratio of 189 which is one more than the molecular mass of 188, as one would expect. Elemental analysis gave very good agreement with carbon value of 63.63 versus the calculated 63.77 and hydrogen value of 10.86 versus the calculated value of 10.70. Infrared spectroscopy gave a strong absorbance at 1067 cm^{-1} typical of episulfoxides. The epoxidation was also shown not to be stereoselective, consequently the first step's product is a racemate. The second oxidation is stereospecific for the anti isomer so the racemic mixture is maintained. Thus the isolated compound is clearly n-octyl thiirane oxide in very high purity.

Determination of Critical Micelle Concentration

The most common process to characterize a surfactant is determination of critical micelle concentration (CMC). The CMC provides a value that can be used to compare surfactants' quality: the lower the CMC, the better the surfactant. This is straightforward since a lower CMC requires less surfactant to solubilize the same amount of organic in a o/w emulsion. Obviously, the CMC also proves the ability of the molecule to create a micellar environment.

Four different methods were used to determine the CMC and the results are shown in figure 5-6. The method of dye solubility was developed by Schott. The dye, Sudan III, absorbs at $\lambda_{\text{max}}=523\text{ nm}$ and has limited solubility in water. At the point where micelles form, the concentration increases dramatically. The intersection of the horizontal line at concentrations below the CMC and the vertical line above the CMC provides a value for the CMC of 6.4 mM. The alternate method is to find the x intercept

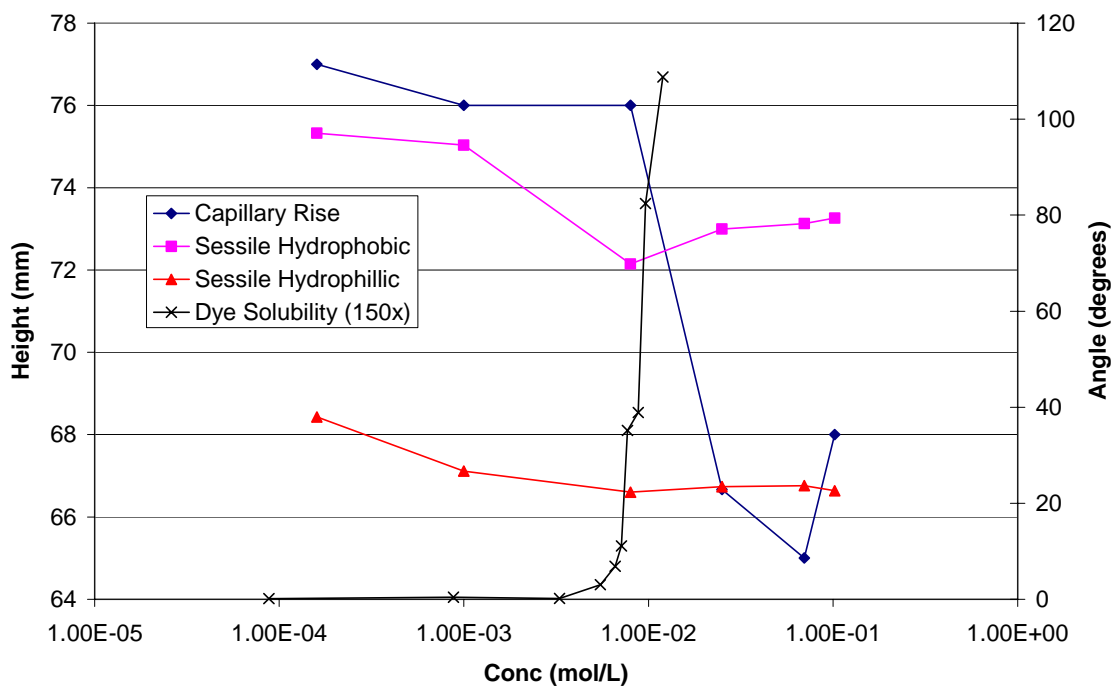


Figure 5-6: Critical Micelle Concentration of 1-octyl thirane-1-oxide in water by capillary rise (diamond), hydrophobic sessile drop contact angle (square), hydrophilic sessile drop contact angle (triangle), and Sudan III dye solubility (x).

of the straight line above the CMC. Using the same data this method gives a CMC of 6.3 mM, essentially the same as the other method. These values compare favorably to the values of common surfactants SDS (8.2 mM), n-dodecyltrimethylammonium bromide (15.2 mM) and chlorpromazine hydrochloride (25.5 mM) (Perez-Rodriguez, Gerardo et al. 1998).

$$\gamma_{SG} - \gamma_{SL} = \gamma_{LG} \cos \theta$$

Equation 5-1: Young's equation

The value from dye solubility was verified by several methods which are all measurements of surface tension which also changes significantly at the CMC. The contact angle of a sessile drop is related to the surface tension by Young's equation (Shah 1992). The surface tension of the solid surface does not change and the surface tension of the gas-liquid interface is assumed to change much less than that of the liquid-solid interface. Thus, the CMC can be shown by plotting the angle versus concentration since the angle is directly proportional to the liquid-solid surface tension. Both the hydrophobic and hydrophilic sessile drop techniques gave similar behavior with a less obvious change of angle with the hydrophilic surface because the bulk fluid is water. Both methods gave a CMC of 8.0 mM which is as close as the concentration series could get to a value of 6.4 mM. Additionally, different methods can result in somewhat different values for CMC.

Finally, capillary rise was also employed to verify CMC. In a capillary, the rise of liquid level is caused by the surface tension (Fuerstenau 2002) and balanced by the

weight of the fluid. Equations 5-2 through 5-4 show this and solve for surface tension which is proportional to the height. Thus the height can be plotted against surfactant concentration to give a CMC. Capillary rise gives a clear change in surface tension at 8.0 mM indicated a CMC. Although the three surface tension measurements did not have enough data points to exactly pinpoint a CMC, they all agree and solidify the value of 6.4 mM found using dye solubility.

$$F_c = W$$

$$2\pi r\gamma = \rho gh(\pi r^2)$$

$$\gamma = \frac{\rho ghr}{2}$$

Equations 5-2,5-3,5-4: Force balance between capillary forces and gravity: solving for surface tension.

Decomposition of Surfactant

The decomposition of the surfactant was verified via GC-MS and LC-MS and then the effect of heating on an emulsion was probed utilizing the same dye experiment used in CMC determination. The decomposition of the surfactant was initially verified in organic solvent in a GC-MS. Even a relatively cold inlet of 100°C resulted in only 1-decene observed on the trace. In an effort to get decomposition rate data, the pure surfactant was heated without solvent in an oil bath. Samples were taken at five and fifteen minutes at 100° and 120°C. At 120° all surfactant had decomposed in five minutes while at 100°C all surfactant had decomposed in fifteen minutes. The only peak observed was 1-decene showing quantitative loss of n-octyl thiirane-1-oxide.

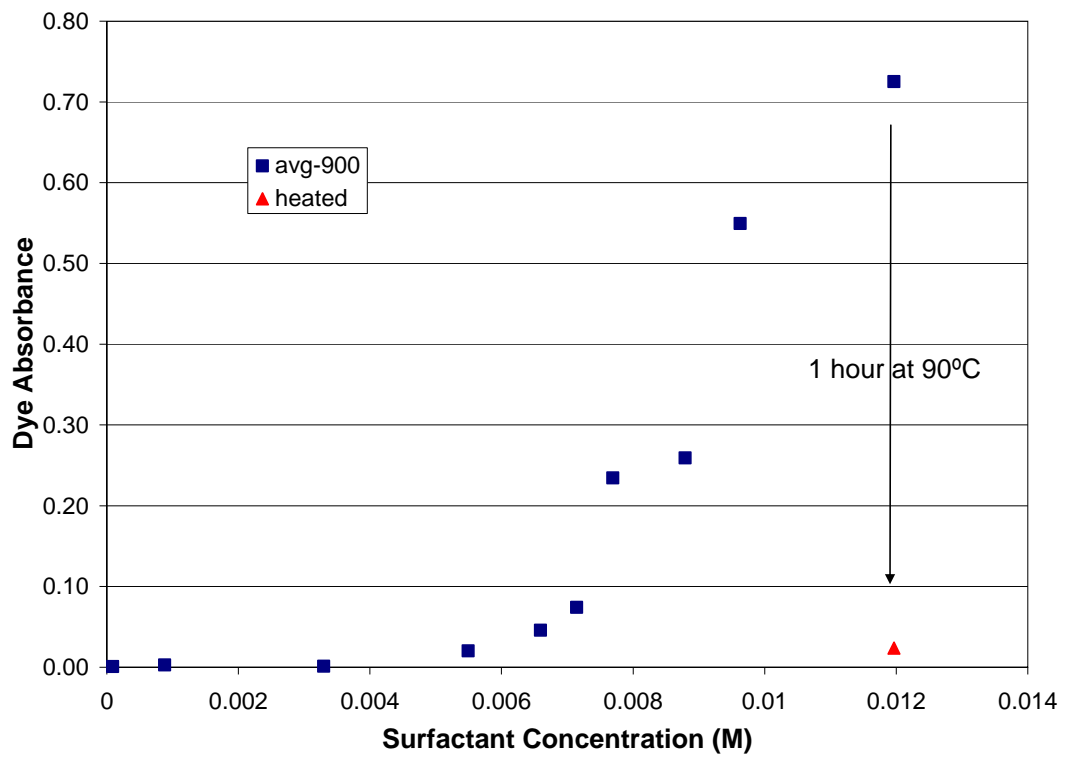


Figure 5-7: Loss of surface activity by heating the solution for 1 hour at 90°C.

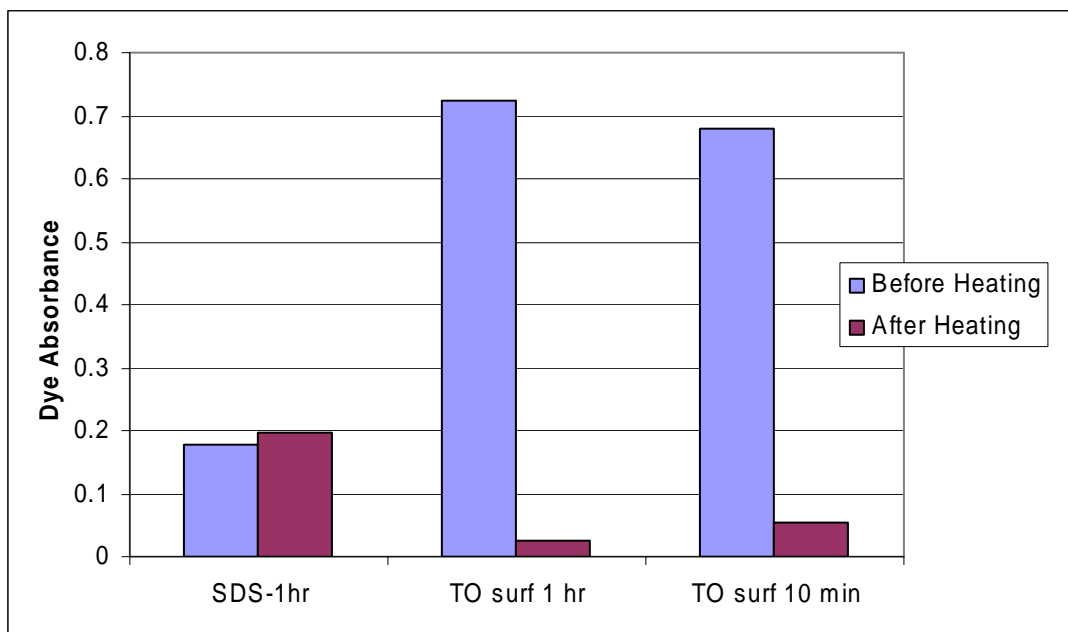


Figure 5-8: Comparison of the dye solubility of 1-octyl thirane-1-oxide and sodium dodecyl sulfate before (blue) and after heating (red) at 90°C for one hour and for ten minutes.

The effect of heating an emulsion was tested by looking at dye solubility of Sudan III. Two samples of n-octyl thiirane-1-oxide and one sample of sodium dodecyl sulfate (SDS) at a concentration of ~12 mM were prepared and their Sudan III solubility was measured as was done with the CMC experiments. Then, one thiirane oxide surfactant solution was heated at 90°C for 10 minutes while the other thiirane oxide solution and the SDS solution were heated at 90°C for one hour. After sonicating, settling, and filtering, a new UV-vis absorbance was measured, also shown in figure 5-7 for the n-octylthiirane-1-oxide heated for 1 hour. Figure 5-8 shows that the thiirane surfactant lost appreciable surface activity in a relatively short amount of time while the SDS remained essentially unchanged. The slight increase in concentration for SDS is expected due to water evaporation at 90°C and means that the actual values for the thiirane surfactant are higher than they should be as well.

Conclusions

We have synthesized and characterized a novel, cleavable surfactant, n-octyl thiirane-1-oxide, which can be broken into a hydrophobic liquid and a gas at elevated temperatures to break emulsions. No matter what the external “trigger” is, all other previously described cleavable surfactants result in a molecule in the aqueous phase. The surfactant described here avoids the downstream processing and possible CMC of the resulting molecule. There are a wide range of possible applications for this cleavable surfactant ranging from biochemistry (Epstein, Jones et al. 1982) to nanoparticle formation (Kitchens, McLeod et al. 2003). The critical micelle concentration was

determined to be 6.4 mM and the loss of CMC was verified by heating at 90°C for only ten minutes.

References

- Adamson, A. W. and A. P. Gast (1997). Physical Chemistry of Surfaces. New York, Wiley-Interscience.
- Bartscherer, K. A., M. Minier, et al. (1995). "Microemulsions in Compressible Fluids- A Review." Fluid Phase Equilibria **107**: 93.
- DeSimone, J. M., Z. Guan, et al. (1992). "Synthesis of Fluoropolymers in Supercritical Carbon Dioxide." Science **257**: 945.
- Dominguez, A., A. Fernandez, et al. (1997). "Determination of Critical Micelle Concentration of Some Surfactants by Three Techniques." Chemical Education **74**(10): 1227.
- Epstein, W. W., D. S. Jones, et al. (1982). "The Synthesis of a Photolabile Detergent and Its Use in the Isolation and Characterization of Protein." Analytical Biochemistry **119**: 304.
- Fromyr, T., F. K. Hansen, et al. (2001). "Adsorption and Surface Elastic Properties of Corresponding Fluorinated and Nonfluorinated Cationic Polymer Films Measured by Drop Shape Analysis." Langmuir **17**(17): 5236.
- Fuerstenau, D. W. (2002). "Equilibrium and Nonequilibrium Phenomena Associated with the Adsorption of Ionic Surfactants at Solid-Water Interfaces." Journal of Colloid and Interface Science **256**(1): 79.
- Hartzel, G. E. and J. N. Paige (1966). "Ethylene Episulfoxide." J. Am. Chem. Soc. **88**(11): 2616.
- Hayashi, Y., F. Shirai, et al. (1985). "Synthesis and Properties of 2-Alkoxy-N,N-Dimethylethylamine N-Oxides." Journal of the American Oil Chemists Society **62**(3): 555.
- Holmberg, K., Ed. (2003). Novel Surfactants: Preparation, Applications, and Biodegradability. Surfactant Science. New York, Marcel Dekker, Inc.
- Itoh, T., K. Nagata, et al. (1997). "Reaction of Nitric Oxide with Amines." J. Org. Chem. **62**(3582-3585).
- Iyer, M., D. G. Hayes, et al. (2001). "Synthesis of pH-Degradable Nonionic Surfactants and Their Application in Microemulsions." Langmuir **17**: 6816.
- Jaegar, D. A., J. Mohebalian, et al. (1990). "Acid-Catalyzed Hydrolysis and Monolayer Properties of Ketal-Based Cleavable Surfactants." Langmuir **6**: 547.

- Jaegar, D. A., J. Wettstein, et al. (1998). "Cleavable Quaternary Hydrazinium Surfactants." Langmuir **14**: 1940.
- Johnston, K. P., K. L. Harrison, et al. (1996). "Water-in-Carbon Dioxide Microemulsions: A New Environment for Hydrophiles Including Proteins." Science **271**: 624.
- Jonsson, B., Lindman, et al. (1998). Surfactants and Polymers in Aqueous Solution, John Wiley and Sons.
- Kastens, M. L. and J. J. Ayo Jr. (1950). "Pioneer Surfactant." Industrial and Engineering Chemistry **42**: 1626.
- Kitchens, C. L., M. C. McLeod, et al. (2003). "Solvent Effects on the Growth and Steric Stabilization of Copper Metallic Nanoparticles in Liquid Alkane/AOT Reverse Micelle Systems." J. Phys. Chem. B **107**(41): 11331.
- Masuyama, A., C. Endo, et al. (2000). "Ozone-Cleavable Gemini Surfactants. Their Surface-Active Properties, Ozonolysis, and Biodegradability." Langmuir **16**: 368.
- Mathias, L. Macrogalleria.
- McElhanon, J. R., T. Zifer, et al. (2005). "Thermally Cleavable Surfactants Based on Furan-Maleimide Diels-Alder Adducts." Langmuir **21**: 3259.
- Metzner, B., K. Meindl, et al. (1994). "UV laser photolysis and quantum yields of para-substituted phenyldiazosulfonate surfactants." J. Photochem. Photobiol. A. Chem. **83**: 129.
- Nuyken, O., K. Meindl, et al. (1994). "Photolabile surfactants based on the diazosulfonate group I. 4-n-Alkylbenzenediazosulfonates." J. Photochem. Photobiol. A. Chem. **81**: 45.
- Nuyken, O., K. Meindl, et al. (1995). "Photolabile Surfactants based on the diazosulphone group 2. 4-(Acyloxy)benzenediazosulphonates and 4-(acylamino)benzenediazosulphonates." J. Photochem. Photobiol. A. Chem. **85**: 291.
- Ryoo, W., S. E. Webb, et al. (2003). "Water-in-Carbon Dioxide Microemulsions with Methylated Branched Hydrocarbon Surfactants." Ind. Eng. Chem. Res. **42**(25): 6348.
- Schott, H. (1966). "Solubilization of a Water-Insoluble Dye as a Method for Determining Micellar Molecular Weights." Journal of Physical Chemistry **70**(9): 2966.

- Schott, H. (1967). "Solubilization of a Water-Insoluble Dye. II." Journal of Physical Chemistry **71**(11): 3611.
- Shah, D. (1992). Introduction to Colloid and Interface Chemistry.
- Smital, T., T. Luckenbach, et al. (2004). "Emerging contaminants- pesticides, PPCPs, microbial degradation products and natural substances as inhibitors of multixenobiotic defense in aquatic organisms." Mutation Research **552**(1-2): 101.
- Texter, J., Ed. (2001). Reactions and Synthesis in Surfactant Systems. Surfactant Science Series. New York, Marcel Dekker, Inc.
- Iyer, M., D. G. Hayes, et al. (2001). "Synthesis of pH-Degradable Nonionic Surfactants and Their Application in Microemulsions." Langmuir **17**: 6816.
- Perez-Rodriguez, M., P. Gerardo, et al. (1998). "A Comparative Study of the Determination of the Critical Micelle Concentration by Conductivity and Dielectric Constant Measurements." Langmuir **14**: 4422.

CHAPTER VI

MELTING POINT DEPRESSION OF IONIC “LIQUIDS” WITH CO₂

Introduction

Ionic liquids represent an exciting alternative to volatile organic solvents commonly used in processing. Their negligible vapor pressure suggests a reduction in emissions relative to other solvents. Furthermore, ionic liquids are also being touted as “designer solvents” in which the cation and anion can be carefully tailored to produce a desired solvent property. However, many of the cation-anion combinations are not actually liquid at room temperature. Combining carbon dioxide with ionic solids produces a large melting point depression and therefore significantly increases the liquid operating range of these substances. We have developed a system for readily quantifying the freezing eutectic of CO₂-ionic liquid mixtures and have done so for tetrabutyl ammonium tetrafluoroborate and tetrahexyl ammonium bromide. The results indicate a high level of control over the melting point of CO₂-IL systems, thus enabling the use of many more ionic compounds for solvent replacement.

An ionic liquid (IL) is an organic salt which melts below 100°C. More commonly, room temperature ionic liquids (RTILs) are those which are liquids at ambient temperatures. Commonly, the cation is organic while the anion is a common inorganic ion but this is not always the case. The majority of ionic liquids employed in research have either had an imidazolium, tetraalkylammonium or tetraalkylphosphonium

cation as shown in Figure 6-1. The length of the alkyl chains vary significantly depending on the intended use of the IL. Many tetralkylammonium cations have all four carbon chains the same length such as: tetrabutylammonium [TBA] and tetraethylammonium [TEA]. Many of these salts were originally used for phase transfer catalysis to transfer ions from aqueous phases into organic phases (Starks, Liotta et al. 1994). Commonly used anions include: tetrafluoroborate [BF₄], hexafluorophosphate [PF₆], bis(trifluoromethylsulfonyl)imide [BTA], bromide [Br], chloride [Cl], and many, many others.

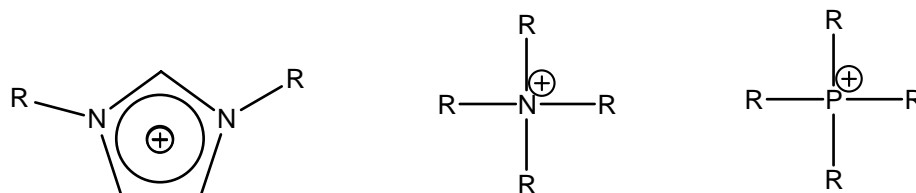


Figure 6-1: Most commonly employed ionic liquid cations

No matter what the ion combination is, the defining characteristic of ILs is their undetectable vapor pressure. Therefore, any application that has concerns of volatile organic compound (VOC) emissions, could potentially utilize ionic liquids. Recently, it has been shown through measurement of octanol-water partition coefficients, that ionic liquids should not bioaccumulate (Ropel, Belveze et al. 2005). Not all toxicity concerns have been resolved, but these preliminary results seem to show ionic liquids are more environmentally friendly than conventional organic solvents.

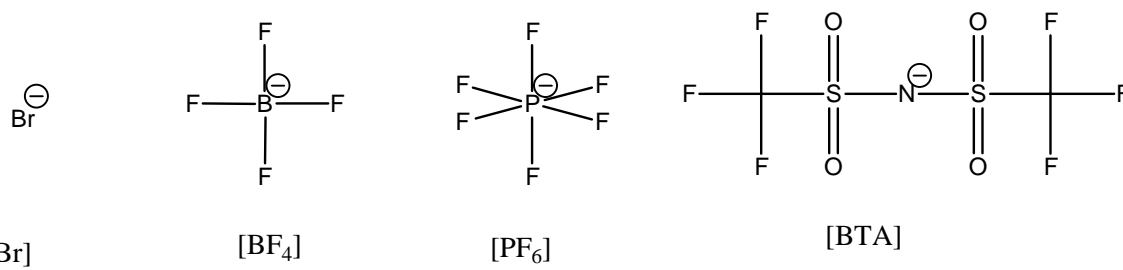
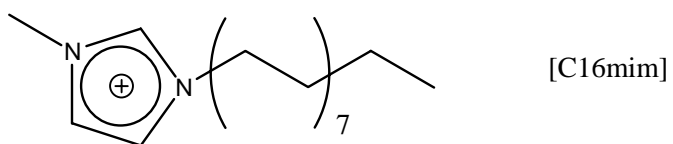
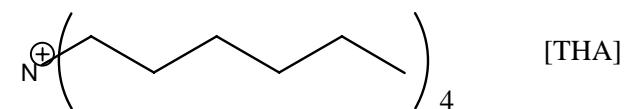
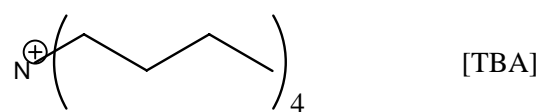


Figure 6-2: Ionic liquid cations and anions used in this work with their abbreviations

Not surprisingly then, ionic liquids have been researched in almost every possible realm of chemistry and chemical engineering at a growing number of laboratories. Examples of uses include every thing from the common organic synthesis (Welton 1999; Gordon 2001; Olivier-Bourbigou and Magna 2002; Wasserscheid and Welton 2002), biocatalysis (Cull, Holbrey et al. 2000; Nara, Harjani et al. 2002), and electrochemistry (Hyk and Stojek 1998) to such fields as energetic materials (Katritzky, Singh et al. 2005) and uranium sequestration (Visser, Jensen et al. 2003). There is still a wide array of untapped possible applications due to the “designer” nature of ionic liquids. Since each ion can be chosen from thousands of different ions, the ion pair can be specifically designed for the application.

Despite the fact that ionic liquids are a very immature field, there has already been one implementation in an industrial process. BASF developed the BASIL (biphasic acid scavenging utilizing ionic liquids) process which creates the ionic liquid, 1-alkylimidazolium salt, after the 1-alkylimidazole reacts with a proton. The ionic liquid is then extracted, deprotonated, and recycled. This system is useful in reactions where acids are a byproduct such as esterifications (Pagano 2004).

Further implementation of ionic liquids into more processes is hindered by two major issues: removal of the product from the ionic liquid and high melting point of a desired ion combination for the application. There has been significant research on the solubility of CO₂ in ionic liquids (Kazarian, Sakellarios et al. 2002; Scurto, Aki et al. 2002; Lu, Liotta et al. 2003; Cadena, Anthony et al. 2004; Solinas, Pfaltz et al. 2004). Carbon dioxide is frequently used in green processing due to its benign characteristics (Eckert, Knutson et al. 1996). From the work of Brennecke, it is known that CO₂ works

much better than any other known extraction solvent for ionic liquids because some organics are soluble in CO₂ but ionic liquids are not soluble in CO₂ (Blanchard, Hancu et al. 1999; Blanchard and Brennecke 2001).

The problem of lowering the melting point of ionic liquids is also significant. As one would expect, when the applications of the ionic liquid class of solvents are so broad, the cation-anion combination is just as varied, particularly in the field on “designer solvents.” While there is some empirical knowledge of which ions will melt lower than others, there are no predictive equations or rules to follow. However, the high melting point can also be solved with CO₂. Carbon dioxide has been shown to reduce the melting point of several known organic solids (Cheong, Zhang et al. 1986; White and Lira 1989; Fukne-Kokot, Skerget et al. 2003). CO₂ has also been shown to accelerate reactions in solventless systems through melting point depression of organic solids (Jessop, Wynne et al. 2000). Additionally, both Scurto (Scurto and Leitner 2005) and Kazarian (Kazarian, Sakellarios et al. 2002) have recently shown that CO₂ can be used to depress the melting point of some ionic liquids quite significantly. Leitner also showed ionic liquid-CO₂ biphasic systems for enzymatic reactions where melting point depression would be ideally suited (Reetz, Wiesenhoefer et al. 2003). Thus, CO₂ could be used as a solvent (to lower the melting point) and as the extraction solvent after the reaction is complete.

Previously, no one has measured the temperature-composition (T-x) diagram of any ionic liquids to explain and quantify the melting point depression observed by Scurto for ionic liquids (Scurto and Leitner 2005). In this work, we utilize a new method for measuring T-x diagrams for several ionic liquids. We also confirmed the accuracy of the

method by comparing data to previously measured data for naphthalene (Cheong, Zhang et al. 1986).

Experimental Materials

All chemical were purchased from Sigma-Aldrich unless otherwise noted. The naphthalene (99%), methanol (extra dry with molecular sieves, <50ppm water, Acros), and Aquastart Combitrant 1 (EMD chemicals) were used as purchased. SFE/SFC grade carbon dioxide was purchased from Airgas and filtered prior to use. All ionic liquids were further purified by drying at room temperature under vacuum of 10^{-3} torr for 48 hours and stored at room temperature under nitrogen atmosphere. The ionic liquids used were: tetrabutylammonium tetrafluoroborate [TBA][BF₄] 99+%, tetrahexylammonium bromide [THA][Br] 99%, tetrabutylammonium bromide [TBA][Br] 99%, tetraethylammonium bis(trifluoromethylsulfonyl)imide [TEA][BTA] 99+%.

Apparatus and Procedures

Cheong et al measured the temperature composition of naphthalene-CO₂ using what they called the “first freezing point method” (Cheong, Zhang et al. 1986). This was done by observing the initial appearance of solid, followed by sampling from a high pressure view cell. An equation of state, paired with pressure, temperature, and volume data, provided the gas phase composition. Gravimetric measurement of the solid phase after dissolution and drying gave the other compositions. Our group developed a first freezing point method where the composition could be determined without sampling.

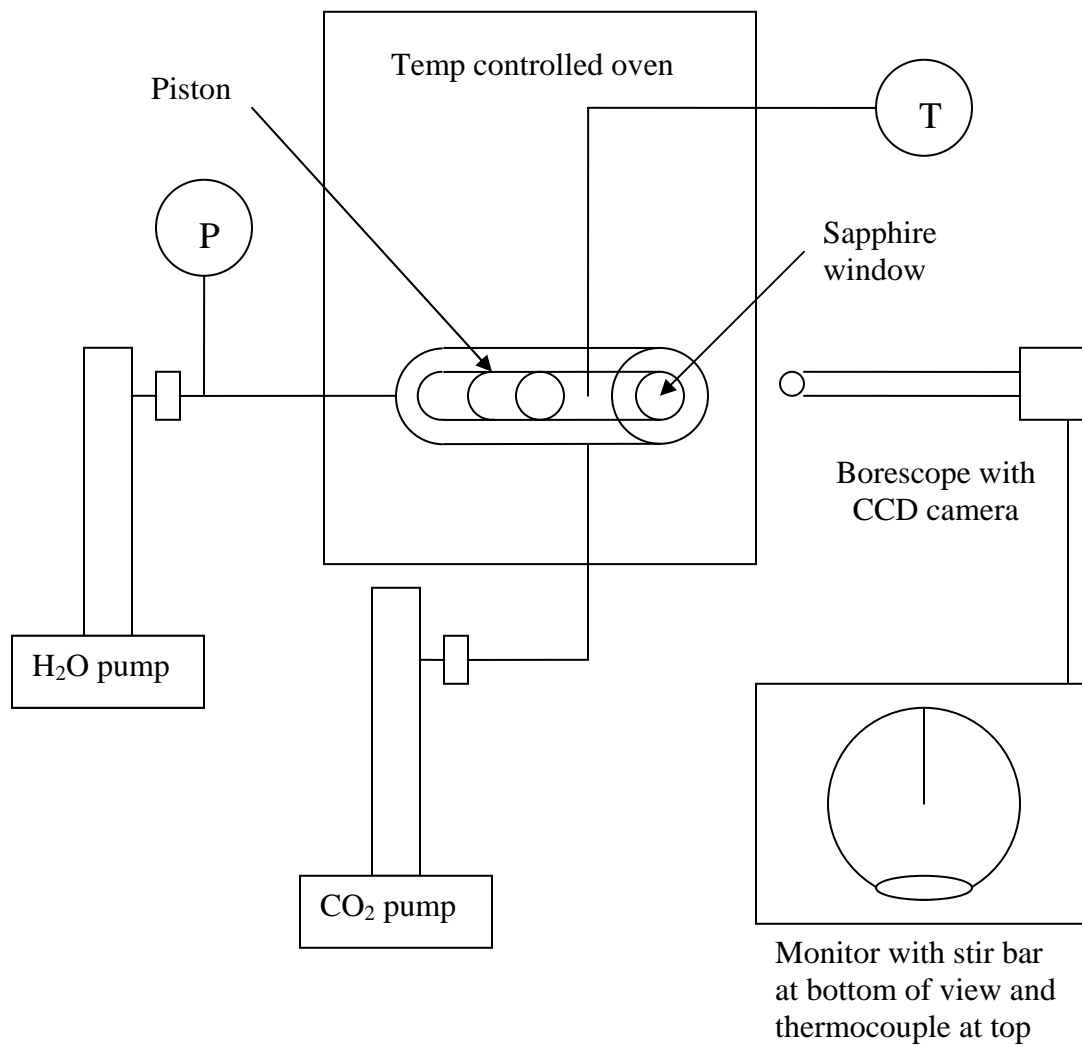


Figure 6-3: Schematic of the melting point apparatus.

First, a known mass of organic solid was loaded into a variable volume high pressure view cell, and the pure solid melting point was confirmed before adding any CO₂. We then loaded the cell with a known quantity of CO₂ from a syringe pump and allowed the cell to reach equilibrium with temperature and pressure such that there was a single liquid phase. Next, we cooled the mixture isobarically until the first crystal formed. Generally the entire contents froze quickly thereafter. We know the composition of the single liquid phase since there are only two components. We assume the first crystal of pure solid has a negligible impact on the overall composition and thus the composition at the freezing point is known. We also assume that the overpressure has no impact on the melting point at the modest pressures used in this study.

After one freezing point is measured, we reheated the system back into one phase and repeated the process. We repeated until two consecutive data points were identical to ensure the system was at equilibrium, which can take up to 24 hours, depending on the solid. The measurements were also done at different cooling rates to ensure accurate melting points.

All measurements were carried out in a variable-volume windowed vessel (1.59 cm i.d., 20 cm³ maximum volume) similar to that used by McHugh (Kirby and McHugh 1999) and previously used in our group shown in Figure 6-3 (Brown, Hallett et al. 2000). The vessel window and variable-volume piston were sealed with Buna-N o-rings. Phase boundaries were measured by visually observing the freezing point through a 2.54 cm diameter sapphire window (1.27 cm viewable area) with a CCD camera (Sony) mounted on a 0.635 cm borescope (Olympus). The borescope and video camera not only allowed for safe observation of the phase equilibria, but also provided a significant magnification

of the viewable area. The binary mixtures were stirred with a Teflon-coated stir bar coupled with an external magnet. The entire cell was placed in a thermostated air bath (modified Varian 3400 gas chromatograph) with temperature control better than ± 0.5 K. Precise temperature control was not required as freezing points were induced and observed while cooling the vessel. The temperature was measured with a hand-held readout (HH-22 Omega) and thermocouple (Omega Type K) inserted into the center of the phase equilibria vessel. The thermocouple response time was on the order of seconds. The combination of thermocouple and readout was accurate to ± 0.2 K and calibrated for each experiment against a platinum RTD (Omega PRP-4) with a DP251 precision RTD bench top thermometer (DP251 Omega) accurate to ± 0.025 K and traceable to NIST. Back-pressure was applied to the piston with a syringe pump (ISCO 100D) operated at constant pressure. To avoid any vapor phase, the pressure was held constant at 210 bar measured with a Druck DPI 260 gauge with PDCR 910 transducer accurate to ± 0.01 bar.

To ensure the validity of our new system, we conducted the new freezing point method on a naphthalene-CO₂ system. Many sources give T-P data for a naphthalene-CO₂ equilibria, but Cheong et al was the only source to provide T-x data (Cheong, Zhang et al. 1986). After verifying our method, we attempted to measure four ionic liquids which were previously purified and stored under nitrogen atmosphere. The high pressure cell was also loaded under nitrogen atmosphere to avoid water introduction into the sample.

After secondary purification, the ionic solids were tested for water content. Samples were prepared by dissolving 1 gram of solid in 0.5 mL extra dry methanol. The water content of both the methanol and the dissolved solids were measured using a Karl

Fisher Titrator, model DL31 from Mettler Toledo. Aquastar Combititrant 1 was used for the titrant.

Results and Discussion

Initially, the new non-sampling first freezing point method needed to be proven accurate. This was done by measuring the temperature-composition (T-x) curve of naphthalene-CO₂ since naphthalene is a solid with a melting point similar to many ionic liquids and there was data in the literature to replicate. One difference of note is naphthalene is known to have higher solubility in CO₂ than most ionic liquids. Figure 6-4 shows a comparison of the literature results (Cheong, Zhang et al. 1986), the results from this work, the ideal prediction and the MOSCED (modified separation of cohesive energy density) prediction (Thomas and Eckert 1984; Lazzaroni, Bush et al. 2005). The ideal solubility is only based on the melting point and enthalpy of fusion (ΔH_{fus}) which are shown in Table 6-1 (McCullough, Finke et al. 1957; Coker, Ambrose et al. 1970). The ideal prediction (Equation 6-1) for this system is a poor predictor so the MOSCED prediction was included for reference. The MOSCED model (Equation 6-2) fits four parameters (hydrogen bond acidity and basicity, polarizability, and dipolarity) to experimental data to calculate infinite dilution activity coefficients. The calculated activity coefficients were used in the Wilson equation to predict the solubility line shown in Figure 6-4. The results presented here are in good agreement with those reported by Cheong and thus the same method was used to measure T-x diagrams for several ionic liquids.

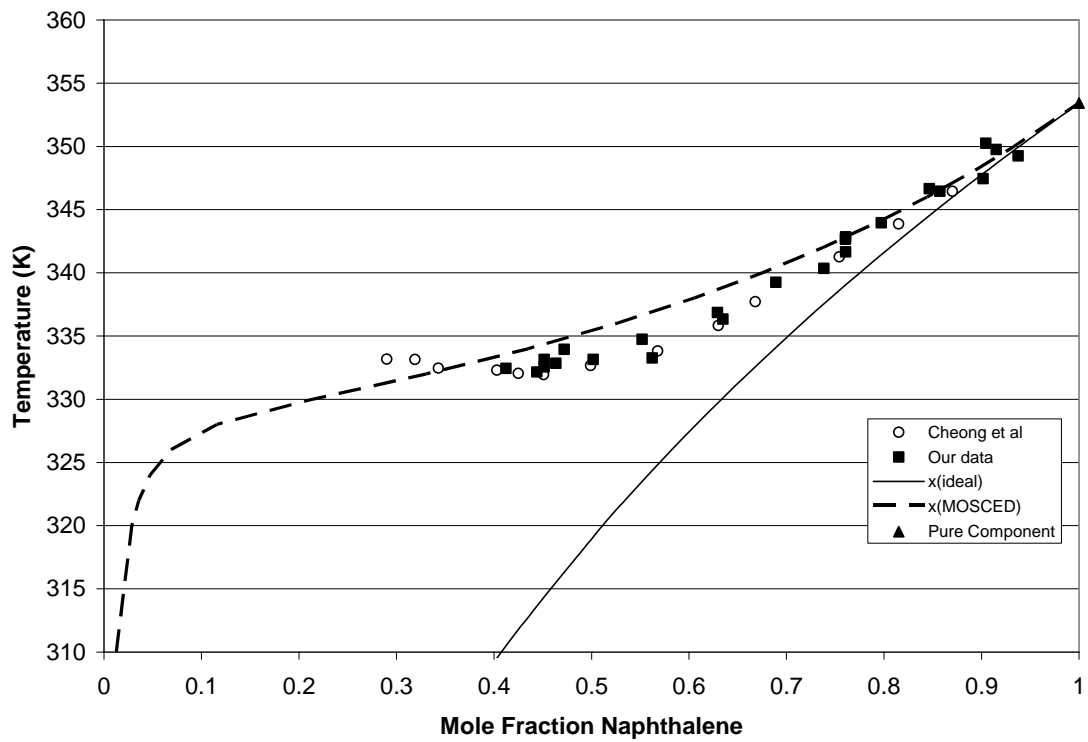


Figure 6-4: Temperature-composition (T-x) diagram for naphthalene-CO₂: (circle-Cheong et al, square-this work, line-ideal solubility, dash line-MOSCED solubility, triangle-pure component value)

$$x = \frac{1}{\exp\left(\frac{\Delta H_{fus}}{R} \left(\frac{T_m - T}{T_m T}\right)\right)}$$

Equation 6-1: Ideal solubility calculation

$$\ln \gamma_2^\infty = \frac{v_2}{RT} \left[(\lambda_1 - \lambda_2)^2 + \frac{q_1^2 q_2^2 (\tau_1 - \tau_2)^2}{\psi_1} + \frac{(\alpha_1 - \alpha_2)(\beta_1 - \beta_2)}{\xi_1} \right] + \ln \left(\frac{v_2}{v_1} \right)^{aa} + 1 - \left(\frac{v_2}{v_1} \right)^{aa}$$

Equation 6-2: MOSCED equation for prediction of infinite dilution activity coefficients.

Table 6-1: Enthalpy of fusion, enthalpy of transition, melting temperature, and transition temperature values and references.

Compound	$\Delta H_{fus}(\text{J/mol})$	Tm (°C)	$\Delta H_{trans}(\text{J/mol})$	Ttrans (°C)	Reference
Naphthalene	18980	80	-	-	McCullough et al
[THA][Br]	15909	100	6688/12122	32/42	Coker et al
[TBA][BF ₄]	10467	160	6688	68	Coker et al
[C16mim][PF ₆]	500	125	37500	75	Gordon et al

Several ionic liquids were chosen to be measured based on the previous results of Scurto and Leitner. They found a melting point depression of 124°C for [TBA][BF₄] with 150 bar of CO₂ pressure. We predicted we could get a significant melting point depression with much less CO₂. Scurto and Leitner also found significant melting point depression with [THA][Br] and [TEA][BTA] so these were investigated as well. Finally, [TBA][Br] was tested because the anion is common with [THA][Br] and the cation is common with [TBA][BF₄] so insight into the impact of changing the cation or anion was expected.

The results for [TBA][BF₄] are shown in Figure 6-5. The ideal solubility calculated from Equation 6-3 is also included as a reference. Since the ionic liquids

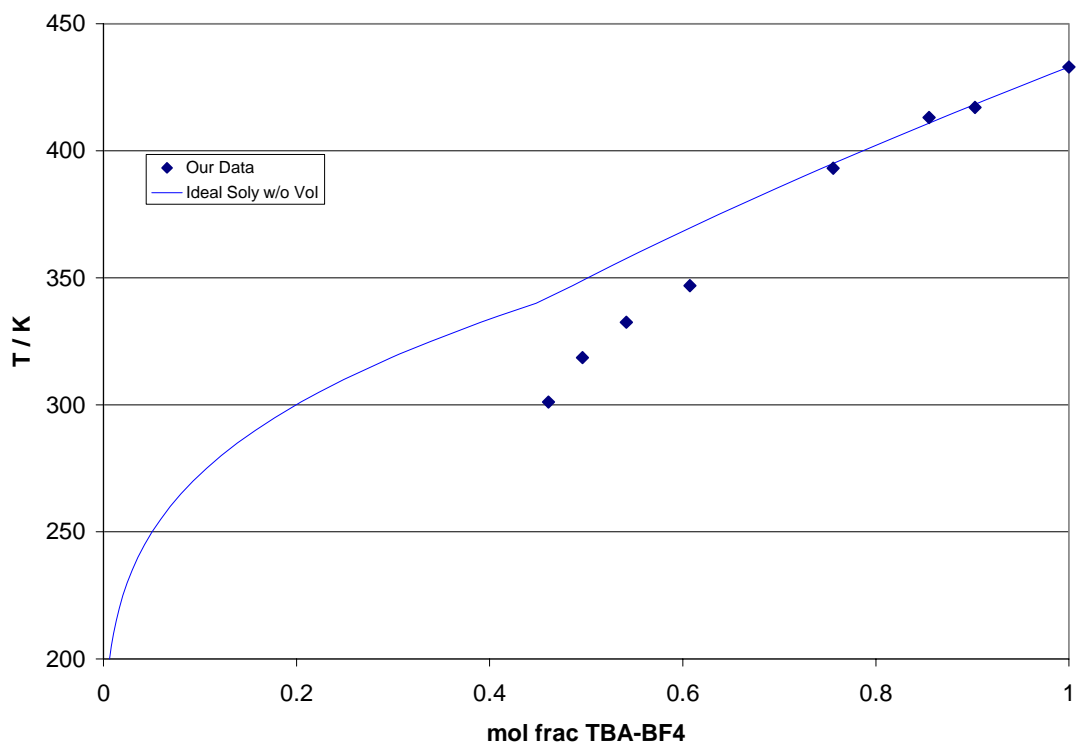


Figure 6-5: Temperature-composition (T-x) diagram for tetrabutylammonium tetrafluoroborate [TBA][BF₄]-CO₂: diamonds-this work, line-ideal solubility.

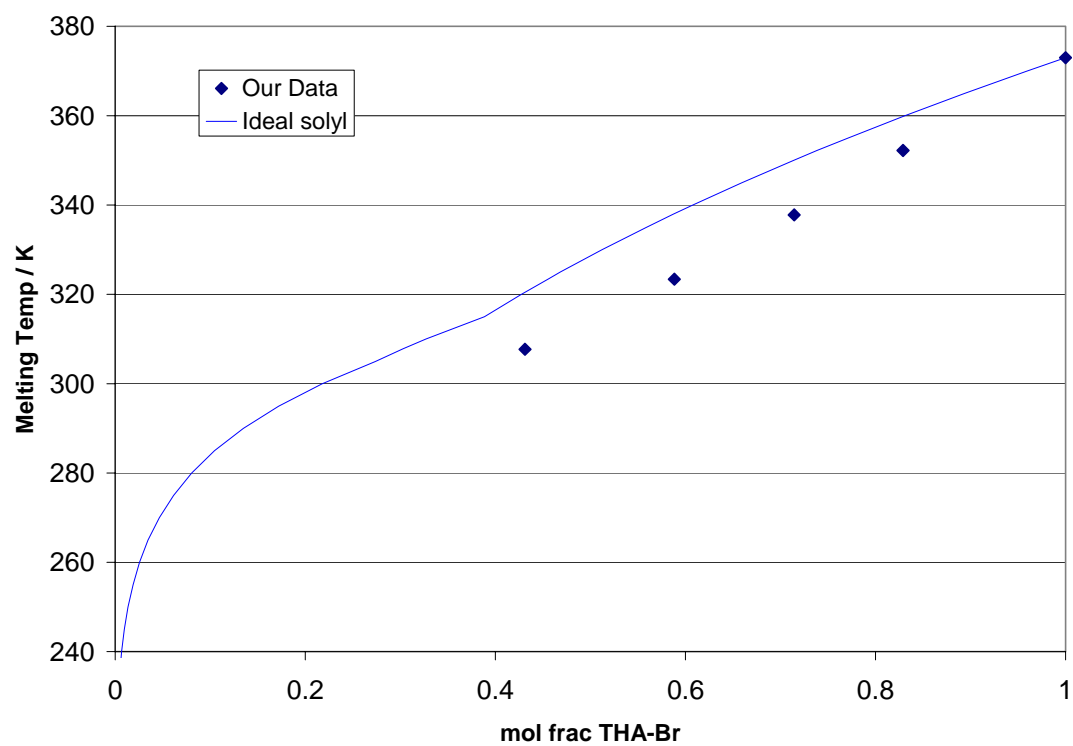


Figure 6-6: Temperature-composition (T-x) diagram for tetrahexylammonium bromide [THA][Br]-CO₂: diamonds-this work, line-ideal solubility.

undergo a solid-solid transition, an additional term is included in the ideal solubility. Above the solid transition temperature Equation 6-1 is used. There is not sufficient data in the literature for a MOSCED prediction and those measurements were outside the scope of this work. The results show a melting point depression of 130° at a mole fraction near 0.5. While the CO₂ pressure cannot be measured in this experimental apparatus, nor can temperatures below ~300°K, the results seem to agree with Scurto and Leitner and elucidate the effect the CO₂ has on [TBA][BF₄].

$$x = \frac{1}{\exp\left(\frac{\Delta H_{fus}}{R} \frac{(T_m - T)}{T_m T} + \frac{\Delta H_{trans}}{R} \frac{(T_{trans} - T)}{T_{trans} T}\right)}$$

Equation 6-3: Ideal solubility with a solid transition state

Figure 6-6 shows the results for [THA][Br] which are very similar to that of [TBA][BF₄]. The ideal solubility is again included and it is clear that for both ionic liquids, the T-x curve falls well below the ideal solubility while for naphthalene the T-x curve is above ideality. This means that both ionic liquids have activity coefficients lower than unity. Since there is no reason to believe there should be a significant specific interaction between the ionic liquid and the CO₂, we believe this effect is due to the size difference between the ionic liquid and CO₂. This effect has been shown in the literature for acetaldehyde and methyl formate in glycol ethers and is of similar magnitude to what is observed here (Schiller and Gmehling 1992).

Using the data of Kazarain et al (Kazarain, Sakellarios et al. 2002) with the ideal solubility (Gordon, Holbrey et al. 1998) of their ionic liquid, [C16mim][PF₆], activity

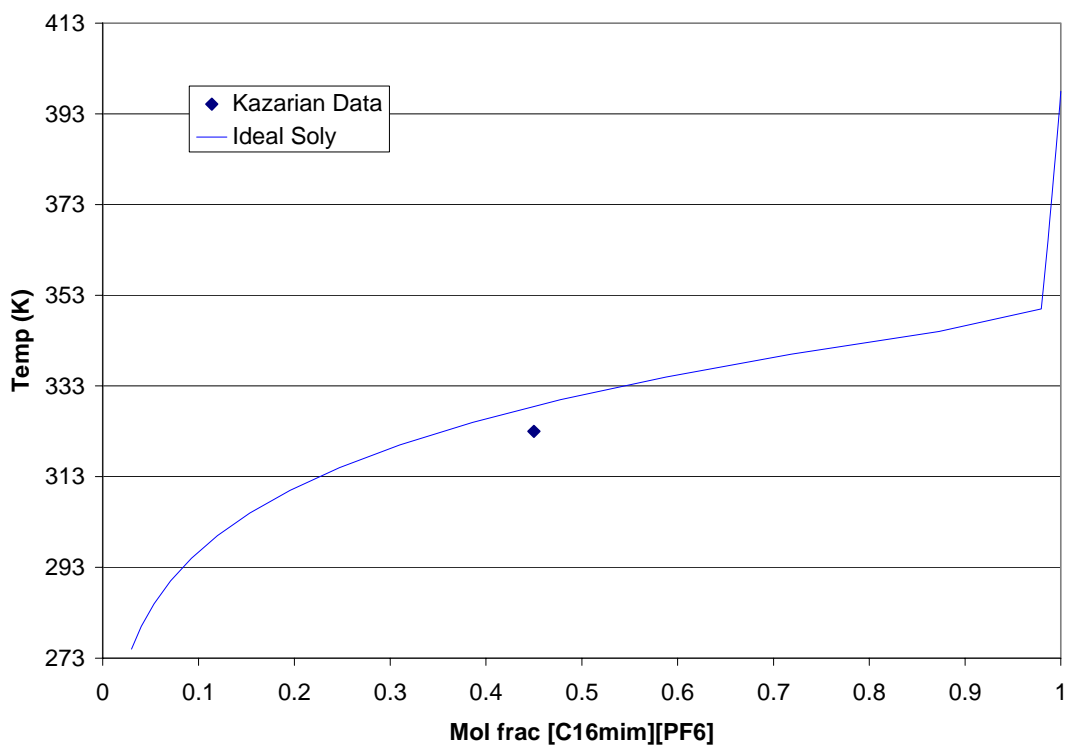


Figure 6-7: Temperature-composition (T-x) diagram for [C16mim][PF₆]-CO₂ from the data of Kazarian et al (2002).

coefficients were again found to be lower than unity (Figure 6-7). Kazarian only measured one melting point and estimated the mole fraction but this data point shows significant nonideality that is greater than the possible error in the estimation.

Similar curves were measured for [TBA][Br] and [TEA][BTA] but repeatability was exceedingly difficult due to long equilibration times. For instance, [TBA][Br] was allowed to equilibrate for 12 hours for a single data point, but the reading had changed after another hour. Some of this effect is due to the stability of the o-rings at high temperature and pressure in the presence of an ionic liquid. However, from these preliminary results, it was clear that both of these ionic liquids would have negative activity coefficients as well. Additionally, melting point depressions of at least 42° and 80° were found for [TBA][Br] and [TEA][BTA] respectively. The latter data point in agreement with the data of Leitner and Scurto while the first was not previously measured.

Table 6-2: Average water content and standard deviation of ionic liquids tested.

Compound	Average Water Content (ppm)	Standard Deviation
[TBA][BF ₄]	194.5	25.7
[THA][Br]	426.5	61.2
[TBA][Br]	125.1	33.1
[TEA][BTA]	161.3	

The water content of all four previously mentioned ionic liquids was also measured. The results from a Karl Fisher titrator are shown in Table 6-2. The water content of all of the ionic liquids were fairly low with the [THA][Br] having the highest by a significant amount. Interestingly, the two ionic liquids that gave problems with their measurement had the lowest water content. This is not surprising since these species are

extremely hygroscopic. Additionally, it is known that the viscosity of ionic liquids is very dependent on their water content (Zhang, Wu et al. 2003). Since it is extremely difficult to get an ionic liquid entirely dry, it is difficult to know the impact of the small amount of water on behavior of the fluids.

In this study only tetraalkylammonium based ionic liquids were investigated but the data of Scurto and Leitner (2005) and Kazarian et al (2002) show the same melting point behavior with CO₂ for imidazolium, tetraalkylphosphonium, and other cations. All tetraalkylammonium and imidazolium based ionic liquids tested give negative deviations from Raoult's law in CO₂. This is not fully understood and further testing of different cations may provide an explanation of this result.

Conclusions

We have developed a unique system for measuring the melting point depression of organic solids, particularly ionic solids. With known concentrations of CO₂ and ionic solid in a pressure view cell, we take the contents of the cell to one phase and visually observe the first crystal form as we reduce the temperature. With this system, no sampling is necessary, and we have proven its accuracy by comparing our data for naphthalene with data from the literature. Our results for [TBA][BF₄] and [THA][Br] of 130 and 65 °C depressions, respectively, indicate that this system can be used to significantly alter the melting point of ionic solids. Additionally, we have shown that all reported literature for ionic liquid-CO₂ mixtures give negative deviations from Raoult's law.

References

- Blanchard, L. A. and J. F. Brennecke (2001). "Recovery of Organic Products from Ionic Liquids Using Supercritical Carbon Dioxide." Ind. Eng. Chem. Res. **40**: 287.
- Blanchard, L. A., D. Hancu, et al. (1999). "Green processing using ionic liquids and CO₂." Nature **399**: 28.
- Brown, J. S., J. P. Hallett, et al. (2000). "Liquid-Liquid Equilibria for Binary Mixtures of Water + Acetophenone, + 1-octanol, + Anisole, and + Toluene from 370K to 550K." J. Chem. Eng. Data **45**: 846.
- Cadena, C., J. L. Anthony, et al. (2004). "Why Is CO₂ So Soluble in Imidazolium-Based Ionic Liquids?" J. Am. Chem. Soc. **126**: 5300.
- Cheong, P. L., D. Zhang, et al. (1986). "High Pressure Phase Equilibria for Binary Systems Involving a Solid Phase." Fluid Phase Equilibria **29**: 555.
- Coker, T. G., J. Ambrose, et al. (1970). "Fusion Properties of Some Ionic Quaternary Ammonium Compounds." J. Am. Chem. Soc. **92**: 5293.
- Cull, S. G., J. D. Holbrey, et al. (2000). "Room-Temperature Ionic Liquids as Replacements for Organic Solvents in Multiphase Bioprocess Operation." Biotechnology and Bioengineering **69**(2): 227.
- Eckert, C. A., B. L. Knutson, et al. (1996). "Supercritical Fluids as Solvents for Chemical and Materials Processing." Nature **383**: 313.
- Fukne-Kokot, K., M. Skerget, et al. (2003). "Modified freezing method for the measuring of gas solubility along the solid-liquid-gas equilibrium line." Fluid Phase Equilibria **205**: 233.
- Gordon, C. M. (2001). "New developments in catalysis using ionic liquids." Appl. Catal. A **222**: 101.
- Gordon, C. M., J. D. Holbrey, et al. (1998). "Ionic liquid crystals: hexafluorophosphate salts." Journal of Materials Chemistry **8**: 2627.
- Hyk, W. and Z. Stojek (1998). "Physicochemical Consequences of Generating a Thin Layer of Ionic Liquid at Microelectrode Surface in Undiluted Redox Liquid." J. Phys. Chem. B **102**: 577.
- Jessop, P., D. C. Wynne, et al. (2000). "Carbon Dioxide gas accelerates solventless synthesis." Chem. Commun.(8): 693.

- Katritzky, A. R., S. Singh, et al. (2005). "1-butyl-3-methylimidazolium 3,5-dinitro-1,2,4-triazolate: a novel ionic liquid containing a rigid planar energetic anion." Chem. Commun.(7): 868.
- Kazarian, S. G., N. Sakellarios, et al. (2002). "High Pressure CO₂-induced reduction of the melting temperature of ionic liquids." Chem. Commun.: 1314.
- Kirby, C. F. and M. A. McHugh (1999). "Phase Behavior of Polymers in Supercritical Fluids Solvents." Chem. Rev. **99**: 565.
- Lazzaroni, M. J., D. Bush, et al. (2005). "Revision of MOSCED Parameters and Extension to Solid Solubility Calculations." Ind. Eng. Chem. Res. **44**: 4075.
- Lu, J., C. L. Liotta, et al. (2003). "Spectroscopically Probing Microscopic Solvent Properties of Room-Temperature Ionic Liquids with the Addition of Carbon Dioxide." J. Phys. Chem. A **107**: 3995.
- McCullough, J. P., H. L. Finke, et al. (1957). "The Low-Temperature Thermodynamic Properties of Naphthalene, 1-Methylnaphthalene, 2-Methylnaphthalene, 1,2,3,4-Tetrahydronaphthalene, trans-decahydronaphthalene, and cis-decahydronaphthalene." J. Phys. Chem. **61**: 1105.
- Nara, S. J., J. R. Harjani, et al. (2002). "Lipase-catalyzed transesterification in ionic liquids and organic solvents: a comparative study." Tetrahedron Letters **43**: 2979.
- Olivier-Bourbigou, H. and L. Magna (2002). "Ionic liquids: perspectives for organic and catalytic reactions." J. Mol. Catal. A: Chemical **182-183**: 419.
- Pagano, B. (2004). BASF to present BASIL™ ionic liquid process at technology transfer forum. Mount Olive, NJ, BASF.
- Reetz, M. T., W. Wiesenhofer, et al. (2003). "Continuous flow enzymatic kinetic resolution and enantiomer separation using ionic liquid/supercritical carbon dioxide media." Advanced Synthesis & Catalysis **345**(11): 1221.
- Ropel, L., L. S. Belveze, et al. (2005). "Octanol-Water partition coefficients of imidazolium-based ionic liquids." Green Chem. **7**: 83.
- Schiller, M. and J. Gmehling (1992). "Measurement of Activity Coefficients at Infinite Dilution Using Gas-Liquid Chromatography. 4. Results for Alkylene Glycol Dialkyl Ethers as Stationary Phases." J. Chem. Eng. Data **37**(4): 503.
- Scurto, A. M., S. N. V. K. Aki, et al. (2002). "CO₂ as a Separation Switch for Ionic Liquid/Organic Mixtures." J. Am. Chem. Soc. **124**: 10276.

- Scurto, A. M. and W. Leitner (2005). Melting Point Depression of Organic Ionic Solids and "Liquids" with Carbon Dioxide for Biphasic Catalytic Reactions.
- Solinas, M., A. Pfaltz, et al. (2004). "Enantioselective Hydrogenation of Imines in Ionic Liquid/Carbon Dioxide Media." J. Am. Chem. Soc. **126**: 16142.
- Starks, C. M., C. L. Liotta, et al. (1994). Phase-transfer catalysis: fundamentals, applications, and industrial perspectives. New York, Chapman & Hall.
- Thomas, E. R. and C. A. Eckert (1984). "Prediction of Limiting Activity Coefficients by a Modified Separation of Cohesive Energy Density Model and UNIFAC." Ind. Eng. Chem. Des. Dev. **23**: 194.
- Visser, A. E., M. P. Jensen, et al. (2003). "Uranyl Coordination Environment in Hydrophobic Ionic Liquids: An in situ Investigation." **42**: 2197.
- Wasserscheid, P. and T. Welton (2002). Ionic Liquids in Synthesis. Weinheim, Germany, Wiley-VCH.
- Welton, T. (1999). "Room-Temperature Ionic Liquids. Solvents for Synthesis and Catalysis." Chem. Rev. **99**: 2071.
- White, G. L. and C. T. Lira (1989). Four-Phase (Solid-Solid-Liquid-Gas) Equilibrium of Two Ternary Organic Systems with Carbon Dioxide. Supercritical Fluids Science and Technology, American Chemical Society: 111-120.
- Zhang, J., W. Wu, et al. (2003). "Conductivities and Viscosities of the Ionic Liquid [bmim][PF6] + Water + Ethanol and [bmim][PF6] + Water + Acetone Ternary Mixtures." **48**: 1315.

CHAPTER VII

CONCLUSIONS AND RECOMMENDATIONS

Alkylcarbonic Acids

In this work, alkylcarbonic acids have been shown to catalyze the hydrolysis of β -pinene and the diazotization of aniline to form methyl yellow and benzyl iodide. The work of West et al (West, Wheeler et al. 2001) was also continued to further characterize and understand the mechanisms by which alkylcarbonic acids catalyze reactions through the decomposition of diazodiphenylmethane. At this point, someone with an interest in applying alkylcarbonic acids to an existing process would have a good basis of knowledge from which to start optimizing their process. There is some work that could be continued to understand alkylcarbonic acids in general, but at this point the focus should shift to finding industrially viable applications. Both of these pursuits are outlined below.

Clearly, a multitude of other acid catalyzed reactions could be tried that would likely prove at worst somewhat successful. Despite the success thus far and the probable success of other acid catalyzed reactions, there is no reason to believe this technology will be implemented in the near future. This is mainly due to the fact that current processes, while having drawbacks, are in place and installing high pressure equipment would only slightly reduce pollution while greatly increasing cost.

The places where alkylcarbonic acids could have the greatest impact are when either pressure is already present or where other advantages of using gas expanded liquids would also contribute to improved product or decreased environmental concerns. An example of this might be to couple alkylcarbonic acids with other GXL research. GXLS often have improved solubility over normal liquids so this is a possibility. However, few reactions between gases and liquids are acid catalyzed. Another possibility would be to combine alkylcarbonic acids with gas anti-solvent (GAS) fractional crystallization (Dixon and Johnston 1991; de la Fuente, Shariati et al. 2004). GAS uses a gas anti-solvent, usually CO₂, to lower the solubility of a compound in the liquid phase to the point where it crystallizes as a solid. In that case, CO₂ would be required for both the reaction and the separation which would help defray the cost of the pressure equipment.

The GAS process could be combined with the synthesis of methyl yellow as shown in Chapter III. The major product is methyl yellow but there is still unreacted N,N-dimethyl aniline, small amounts of coupled byproducts such as azobenzene or diphenylamine, and some salt from the sodium nitrite. Adding CO₂ pressure would likely first drop out the salt but next would be the methyl yellow product. A liquid-liquid extraction should separate the salt from the methyl yellow. A system to conduct GAS experiments is already setup in our laboratory and several previous experiments on GAS have been done.

In the pursuit of further understanding alkylcarbonic acids, another set of experiments utilizing the reaction of diazodiphenylmethane (DDM) could be run. The comparison of n-butyl alcohol, iso-butyl alcohol, sec-butyl alcohol, and tert-butyl alcohol

(Figure 7-1) would show the difference in a primary to a tertiary alcohol to forming alkylcarboxylic acids. The comparison between iso-butyl and n-butyl should provide information about isomer effect without changing the primary alcohol.

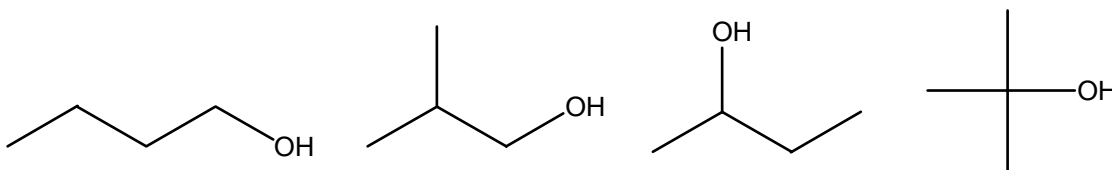


Figure 7-1: Series of alcohols for further study of alkylcarboxylic acids reacting with DDM

Also, since polyethylene glycols (PEGs) are receiving increased research interest as solvents with CO₂, it would be interesting to measure the DDM conversion with PEG. The rate could be compared to that for PEG without CO₂ and to other alcohols previously measured to see just how much acid catalysis occurs in CO₂-PEG systems. The effect of PEG polymerization (average molecular weight) could also be investigated with PEG-180, PEG-300, PEG-400, etc.

Cleavable Surfactants

In this work, a novel cleavable surfactant, n-octyl thiirane-1-oxide is characterized and demonstrated to be an effective surfactant. It is also shown to be easily cleavable into a gas and a hydrophobic liquid. This provides advantages over current cleavable surfactants which result in a hydrophilic liquid which requires wastewater treatment for removal and could still form micelles. Several derivatives of this technology are presented here as well as some continued research on the current molecule.

The intent of the cleavable surfactant presented here is to have the polar head group of the surfactant decompose into a gas rather than a liquid. Using the same head group functionality, thiirane oxide, but attaching a phenyl ring as shown in Figure 7-2, a photolabile cleavable surfactant would be created. The light sensitive surfactant may require less energy to decompose the surfactant since the energy input would ideally all go to the surfactant whereas when heating, the entire solution must be heated to the decomposition point of the surfactant.

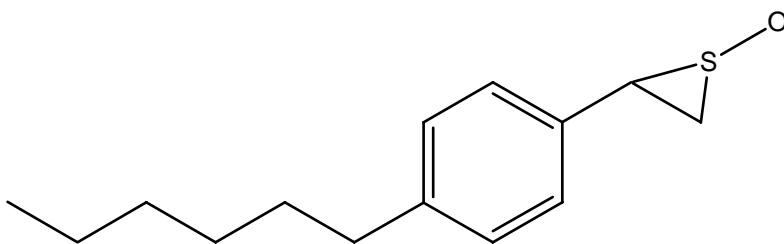


Figure 7-2: Photolabile analog of thiirane oxide cleavable surfactant

Alternatively, the thiirane oxide group could be attached to a CO₂-philic tail for use in w/c emulsions. Typically, fluorocarbons or fluoroether functional groups have been used as CO₂-philic moieties. Johnston et al have also created more environmentally friendly branched hydrocarbon chains that work well in w/c emulsions (Johnston, Harrison et al. 1996). Potential surfactants of this type are shown in Figure 7-3.

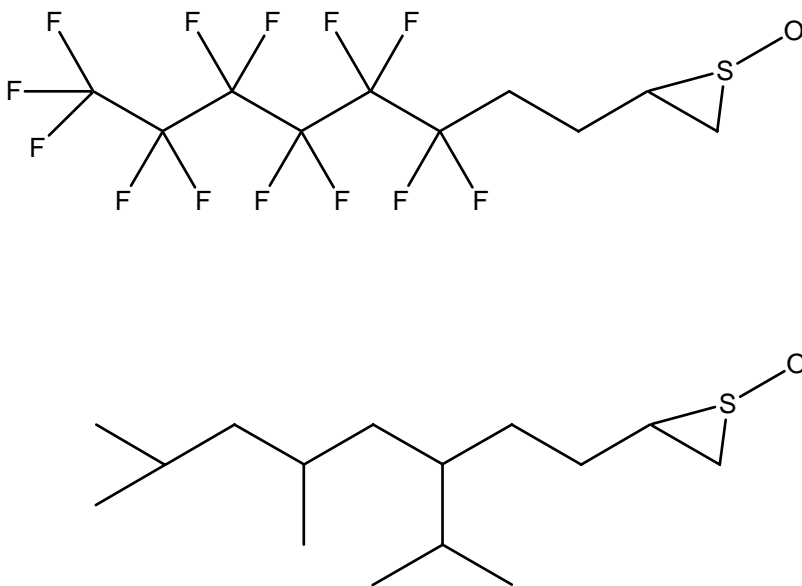


Figure 7-3: CO₂-philic analogs of thiirane oxide cleavable surfactant

There are several other potential head groups shown in Figure 7-4 that have advantages over the thiirane oxide functionality. The only disadvantage of thiirane oxide is that it releases sulfur oxide which is very reactive. It has been shown that SO quickly reacts to form SO₂ and elemental sulfur when in contact with another SO molecule. Also, the SO could react with other species present such as 1-decene to form a surfactant molecule, thus reducing the loss of CMC. So, a surfactant with a sulfone head group may be more advantageous since it would release SO₂ which is much less reactive. However, SO₂ is malodorous and a toxic gas. Therefore, releasing CO₂ may be even better. Figure 7-4 also shows two potential surfactants based on the cyclic ester head group. These surfactants may not have as low of a CMC but this could be accommodated by multiple head groups of additional polar functionality on the ring.

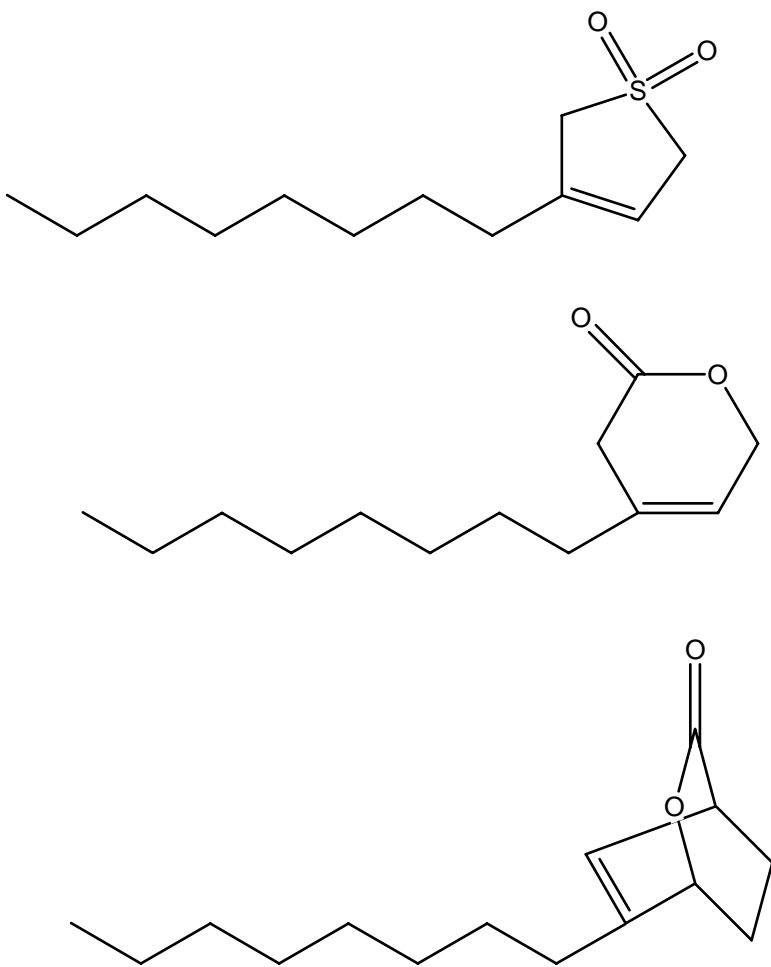


Figure 7-4: SO_2 and CO_2 emitting cleavable surfactants

In addition to the different types of surfactants that could be designed, it is important to further classify the current and any future surfactants fully. While the chemical characterization is complete and the CMC measured, the micelle structure was not probed. The current surfactant already is planned to be run in a small angle neutron scattering (SANS) apparatus at NIST in Gaithersburg, Maryland. Small angle neutron scattering is commonly used to determine whether the micelles are spherical or cylindrical or a different shape (McElhanon, Zifer et al. 2005). These measurements are fairly straightforward and can be carried out on any further surfactant that is synthesized.

Finally, it would be very powerful to utilize a cleavable surfactant in a useful application. Ideally the reaction would be run in the emulsion and then separated by decomposing the surfactant allowing a simple isolation of the desired product. A simple reaction to initially test this could be the hydrolysis of benzyl chloride to benzyl alcohol as shown in Figure 7-5. The reaction would be run by loading benzyl chloride, water, and the surfactant above the CMC along with a little base. Then after letting the reaction run, heat the mixture to 90°C and then allow it to cool back to room temperature. Then the product will be immiscible in the water phase and should be in an oil phase with the 1-decene from the surfactant.

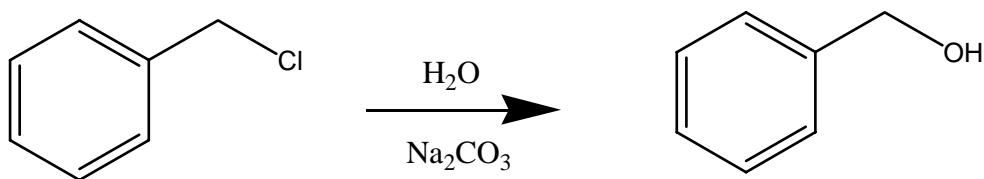


Figure 7-5: Base catalyzed hydrolysis of benzyl chloride to benzyl alcohol.

Another possible reaction would be emulsion polymerization. These reactions are much more complicated than a base catalyzed hydrolysis, but much more compelling to industry since polymerization is the primary use of surfactants in industrial synthesis. Beckman has previously polymerized acrylamide in CO₂ based emulsions as shown in Figure 7-6 (Adamsky and Beckman 1994). This is a good choice for reaction because of our group's previous experience with surfactants and our growing interest in cleavable surfactants. Additionally, we have very close connections with Beckman who could serve as a collaborator on the project because of his polymer science background and experience with this particular reaction. Additionally, the group of Johnston at the University of Texas has a strong interest in w/c emulsions and could provide help and possible collaboration on this interesting project.

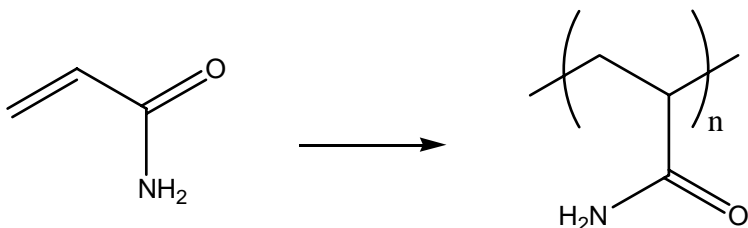


Figure 7-6: Polymerization of acrylamide to polyacrylamide.

Another interesting possibility utilizing cleavable surfactants is the synthesis and isolation of nanoparticles. The Eckert-Liotta group has researchers with experience in this area as well as collaborators at Auburn and Texas with significant experience. Kitchens et al demonstrated copper nanoparticle growth using bis-(2-ethylhexyl) sulfosuccinate sodium salt (AOT) as the surfactant in alkanes and CO₂ (Kitchens, McLeod et al. 2003; Kitchens and Roberts 2004). It would be very interesting to

synthesize nanoparticles and isolate them in a process that was easier than the current one.

Obviously the list of possible applications could be quite long but another brief idea, given the research group's current interest in biomolecules, is the extraction of enzymes which Johnston has also demonstrated (Lemert and Johnston 1990).

Melting Point Depression Measurements

The work present here on the measurement of melting point depression provides a new, simplified way to get accurate data. The melting point depression for two ionic liquids is also quantified and activity coefficients can be derived from these measurements. This work could be important for ionic liquid biphasic systems in the future.

However, these results on ionic liquids are only preliminary. While a basic understanding of the T-x curve for two ionic liquids was found, the study was not wide reaching enough to draw firm conclusions about all ionic liquids. For that reason, it would be wise to try a series of different cations with the same anion to understand if all ionic liquids exhibit negative deviations. Additionally, a series of cations with the same anion could be run to give further understanding of the effect cation size on melting point depression and deviation from idealality. A series of potential cations is in figure 7-7.

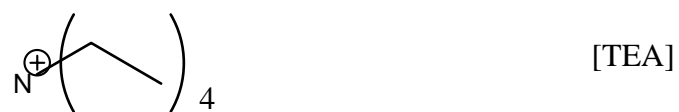
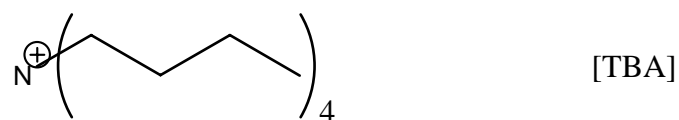
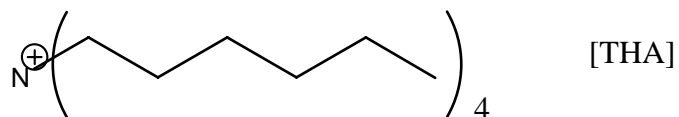


Figure 7-7: Series of cations with decreasing alkylchain length from tetrahexyl to tetramethyl ammonium cation with abbreviations.

Similarly, the effect of functional groups on the melting point of naphthalene could be easily studied. Substitution of hydrogen with several functional groups such as methyl, ethyl, methoxy, nitro, chloro and others could give a picture of what the interaction of CO₂ with that functional group does to the melting point.

Another class of solvents that is gaining popularity as a potential 'green' solvent is polyethyleneglycols, or PEGs. Like, ionic liquids, they exhibit very low vapor pressures making them good replacements for VOCs. Also, PEGs have good organic and aqueous solubilities so they are good solvents for a wide range of applications. However, at higher molecular weights PEGs get very viscous and eventually are solids. Thus, a system very similar to that described for ILs would work equally well for PEGs. CO₂ could be used to depress the melting point of the solvent and then extract the product out or used in a basphic regime. Measurement of the T-x curve for various molecular weight PEGs could be done in the same apparatus as was used for the ILs.

References

- Adamsky, F. A. and E. J. Beckman (1994). "Inverse Emulsion Polymerization of Acrylamide in Supercritical Carbon Dioxide." Macromolecules **27**: 312.
- de la Fuente, J. C., A. Shariati, et al. (2004). "On the selection of optimum thermodynamic conditions for the GAS process." J. Supercrit. Fluids **32**(1-3): 55.
- Dixon, D. J. and K. P. Johnston (1991). "Molecular Thermodynamics of solubilities in gas antisolvent crystallization." AICHE J. **37**(10): 1441.
- Johnston, K. P., K. L. Harrison, et al. (1996). "Water-in-Carbon Dioxide Microemulsions: A New Environment for Hydrophiles Including Proteins." Science **271**: 624.
- Kitchens, C. L., M. C. McLeod, et al. (2003). "Solvent Effects on the Growth and Steric Stabilization of Copper Metallic Nanoparticles in Liquid Alkane/AOT Reverse Micelle Systems." J. Phys. Chem. B **107**(41): 11331.
- Kitchens, C. L. and C. B. Roberts (2004). "Copper Nanoparticle Synthesis in Compressed Liquid and Supercritical Fluid Reverse Micelle Systems." Ind. Eng. Chem. Res. **43**(19): 6070.
- Lemert, R. M. and K. P. Johnston (1990). "Reverse Micelles in Supercritical Fluids. 3. Amino Acid Solubilization in Ethane and Propane." J. Phys. Chem. **94**(15): 6021.
- McElhanon, J. R., T. Zifer, et al. (2005). "Thermally Cleavable Surfactants Based on Furan-Maleimide Diels-Alder Adducts." Langmuir **21**: 3259.
- West, K. N., C. Wheeler, et al. (2001). "In Situ Formation of Alkylcarbonic Acid with CO₂." J. Phys. Chem. A **105**: 3947.

VITA

Ross Ritchie Weikel was born in Raleigh, North Carolina on February 17, 1979 and grew up there as well. He is the son of Scott Jay Weikel and Jean Ritchie Weikel. He attended high school at Jesse O. Sanderson HS in Raleigh. Ross graduated *magna cum laude* from North Carolina State University in 2001 with a Bachelor of Science in Chemical Engineering. While there, he competed on the varsity soccer team and met his wife, Blair Schultea (Weikel) whom he married in April of 2005. In 2001, he enrolled at the Georgia Institute of Technology. His graduate studies were directed by Professor Charles A. Eckert and Professor Charles L. Liotta. He will complete his Ph.D. in Chemical Engineering in the summer of 2005. Selected publications and presentations follow.

Publications

Ross R. Weikel, Jason P. Hallett, Charles L. Liotta, and Charles A. Eckert, "Self Neutralizing Acid Catalysis from CO₂ and Its Application" Topics Catalysis (2005) *submitted*.

Ross R. Weikel, Colin Thomas, Charles L. Liotta, and Charles A. Eckert, "Thiirane Oxide Based Thermally Cleavable Surfactants" Langmuir (2005) *in preparation*.

Ross R. Weikel, Charles L. Liotta, Charles A. Eckert, "Self-neutralizing *in situ* acid catalysis for single pot synthesis of aryl halides and azo dyes in gas expanded liquids" Green Chem (2005) *submitted*.

Elizabeth Newton, Ross R. Weikel, Charles L. Liotta, and Charles A. Eckert, "Melting Point Depression of Ionic Liquids with CO₂" *in preparation*.

Selma Bektesevic, Julie C. Beier, Liang Chen, Nicolas Eghbali, Stephanie King, Galit Levetin, Geeta Mehta, Richard J. Mullins, Jessica L. Reiner, Ross Weikel, Songweng Xie, and Erica Gunn, "Green challenges: student perspectives from the 2004 ACS-PRF Summer School on Green Chemistry" Green Chem (2005) 7, 403-407.

Theresa Chamblee, Ross R Weikel, Shane Nolen, Charles L. Liotta, and Charles A. Eckert, Reversible *in situ* acid formation for b-pinene hydrolysis using CO₂ expanded liquid and hot water" Green Chem (2004) 6(8), 382-386.

Presentations

Ross R. Weikel(speaker), Charles L. Liotta, Charles A. Eckert, "Self Neutralizing Acid Catalysis from CO₂" Canadian Symposium on Catalysis, Montreal, Canada, May 18, 2004

Ross R. Weikel(presenter), Xiaofeng Xie, Charles L. Liotta, Charles A. Eckert "Self Neutralizing Acid Catalysis from CO₂" ACS-PRF Summer School on Green Chemistry, Pittsburgh, PA, August 3, 2004

Theresa Chamblee (speaker), Ross Weikel, Shane Nolen, Charles L. Liotta, and Charles A. Eckert, "The Use of New Technologies to Develop Environmentally Benign Processes: Acid-Catalyzed Hydrolysis of Pinene in Aqueous Media" 35th International Symposium on Essential Oils, September 29, 2004, Messina, Italy

Ross R. Weikel(speaker), Theresa Chamblee, Charles L. Liotta, Charles A. Eckert, "Self Neutralizing Acid Catalysis from CO₂" AIChE Annual Meeting, Austin, TX, November 12, 2004

Jason P. Hallett(speaker), Ross R. Weikel, Charles L. Liotta, and Charles A. Eckert, "Catalysis Using *In Situ* Acids Formed in CO₂-Expanded Alcohols" International Symposium on Supercritical Fluids, Orlando, FL, May 1-4, 2005

Joshua D. Grilly, Colin A. Thomas, Ross R. Weikel, Christopher L. Kitchens, Jason P. Hallett, Philip G. Jessop, Charles L. Liotta, Charles A. Eckert, "Sulfoxide Solvents and Surfactants for Facile Separations" AIChE Annual Meeting, Cincinnati, OH, November 2005